new 82-10

LEGAL NOTICE

This report was prepared by Ontario Hydro and, while effort has been made to assure the accuracy and applicability of the material contained herein, neither Ontario Hydro nor any person acting on its behalf:

(a) makes any warranty, express or implied with respect to the use of any information, apparatus, method or process disclosed in this report or that such use may not infringe privately owned rights; or

(b) assumes any liabilities with respect to the use of, or for damages resulting from the use of, any information, apparatus, method or process disclosed in this report.

ontario hydro
research division

THE METALLURGY OF PRESSURE TUBES

Report No. 89-271-K

R.G. Fleck
Supervising Engineer
Materials Integrity Section
Metallurgical Research Department

ABSTRACT

The purpose of this report is to introduce the various metallurgical aspects of zirconium and to discuss their impact on the service performance of CANDU pressure tubes. A review of the physical metallurgy of zirconium is the starting point. The concept of anisotropy is presented and the role of dislocations in deformation is outlined. Pressure tube manufacture is presented from the extraction of the zirconium to the variations in extrusion and cold reduction, drawing and pilgering, processes that have been investigated. The basic mechanisms that have resulted in concerns with the operational life of pressure tubes are discussed. Irradiation damage and deformation, delayed hydride cracking and fracture and corrosion and hydrogen ingress are reviewed along with the experimental programs to investigate these mechanisms. Finally a review of alloy development programs that have been performed is presented.

job	file	date	report no.
84-539-000	100	January 16, 1990	89-271-K

91602
new 82-10

ontario hydro
research division

EXECUTIVE SUMMARY

THE METALLURGY OF PRESSURE TUBES

R.G. Fleck
Materials Integrity Section
Metallurgical Research Department

A number of occasions arise where it is required to present overviews on the metallurgy of pressure tubes. The information presented in this report is an attempt to collect relevant information on key aspects of pressure tube metallurgy. Consequently, the information presented has been collected from a number of sources in AECL-CO, AECL-RC and Ontario Hydro Research Division.

A brief description of the pressure tube and the operating conditions is presented. The report then concentrates on the physical and mechanical metallurgical aspects of pressure tubes.

The crystal structure of zirconium is discussed and the concept of dislocations, grains and grain boundaries are presented. The introduction of these principles is included to help clarify discussions on the properties and performance of pressure tubes. Pressure tube manufacture is presented to cover the extraction of zirconium from the ore, the production of the alloy (Zr-2.5 wt% Nb) and billet and tube processing. Various developmental aspects related to production are presented such as pilgering and modified cold draw schedules. The metallurgical structure of the pressure tubes is then discussed.

Processes that have caused concern with the operational life of pressure tubes are discussed such as; irradiation damage and deformation, delayed hydride cracking and fracture and corrosion and hydrogen ingress. The various alloy development programs that have been carried out are also discussed.

job	file	date	report no.
84-539-000	100	January 16, 1990	89-271-K

TABLE OF CONTENTS

		Page
1.0	INTRODUCTION	1
2.0	BASIC METALLURGY	5
3.0	ZIRCONIUM EXTRACTION AND ALLOY PRODUCTION	12
4.0	TUBE PRODUCTION	17
5.0	MECHANICAL PROPERTIES	31
6.0	OPERATING EXPERIENCE	42
7.0	DISCUSSION	44
	7.1 Irradiation Damage and Deformation	45
	7.2 Pressure Tube Fracture	55
	7.3 Hydrogen Ingress and Corrosion	82
8.0	ALLOY DEVELOPMENT	93
9.0	SUMMARY	94
10.0	ACKNOWLEDGEMENTS	96
BIBLIOGRAPHY		97

LIST OF FIGURES

		PAGE
FIGURE 1.1(a)	Simplified Description of a Fuel Channel	2
FIGURE 1.1(b)	Schematic Diagram of a Pickering Generating Station "A" Fuel Channel (From CANDU 500 Pickering Generating Station 1969)	3
FIGURE 1.2	Pickering "A" Reactor Face Showing Feeder Pipe Assembly (From CANDU 500 Pickering Generating Station 1969)	4
FIGURE 2.1	The Three Common Crystal Structures of Metals	6
FIGURE 2.2	Illustration of the principal Crystallographic Planes in Zirconium. The Normals to these Planes are the Principal Directions, eg, Basal Plane Normal is the <0001> Direction	7
FIGURE 2.3	Hexagonal Crystal Structure of Zirconium. Texture Measurements on Pressure Tubes have been Mainly Concerned with the Distribution of the Basal Plane Poles in the three Principal Directions of the Pressure Tube	8
FIGURE 2.4	Illustration of the Transition Temperature for Zirconium where the Crystal Structure Changes from Hexagonal Close Packed to Body Centered Cubic	9
FIGURE 2.5	The Result of Dislocation Motion Through a Crystal Lattice is Deformation of the Lattice	10
FIGURE 2.6	Transmission Electron Micrograph (Mag 33,000 X) of Annealed Zr-2.5 wt% Nb showing Grains of Alpha Zirconium (A) and Grain Boundaries (B)	11
FIGURE 2.7	Phase Diagram for the Zirconium-Hydrogen system	13
FIGURE 2.8	Summary of Terminal Solid Solubility of Hydrogen Isotopes in Cold-Worked Zr-2.5 WT% Nb	14
FIGURE 3.1	Flow Diagram for the Production of Zirconium and Zirconium Alloys	15
FIGURE 3.2	Schematic Diagram to Illustrate how Ingot Defects are Produced as a Result of a Fast (5-15 min) Hottop Procedure.	18

LIST OF FIGURES (Cont'd)

		PAGE
FIGURE 4.1	Present Fabrication Route for Zr-2-1/2% Nb Pressure Tubes	19
FIGURE 4.2	Equilibrium Phase Diagram for the Zirconium-Nobium System	20
FIGURE 4.3	Transmission Electron Micrograph (Mag 47,000 X) of Zr-2.5 wt% Nb Pressure Tube Material showing Alpha Grains (A), Beta Phase (B) and Dislocations (C)	21
FIGURE 4.4	Illustration of the Breakdown Sequence of an Ingot for the Production of Pressure Tubes. With the use of a Sequential Numbering System a Pressure Tube can be Traced Back to a Specific Position in a Log	23
FIGURE 4.5	(A) & (B) are respectively Microstructures from a Forged and Air-Cooled and a β-Quenced Zr-2.5% Nb Forged Bar (x 0.6).	24
FIGURE 4.6	Extrusion Process	26
FIGURE 4.7	Schematic of Plug Drawing Process	26
FIGURE 4.8 (a)	Schematic representation of the Preferred Orientation of C-Axis (Basal Poles) of Zirconium Crystals (Grains) in present CANDU Pressure Tubes. The Fraction of the Basal Poles in the Three Principal Directions are Determined	27
FIGURE 4.8 (b)	Schematic representation of Basal Poles Oriented in the Transverse Direction of a Pressure Tube and Typical Basal Pole Figure for such a Texture	28
FIGURE 4.9	Defect in Pressure Tube as a Result of Ingot Pipe Remnant in Trepanned Billet	30
FIGURE 4.10	Production Routes for the Fabrication of Cold-Worked Zr-2.5 wt% Nb Tubes	32
FIGURE 4.11(a)	Principles of the Pilger Process	33
FIGURE 4.11(b)	Pilger Rolls in the 'Open' Position	34

LIST OF FIGURES (Cont'd)

		PAGE
FIGURE 5.1	Schematic diagram of the Tensile Specimen used to determine the Tensile Properties to Qualify Pressure Tubes	36
FIGURE 5.2	Representative Engineering Stress vs Engineering Strain Plots for Longitudinal Specimens from Front and Back Ends of a Zr-2.5 Nb Pressure Tube	37
FIGURE 5.3	The Effect of Grain Thickness on the Yield Strength of Zr-2.5 Nb Extrusions	38
FIGURE 5.4	Engineering Stress vs Engineering Strain Plots illustrating the large differences in Tensile Properties between Longitudinal and Circumferential specimens at ambient temperature	40
FIGURE 5.5	Plots illustrating the decrease in 0.2% Yield Strength and Tensile Strength with increasing Stress Relieving Temperatures	41
FIGURE 6.1	Schematic drawing to illustrate correct and incorrect Rolling of Pressure Tube into the End Fitting	43
FIGURE 7.1.1	Schematic diagram of a displacement or Seeger Zone.	46
FIGURE 7.1.2	An illustration of the influence of a Fast Neutron Flux on the Thermal (Out Reactor) Creep Rate	48
FIGURE 7.1.3(a)	Dislocation Motion by Climb due to Vacancy or Interstitial	49
FIGURE 7.1.3(b)	Schematic description of how a Dislocation can Climb past barriers (particles) and then continue to glide	50
FIGURE 7.1.4	Influence of Grain Shape on Irradiation Induced Vacancy Flux	52
FIGURE 7.1.5	Irradiation Growth Behaviour of Darlington Pressure Tube Material at 553, 583 and 623 K. Samples cut Longitudinally	54

LIST OF FIGURES (Cont'd)

		PAGE
FIGURE 7.1.6	Irradiation Growth Behaviour of Zr-2.5 wt% Nb material at ~280°C. Samples cut Transversely from the Pressure Tube	56
FIGURE 7.1.7	Microstructure of a Current Zr-2.5 Nb & TG3 Pressure Tube in the Longitudinal Section	57
FIGURE 7.2.1	A Schematic illustration of how the Orientation of Hydrides in relation to the Applied Stress influences the Ductility of Zirconium	59
FIGURE 7.2.2	Large Hydride Precipitated at the root of a Notch (Mag 160X)	60
FIGURE 7.2.3	Schematic illustration of Delayed Hydride Cracking	61
FIGURE 7.2.4	Schematic diagram to illustrate the relationship between Notch Size and Stress Concentration	62
FIGURE 7.2.5	Schematic diagram of the dependence of Crack Velocity on Stress Intensity Factor	63
FIGURE 7.2.6	The influence of Applied Stress during Hydriding on the Distribution of Hydrides	65
FIGURE 7.2.7	Optical Micrograph (Mag 115X) of Hydrides in Zr-2.5 wt% Nb	67
FIGURE 7.2.8	Transmission Electron Micrograph (Mag 122,000 X) which shows Stacking of Small Hydrides that Form a "Single" Hydride	68
FIGURE 7.2.9	Transmission Electron Micrograph (Mag 85,000 X) of a Hydride (A) lying (a) along a Smooth Beta Boundary and (b) at an angle to an Irregular Beta Boundary	69
FIGURE 7.2.10	Cantilever Beam Test Specimen used to study the Delayed Hydride Cracking behaviour of Zr-2.5 Nb showing orientation relative to the Pressure Tube from which it was cut	71

LIST OF FIGURES (Cont'd)

		PAGE
FIGURE 7.2.11	Schematic Diagram for 4-Point Bend Loading	72
FIGURE 7.2.12	Specimen used to investigate Crack Initiation into a region of continuous Increase in Hydrogen Concentration	73
FIGURE 7.2.13	The effect of direction of approach to Test Temperature on the subsequent Velocity of Delayed Hydride Cracks	74
FIGURE 7.2.14	Crack Growth Dependence on Stress Concentration K. After a Decrease in K there is an Incubation period before Cracking occurs at the Lower K value	76
FIGURE 7.2.15	Schematic drawing of a Compact Tension Specimen	77
FIGURE 7.2.16	Schematic diagram to show Crack Dimensions at onset of Leakage	78
FIGURE 7.2.17	Pressure Tube Sag into Contact with Calandria Tube as a Result of a Spacer Moved Out of Design Position as a Result of Vibration During Commissioning	80
FIGURE 7.2.18	Hydride Blisters on Pressure Tubes	81
FIGURE 7.2.19	Comparison of Measured and Calculated Deuterium Profiles through the Blister shown in the above Micrograph	83
Figure 7.2.20	Applied Tensile Stress to cause Cracking plotted against Blister Depth for all Blisters	84
FIGURE 7.3.1	Deuterium Buildup at Pressure Tube Ends of PNGS Unit 4 Fuel Channels	85
FIGURE 7.3.2	Potential Routes for Deuterium Ingress at Rolled Joints	87
FIGURE 7.3.3	Location of Yttrium Sink, Attachment Ring on Pressure Tube in Relation to Rolled Joint	89

LIST OF FIGURES (Cont'd)

		PAGE
FIGURE 7.3.4	Corrosion of Pickering 1 and 2 Zircaloy-2 Pressure Tubes	90
FIGURE 7.3.5	Breakdown of Protective Oxide along the outside of P3L09 compared to Deuterium Concentration	92
FIGURE 8.1	Atomic Arrangement for the Ordered Alloy - Zr_3Al	95

TO: D. Mills
Director of Research

ontario hydro
research division

THE METALLURGY OF PRESSURE TUBES

1.0 INTRODUCTION

The CANDU reactor design is based on a number of individual pressure vessels (pressure tubes) per reactor as opposed to the single pressure vessel concept of the PWR's. Dependent on the specific CANDU reactor there are either 390 or 480 individual pressure vessels per reactor. Figures 1.1(a) and 1.1(b) are schematic diagrams which show the location of the pressure tube in a fuel channel and Figure 1.2 shows the arrangement of the fuel channels in a typical CANDU reactor.

Pressure tubes are required to operate in an environment of elevated temperature (300°C), internal pressure (10 MPa), fast (E>1MeV) neutron flux (2.5×10^{17} $n/m^2/s$) and water. The CANDU reactors use natural uranium and therefore neutron economy is important. The only suitable material which can provide the desired neutron economy (i.e. has a low capacity for neutron absorption) and still maintain it's mechanical properties along with corrosion resistance for the above operating conditions is zirconium. Two alloys have been used for the production of pressure tubes; Zircaloy and Zr-2.5 wt% Nb, with the latter being the only one now used in CANDU reactors as operated in Canada. Exposure to the above operating conditions for a design life of about 30 years places an emphasis on the evaluation of the long term material properties of pressure tubes. The longest running Ontario Hydro CANDU reactors have operated for about 15 years and several pressure tube related outages have occurred. The Pickering Units 1 & 2, which originally used Zircaloy tubes, were completely retubed in 1986-88. For CANDU reactors it is desirable to have pressure tubes that have a service life comparable to the 40 year life of the total generating station.

This report will present information on the basic metallurgical properties of zirconium, the production of zirconium alloys and the manufacture of pressure tubes. The various pressure tube problems which have occurred will also be discussed. As the report is to provide an overview of pressure tube technology a bibliography is provided for each section as opposed to detailed references for specific points. The information presented is a result of discussions over a period of years with staff, referenced at the end of the report, in AECL-CO, AECL-RC and OH.

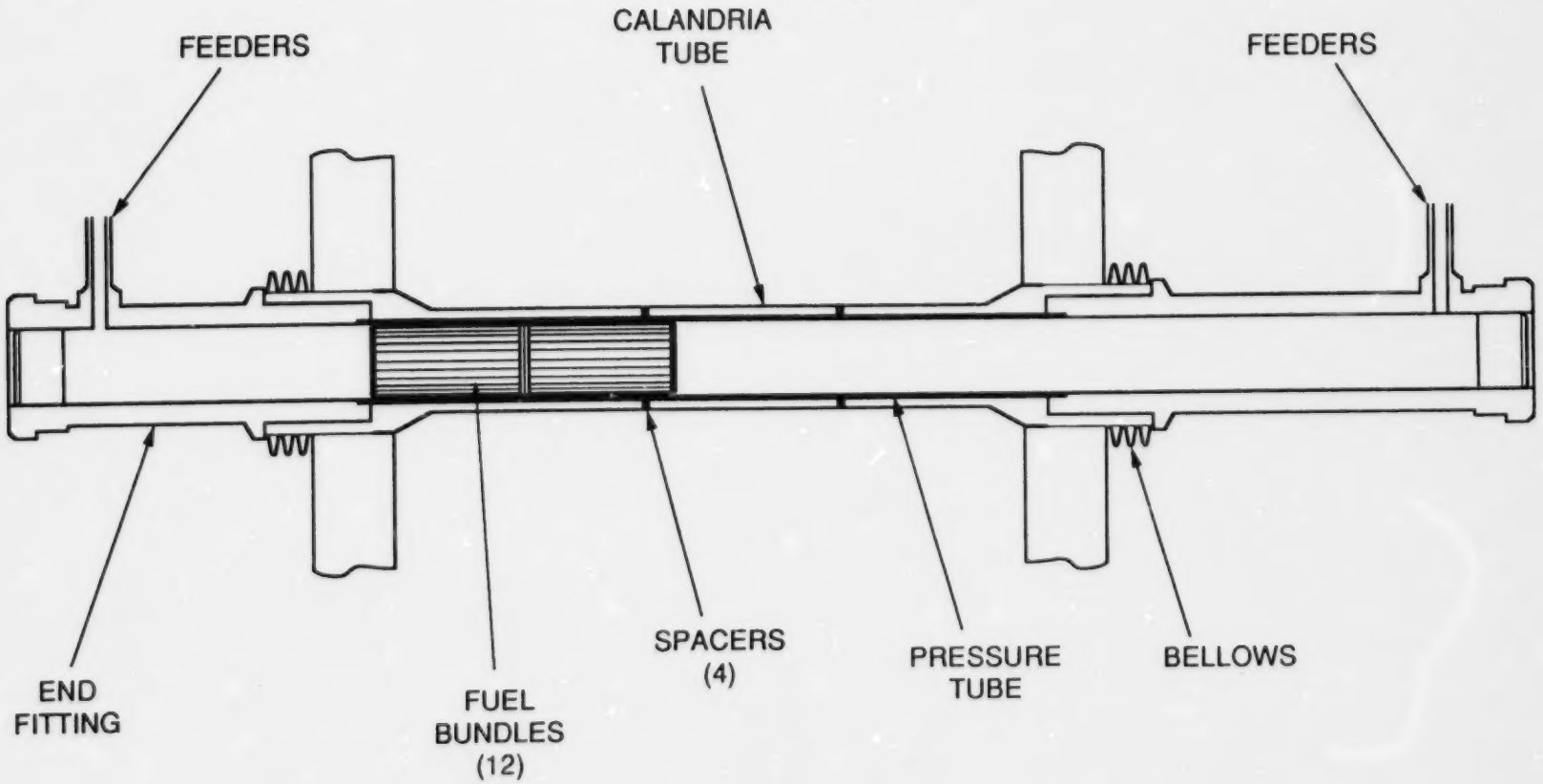

FIGURE 1.1 (a)

SIMPLIFIED DESCRIPTION OF A FUEL CHANNEL

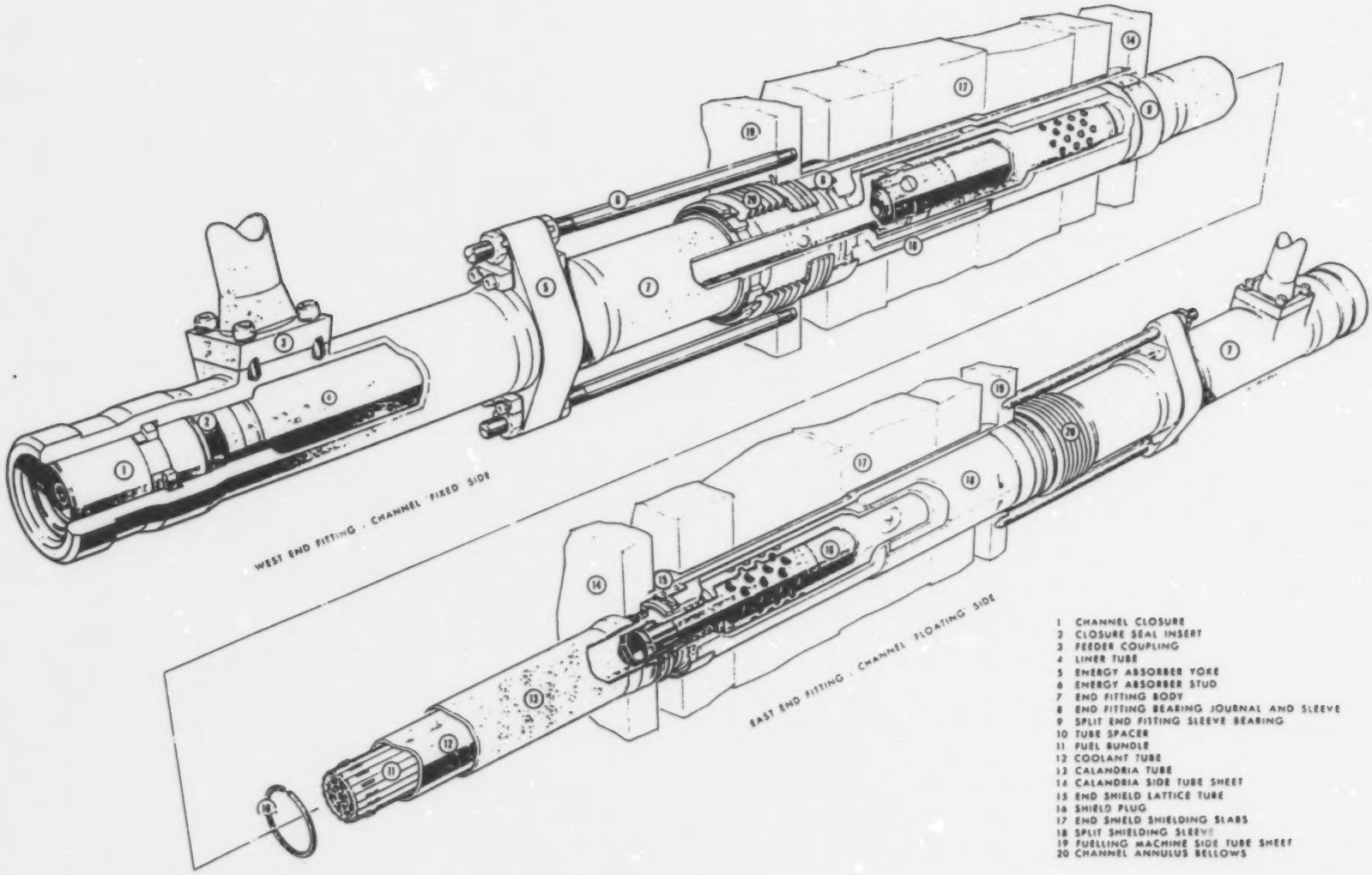
WEST END FITTING - CHANNEL FIXED SIDE
EAST END FITTING - CHANNEL FLOATING SIDE
1 CHANNEL CLOSURE
2 CLOSURE SEAL INSERT
3 FEEDER COUPLING
4 LINER TUBE
5 ENERGY ABSORBER YOKE
6 ENERGY ABSORBER STUD
7 END FITTING BODY
8 END FITTING BEARING JOURNAL AND SLEEVE
9 SPLIT END FITTING SLEEVE BEARING
10 TUBE SPACER
11 FUEL BUNDLE
12 COOLANT TUBE
13 CALANDRIA TUBE
14 CALANDRIA SIDE TUBE SHEET
15 END SHIELD LATTICE TUBE
16 SHIELD PLUG
17 END SHIELD SHIELDING SLABS
18 SPLIT SHIELDING SLEEVE
19 FUELLING MACHINE SIDE TUBE SHEET
20 CHANNEL ANNULUS BELLOWS

FIGURE 1.1 (b)

SCHEMATIC DIAGRAM OF A PICKERING GENERATING STATION "A" FUEL CHANNEL
(FROM CANDU 500 PICKERING GENERATING STATION 1969)

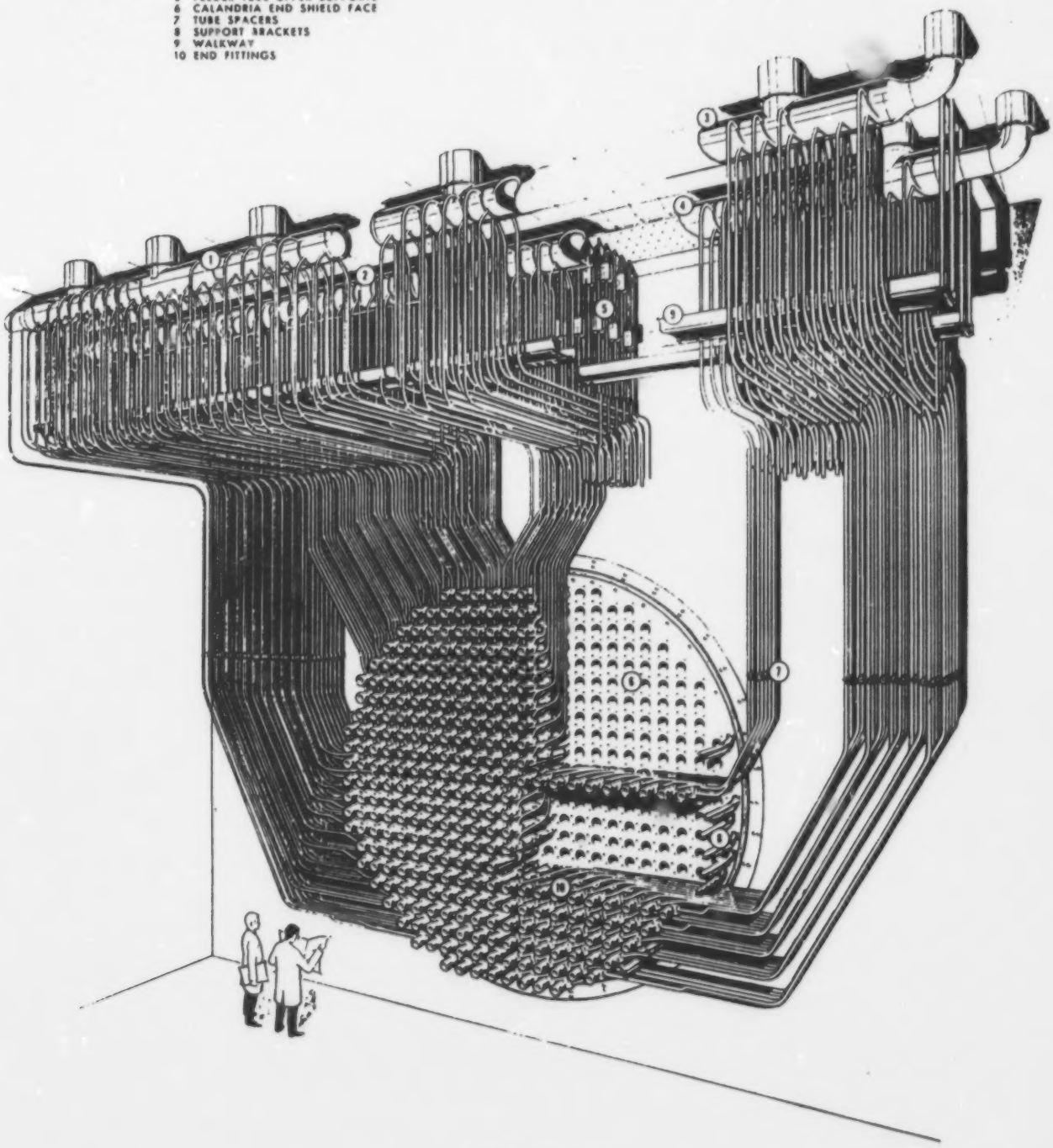

FIGURE 1.2

PICKERING "A" REACTOR FACE SHOWING
FEEDER PIPE ASSEMBLY
(FROM CANDU 500 PICKERING GENERATING STATION 1969)

2.0 BASIC METALLURGY

Many of the in service characteristics of pressure tubes are a result of the basic properties of zirconium.

Crystallography is the study of atomic arrangements in crystalline solids such as a metals. From studies of the crystal structure deformation and fracture mechanisms can be understood. The majority of engineering metals e.g. steels, nickel alloys, aluminum etc., have either a body centered cubic or face centered cubic crystal structure as shown in Figure 2.1. These crystal structures are relatively isotropic.

For zirconium the crystal structure is hexagonal close packed (hcp), see Figure 2.1. Within the crystal structure there are various planes of atoms that can be identified and Figure 2.2 illustrates the major planes in the hexagonal close packed crystal structure. The normals to these planes are used to identify the directions within the crystal structure. For a given crystal structure there are certain combinations of crystal planes and directions that are preferential for deformation. These planes and directions invariably contain the closest atomic packing for a given crystal structure. For metals with the hcp structure the mechanical properties are anisotropic (Figure 2.3). The hcp zirconium undergoes a crystallographic change from hexagonal close packed to body centered cubic, on heating, at a temperature of 862°C as illustrated in Figure 2.4.

From the above basic information on the crystallography of zirconium subsequent discussions on the anisotropic behaviour of pressure tube will be easier to understand.

Another basic crystallographic feature that should be described is the dislocation. A metal is built up from atoms arranged or stacked in a particular sequence, Figure 2.5, which determines the crystal structure as discussed above. As in all aspects of nature nothing is absolutely perfect and so in the stacking of the atoms imperfections occur. A particular imperfection that occurs is the introduction of an extra half plane of atoms into the atomic stacking arrangement. This results in a dislocation of the perfect atomic arrangement, Figure 2.5. The situation presented in Figure 2.5 is a simplification but it does convey the correct idea of a dislocation and will be useful when deformation is discussed. Deformation occurs when the dislocation moves as illustrated in Figure 2.5. If the dislocation motion is restricted then deformation becomes more difficult i.e. higher stress levels are required. For a given crystal structure there are preferred directions and planes for dislocation motion.

Metals are crystalline materials and consist of a number of crystals, in which atoms are packed in a periodic sequence, joined together. The individual crystals are referred to as grains and the individual grains are separated by grain boundaries, Figure 2.6. In alloys more than one phase can be present and in such cases phase boundaries also occur.

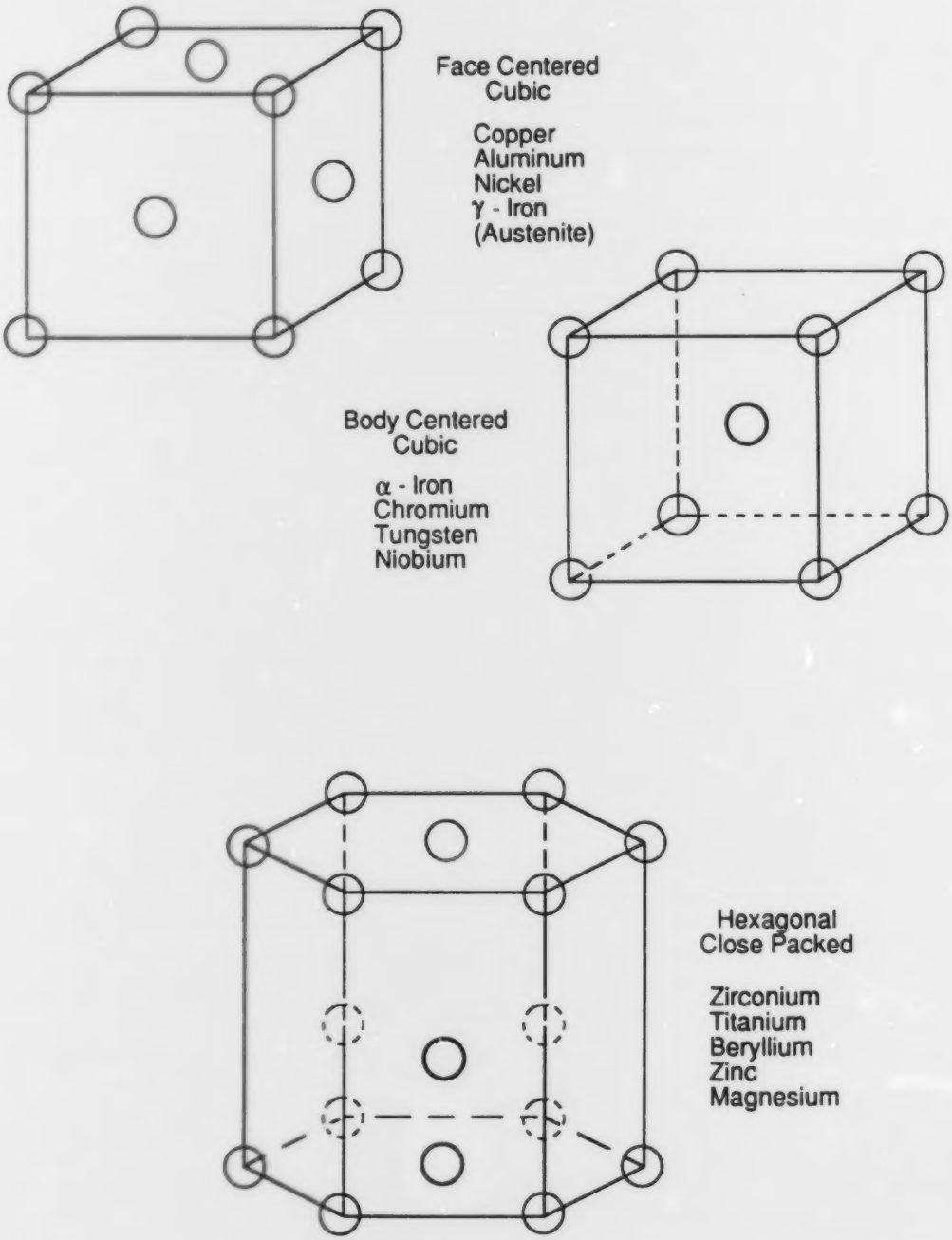

FIGURE 2.1

THE THREE COMMON CRYSTAL STRUCTURES OF METALS

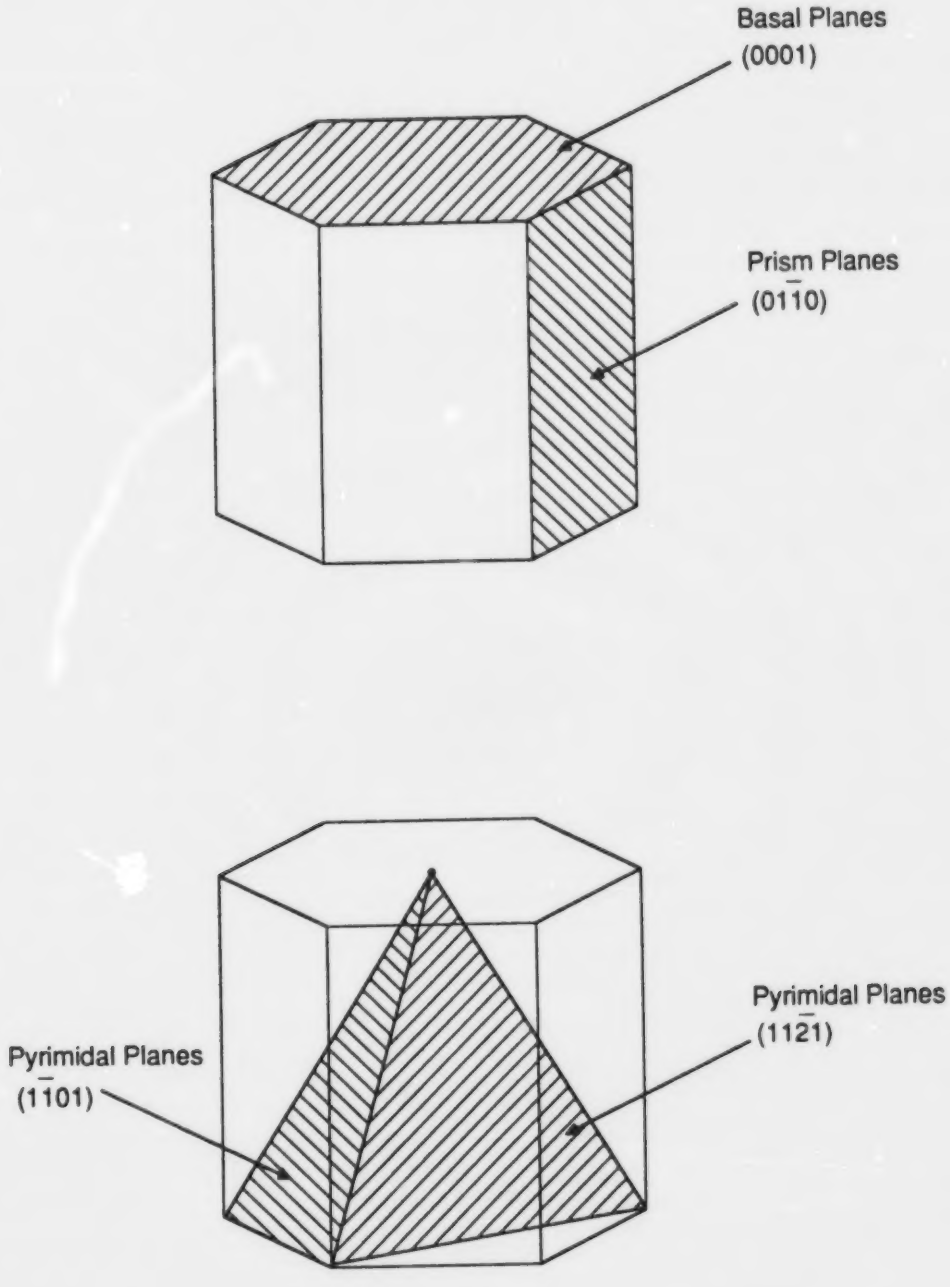

FIGURE 2.2

ILLUSTRATION OF THE PRINCIPAL CRYSTALLOGRAPHIC PLANES IN ZIRCONIUM. THE NORMALS TO THESE PLANES ARE THE PRINCIPAL DIRECTIONS e.g. BASAL PLANE NORMAL IS THE < 0001 > DIRECTION

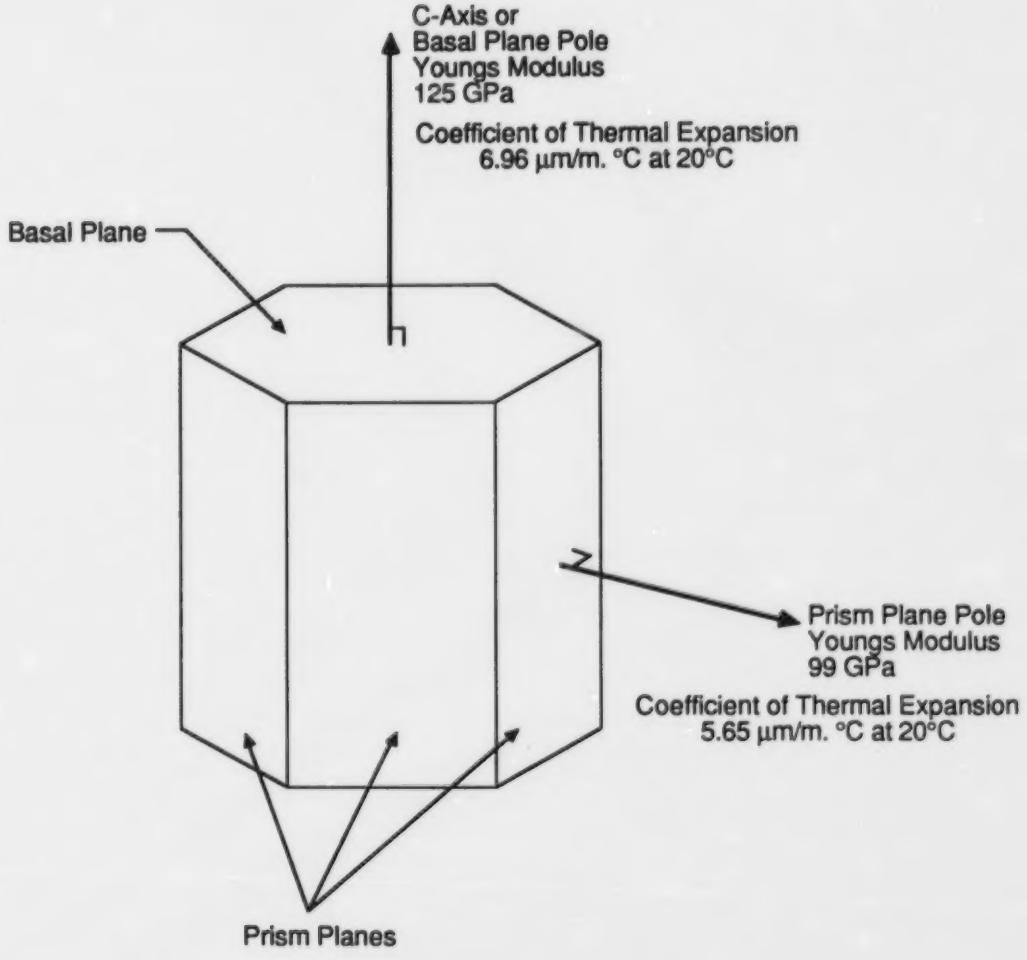

FIGURE 2.3

HEXAGONAL CRYSTAL STRUCTURE OF ZIRCONIUM. TEXTURE MEASUREMENTS ON PRESSURE TUBES HAVE BEEN MAINLY CONCERNED WITH THE DISTRIBUTION OF THE BASAL PLANE POLES IN THE THREE PRINCIPAL DIRECTIONS OF THE PRESSURE TUBE

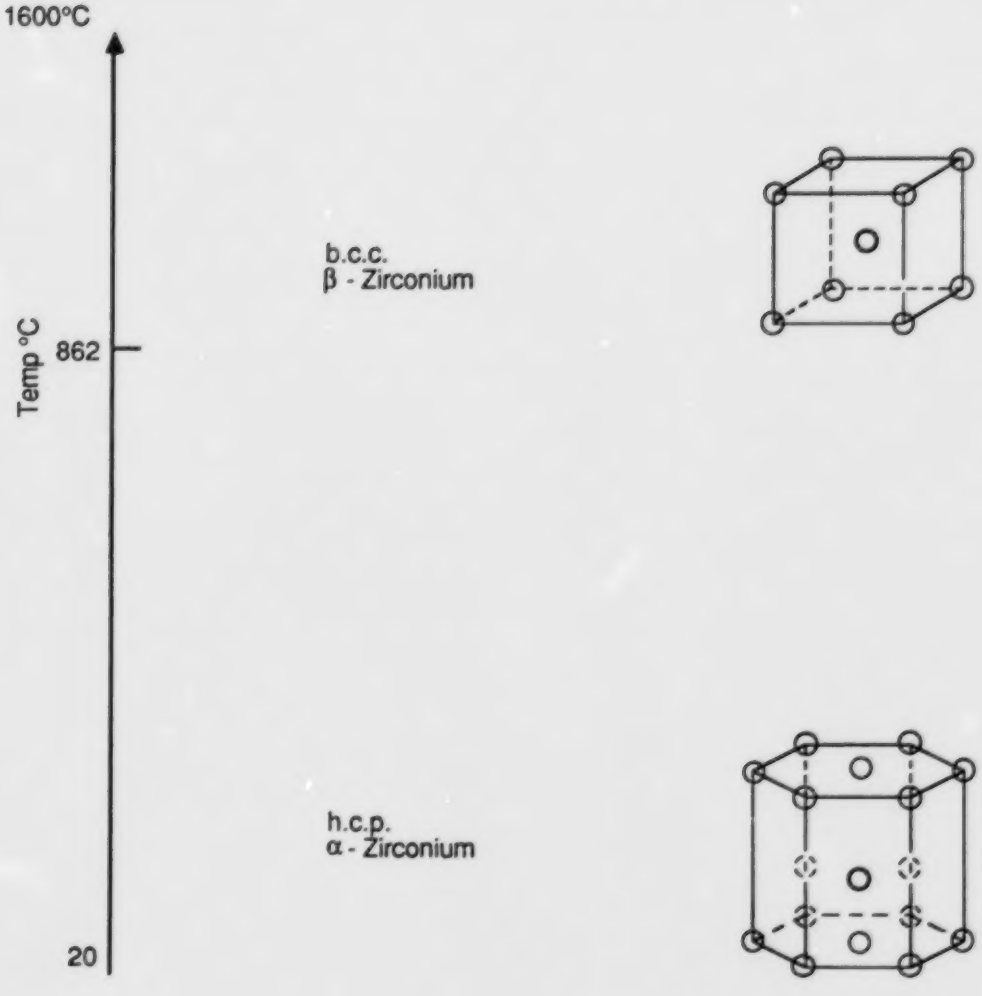

FIGURE 2.4

ILLUSTRATION OF THE TRANSITION TEMPERATURE FOR ZIRCONIUM WHERE THE CRYSTAL STRUCTURE CHANGES FROM HEXAGONAL CLOSE PACKED TO BODY CENTERED CUBIC

FIGURE 2.5

THE RESULT OF DISLOCATION MOTION THROUGH A CRYSTAL LATTICE IS DEFORMATION OF THE LATTICE

FLECK 9
CAZ-4

FIGURE 2.6

TRANSMISSION ELECTRON MICROGRAPH (MAG 33,000 X) OF ANNEALED Zr-2.5 wt % Nb SHOWING GRAINS OF ALPHA ZIRCONIUM (A) AND GRAIN BOUNDARIES (B) (V Perovic OHRD)

Zirconium has a high affinity for hydrogen and the Zr-H phase diagram is presented in Figure 2.7. The solubility of hydrogen in zirconium is very low and as a result the precipitation of zirconium hydrides ($ZrH_{1.5}$) occurs when hydrogen is absorbed by the zirconium. As the temperature is increased the solubility of the hydrogen increases such that at CANDU operating temperatures hydrides will not be present until the hydrogen concentration is in the range of 30 - 60 ppm by weight (Figure 2.8).

3.0 ZIRCONIUM EXTRACTION AND ALLOY PRODUCTION

Zirconium occurs most abundantly as the mineral Zircon which has the composition $ZrO_2.SiO_2$. In the extraction of the zirconium, for nuclear applications, it is important to remove the impurity hafnium. Zirconium and hafnium have similar chemical properties and the difficulty of their separation is not unlike that encountered in the separation of two isotopes of the same element. The removal of hafnium is important as its' thermal neutron capture cross-section is almost three orders of magnitude higher than that of zirconium.

The most common process used to extract zirconium is the Kroll process. This depends on the formation of a zirconium chloride which is then reduced by magnesium to produce a high purity metal known as sponge zirconium. An outline of the Kroll process is presented in Figure 3.1 and each step is discussed as follows:

1. **Ore Dressing**. At this stage the ore is concentrated by the removal of unwanted material which is associated with the removal of the ore from the ground. Flotation, magnetic and electrostatic techniques are used to concentrate the $ZrO_2.SiO_2$. No hafnium is removed at this stage.

2. **Ball Milling**. The ore is mixed with coke at this stage.

3. **Sand Chlorination**. A fluidized bed technique is used in which the ore and carbon are chlorinated in an endothermic reaction, see below, which is performed at temperatures in excess of 1150°C.

$$ZrO_2.SiO_2 + 2C + 4Cl_2 \text{ ------> } ZrCl_4 + SiCl_4 + 2CO_2$$

   The hafnium impurity is also converted to the tetrachloride at this stage.

4. **Feed Makeup**. The zirconium and hafnium tetrachlorides are mixed with water and all solid particles are filtered out.

5. **Separation System**. Liquid extraction columns are used to remove the hafnium. The process uses methylisobutyl ketone (MIBK) as a solvent which extracts the hafnium from the feed solution. The feed solution is a mixture of the zirconium and hafnium tetrachlorides, ammonium hydroxide and ammonium thiocyanate.

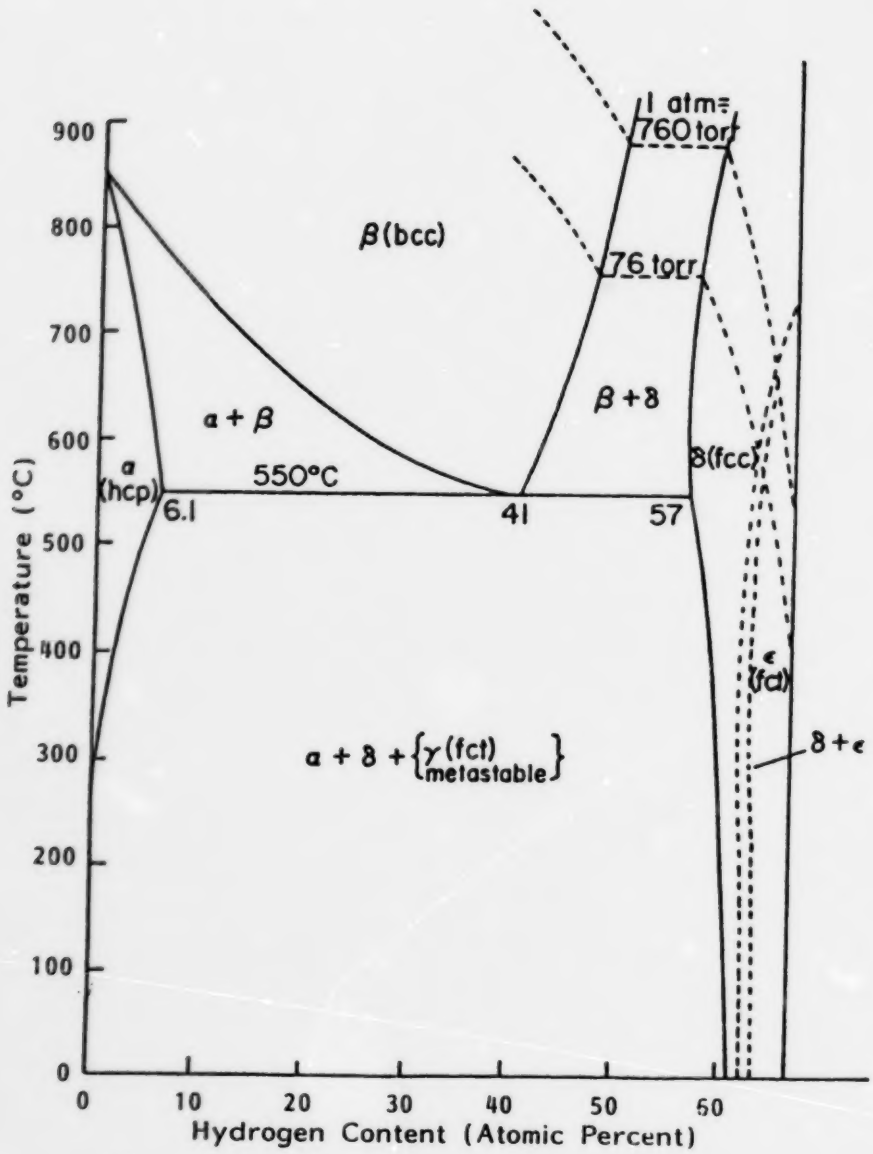

FIGURE 2.7

PHASE DIAGRAM FOR THE ZIRCONIUM-HYDROGEN SYSTEM

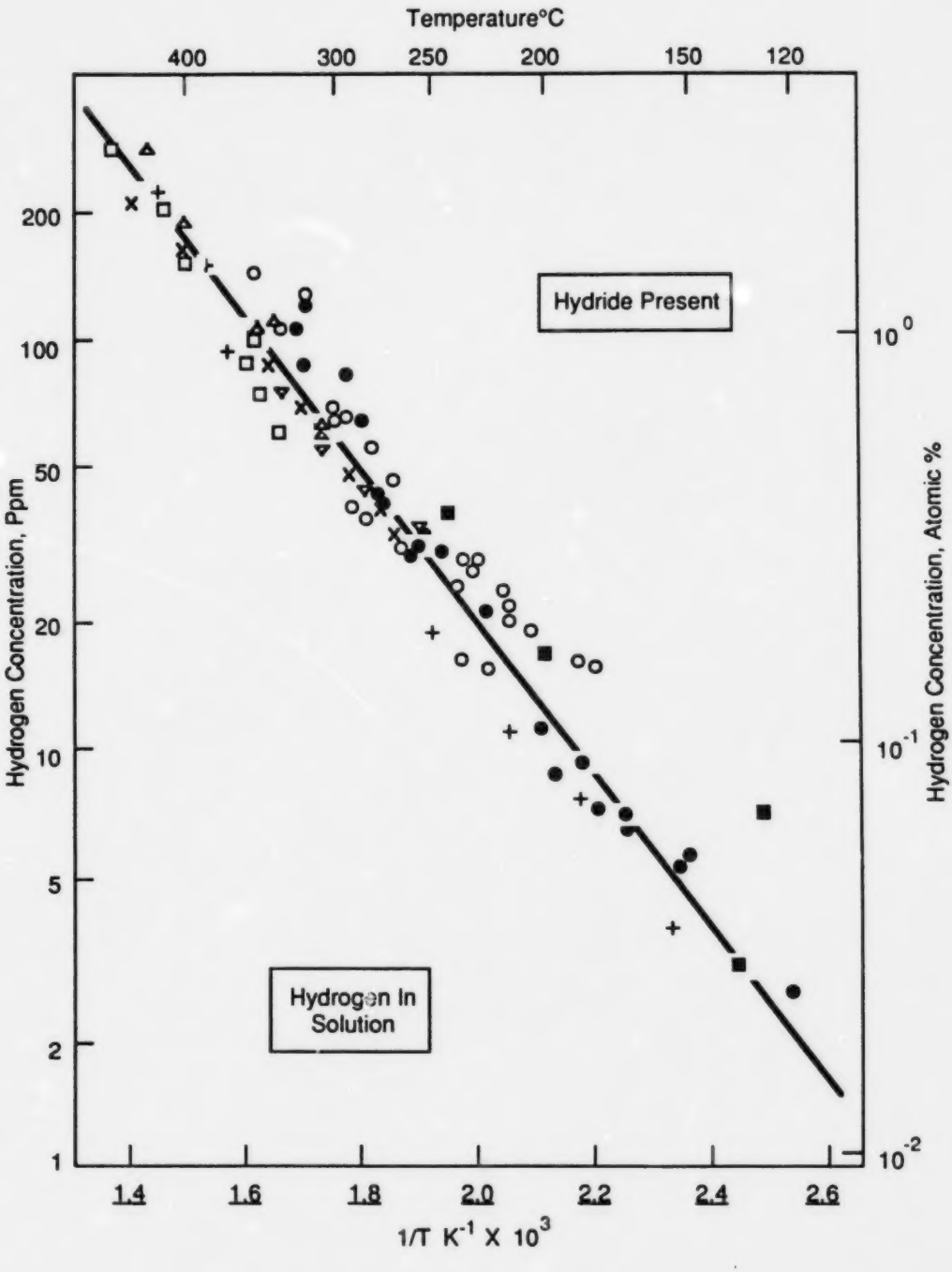

FIGURE 2.8

SUMMARY OF TERMINAL SOLUBILITY OF HYDROGEN ISOTOPES IN COLD-WORKED Zr-2.5 WT % Nb

(The various data points relate to studies by different researchers)

89-271
Fleck 11-A13

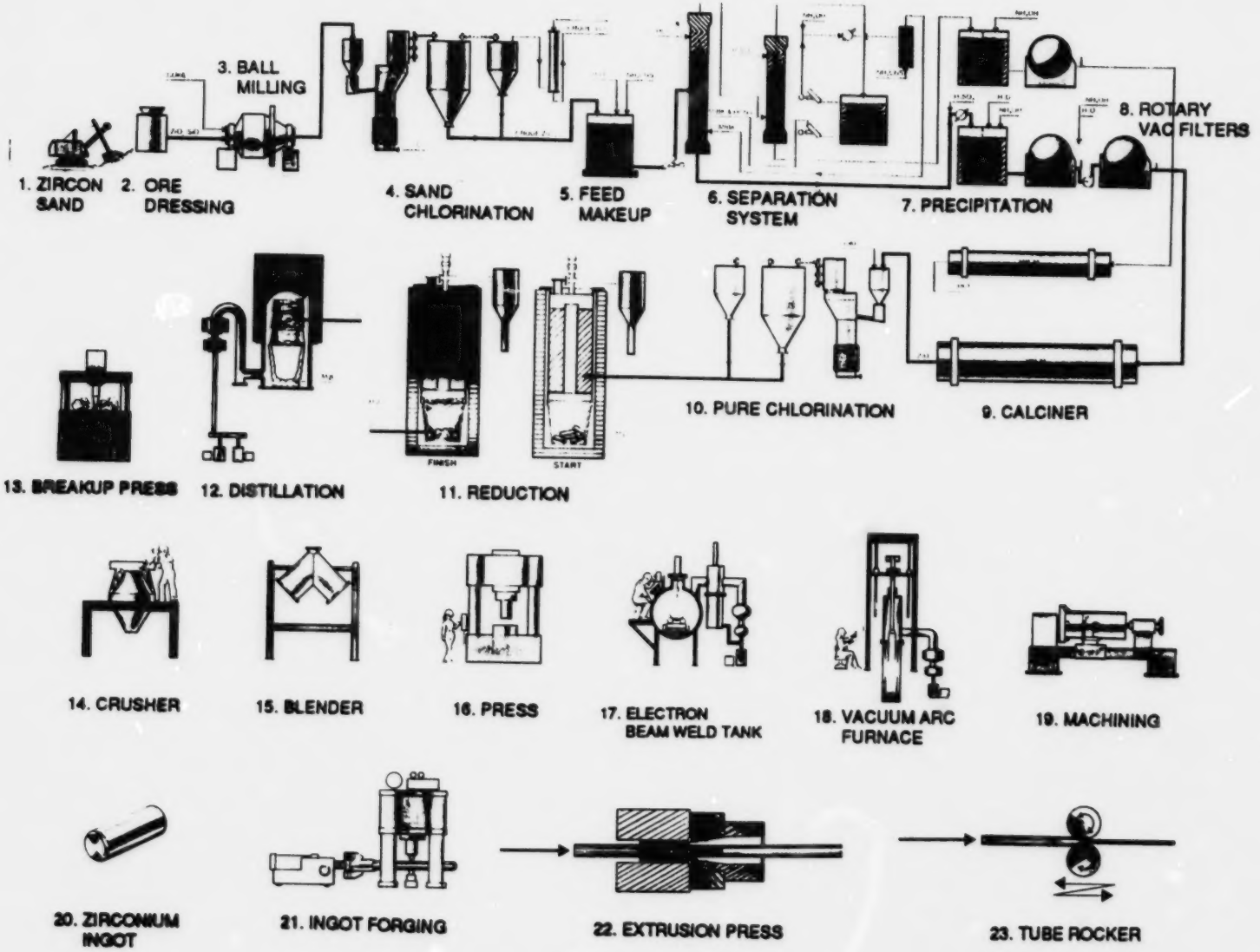

FIGURE 3.1

FLOW DIAGRAM FOR THE PRODUCTION OF ZIRCONIUM AND ZIRCONIUM ALLOYS

6. **Hafnium Extraction**. The MIBK solvent from the separation system enters scrubbing columns where it is exposed to a counter-current of sulphuric acid. The hafnium and other metal impurities such as boron and titanium are scrubbed into the sulphuric acid solution.

7. **Precipitation**. The zirconium rich liquid is diluted and reacted with sulphuric acid to precipitate zirconium sulphate:

$$ZrCl_4 + H_2SO_4 \text{ -------> } Zr(SO_4) + HCl$$

The sulphate is then reacted with ammonia:

$$Zr(SO_4) + NH_4OH \text{ --------> } Zr(OH)_4$$

8. **Calciner**. The zirconium hydroxide is now heated to produce the oxide:

$$Zr(OH)_4 \text{ ---------> } ZrO_2 + 2H_2O$$

9. **Pure Chlorination**. In this process a repeat of step 4 takes place except the zirconium is now free of the hafnium:

$$ZrO_2 + C + 2Cl_2 \text{ ------------> } ZrCl_4 + CO_2$$

10. **Reduction**. The zirconium chloride is now reduced by magnesium in an inert atmosphere. The major problem with this process is that the zirconium tetrachloride is a solid at room temperature and sublimes at 331°C. Liquid tetrachloride can only be obtained under pressure. The reduction is performed by bringing gaseous tetrachloride into contact with the magnesium:

$$ZrCl_4 + Mg \text{ ---------> } 2MgCl_2 + Zr$$

11. **Distillation**. This process separates the magnesium chloride from the zirconium. A vertical vacuum furnace is used where the top region is at 950°C and the bottom zone is cooler. The magnesium melts in the upper zone of the furnace and falls to the lower zone. When the process is complete helium is used to accelerate the cooling of the furnace. The product is sponge zirconium.

The Kroll process is a batch process and to increase the capacity of an extraction plant more reduction and distillation furnaces would have to be added.

Zirconium is also produced by the Van Arkel process which depends on the decomposition of zirconium iodide when exposed to a hot filament. The process is expensive and does not lend itself to the production of large quantities of zirconium. However, the zirconium produced by this process has a higher purity than zirconium extracted by the Kroll process, especially in terms of oxygen and nitrogen.

For pressure tube manufacture the alloy Zr-2.5 wt% Nb has to be produced to the desired chemical specifications. The sponge zirconium production controls some of the impurities. For example the iron concentration depends on the iron impurity level in the magnesium used in the reduction process. The oxygen concentration is also controlled by the extraction process. For a particular chemical specification of the final ingot suitable zirconium sponge is selected.

Alloying is performed in a vacuum electric arc furnace with the alloying additions incorporated as part of the metal electrode. The metal electrode is formed by mechanically compacting sponge zirconium with a master alloy (which is 50% Zr and 50% Nb). A number of such compacts along with appropriate scrap additions are electron beam welded together to form the electrode which is about 3 m in length. A two stage vacuum arc remelt process is used to ensure a homogeneous distribution of the alloying elements in the ingot. The crucial stage in the process is towards the end of the melt. The process is known as "hottopping" and requires the power to be decreased in a controlled manner to eliminate entrapment of impurities or of shrinkage defects. To eliminate shrink defects the power decrease to the electrode towards the end of the melt sequence has to be performed slowly. This eliminates the risk of the surface freezing and leaving liquid trapped below the surface, Figure 3.2. If the hot top procedure occurs too rapidly defects can be created at depths of up to 300 mm in the ingot. These defects form when small pockets of liquid metal are trapped by the rapid reduction in size of the melt pool. Details of the melting process tend to be restricted by the producer because of commercial propriety. For pressure tubes the ingot produced is approximately 580 mm in diameter and weighs 5400 kgs. The outside surface of the ingot is cleaned by a machining operation and samples for chemical analysis are taken from a number of different locations along the length of the ingot.

4.0 TUBE PRODUCTION

A flow diagram of the pressure tube production sequence is presented in Figure 4.1 and a discussion of each step is presented below. Pressure tubes are now solely manufactured from the alloy Zr - 2.5 wt% Nb the composition of which is presented in Table 4.1 along with that of Zircaloy 2 and 4. For the earlier reactors (NPD, Douglas Point and Pickering 1 & 2) Zircaloy 2 was used for the pressure tubes. The re-tubing of Pickering 1 & 2 used the Zr - 2.5 wt% Nb alloy. The phase diagram for the Zr - Nb system is presented in Figure 4.2. The alloy is two phase as shown in the electron micrograph in Figure 4.3, where the α-zirconium grains are surrounded by a β phase. For the true equilibrium conditions the β phase is β-niobium but for the pressure tubes the β phase is mainly β-zirconium that has some degree of transformation phases present.

1. **Ingot Breakdown**. The ingot is reduced in cross section and also divided into sections (about 6) of equal length. A press forge is used to perform this operation. A number of forging stages are carried out with ingot re-heats between each stage. The initial reduction is performed at about 985°C and the subsequent reductions occur at about 900°C with

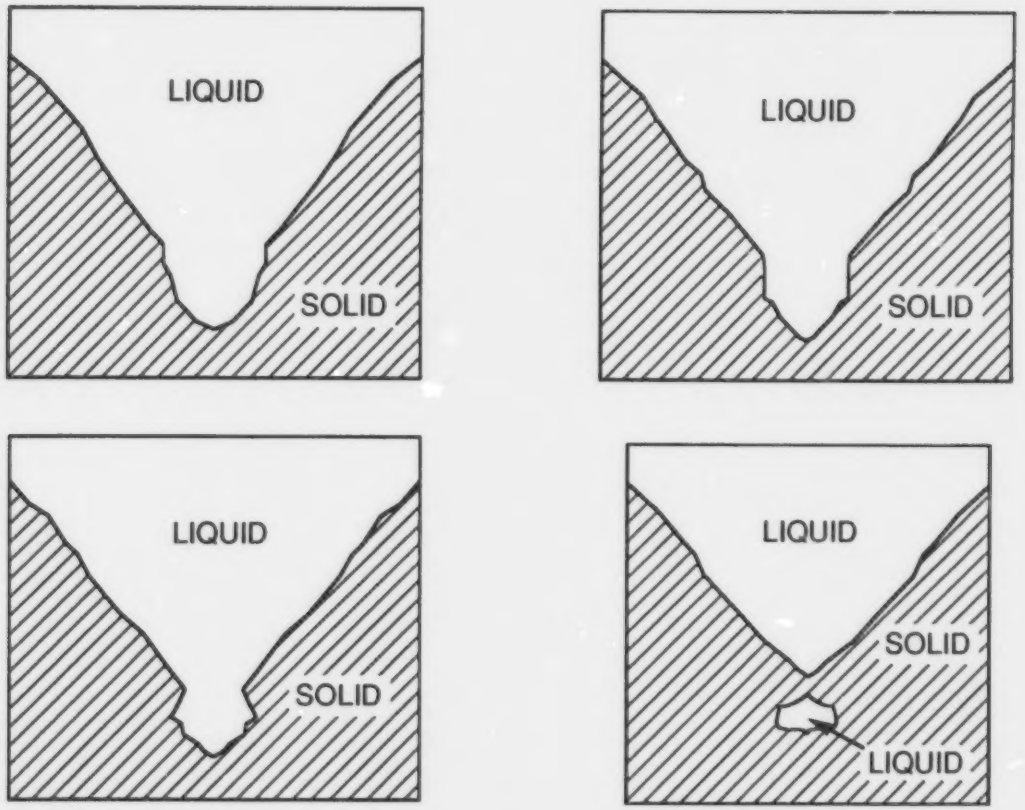

FIGURE 3.2

SCHEMATIC DIAGRAM TO ILLUSTRATE HOW INGOT DEFECTS ARE PRODUCED AS A RESULT OF A FAST (5-15 min) HOTTOP PROCEDURE. THE MOLTEN POOL IS CONSTRICTED BY HEAT LOSS IN THE RADIAL DIRECTION OF THE INGOT. THE RESULT IS THE ENCAPSULATION OF LIQUID METAL WHICH EVENTUALLY SOLIDIFIES AND RESULTS IN A SHRINK CAVITY

89-271
FLECK-24
CAZ-4

FIGURE 4.1

PRESENT FABRICATION ROUTE FOR Zr - 2-1/2% Nb PRESSURE TUBES

1	ORE	SOURCES OF ORE: AUSTRALIA
2	EXTRACTION	CARRIED OUT BY WAH CHANG
3	ALLOYING	CARRIED OUT BY WAH CHANG SPECIFICATIONS:Nb:2.4 - 2.8 wt% OXYGEN 900 - 1300 ppm. RECYCLED MATERIAL ALSO USED
4	INGOT	DIMENSIONS 5400 kg, 580 mm DIA.
5	FORGE	DIMENSIONS 584 mm , TEMPERATURE: 985°C
6	CUT INTO SECTIONS	NUMBER OF SECTIONS - 3
7	RE-HEAT	NUMBER OF SECTIONS - 2
8	FORGE	DIMENSIONS 380 mm , TEMPERATURE: 900°C
9	FORGE	DIMENSIONS 254 mm HEXAGON, TEMPERATURE: 900°C
10	RE-HEAT	TEMPERATURE 1010°C
11	QUENCH	
12	RE-HEAT	TEMPERATURE 8[illegible]°C
13	ROTARY FORGE	DIMENSIONS 230 mm DIAMETER LOG TEMPERATURE: 820°C
14	CUT INTO BILLETS	NUMBER OF BILLETS 30 - 40
15	MACHINE (TREPAN)	PURPOSE: PRODUCE HOLLOW BILLET.
16	RE-HEAT	TEMPERATURE 820 °C, TIME 200 - 700 min
17	EXTRUDE	RATIO ~11:1 TEMPERATURE: 820 - 860°C RATE < 8 mm/s
18	COLD DRAW	
19	COLD DRAW	TOTAL COLD REDUCTION ABOUT 25%
20	AUTOCLAVE	TEMPERATURE: 400°C TIME: 24 h ENVIRONMENT: STEAM

FLECK 0
CAZ-4
89-271

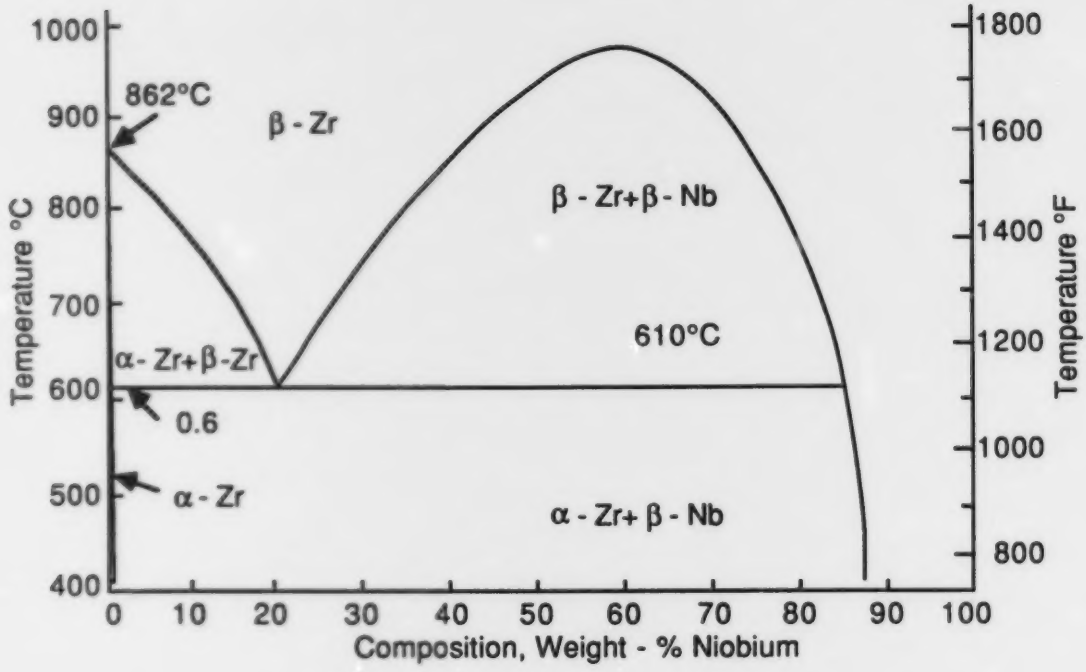

FIGURE 4.2

EQUILIBRIUM PHASE DIAGRAM FOR THE ZIRCONIUM-NIOBIUM SYSTEM

89-271
FLECK 12
CAZ-4

FIGURE 4.3

TRANSMISSION ELECTRON MICROGRAPH (MAG 47,000 X) OF Zr-2.5 wt % Nb PRESSURE TUBE MATERIAL SHOWING ALPHA GRAINS (A), BETA PHASE (B) AND DISLOCATIONS (C) (V Perovic OHRD)

TABLE 4.1

COMPOSITION OF ZIRCONIUM ALLOYS, ZIRCALOY 2 AND 4 AND Zr - 2.5 wt% Nb

	ZIRCALOY 2	ZIRCALOY 4	Zr-2.5 wt% Nb
Tin (wt%)	1.2 - 1.7	1.2 - 1.7	
Iron (wt%)	0.07 - 0.2	0.18 - 0.24	
Chronium (wt%)	0.05 - 0.15	0.07 - 0.13	
Nickel (wt%)	0.03 - 0.08		
Niobium (wt%)	-	-	2.4 - 2.8
Oxygen (ppm)	1000 - 1400	1000 - 1400	900 - 1300

the re-heats performed in furnaces located about 9 m from the press. The sections produced from the ingot are referred to as forging logs which are numbered such that their position in the ingot can be determined, Figure 4.4. The forge process initially reduces the cylindrical ingot to a square cross-section (380 mm square) and in the final stage produces logs with a hexagonal cross section (254 mm).

2. **Heat Treatment**. The heat treatment is performed either on the logs after press forging or after the actual extrusion billets have been produced. The heat treatment consists of the logs, or billets, being heated to about 1010°C and then quenched in water. The purpose of the heat treatment is to improve the dimensional tolerances of the subsequent extrusion. The improved extrusion properties result from the more uniform grain structure, Figure 4.5.

3. **Billet Production**. The hexagonal logs are rotary forged at about 820°C to a 230 mm diameter. From these logs equal length billets are machined which are then trepanned to produce the hollow extrusion billets. From a given ingot about 30 billets are produced with the dimensions: 575 mm long and 200 mm OD.

4. **Extrusion**. Prior to extrusion a steel and copper clad is put on the billets. The copper is to improve the extrusion characteristics of the billet and the steel is to prevent the formation of a low melting zirconium/copper alloy. The clad billets are then placed in a movable hearth furnace at a temperature of about 820°C and the residence time of the billets in the furnace has been in the range 200-700 mins. The furnace and the extrusion press are arranged such that the transfer of the billets takes less than a minute. The billets are extruded, Figure 4.6, at a rate of about 8 mm/sec and the extrusion ratio is calculated from:

Metal cross-sectional area of billet/Metal cross-sectional area of tube.

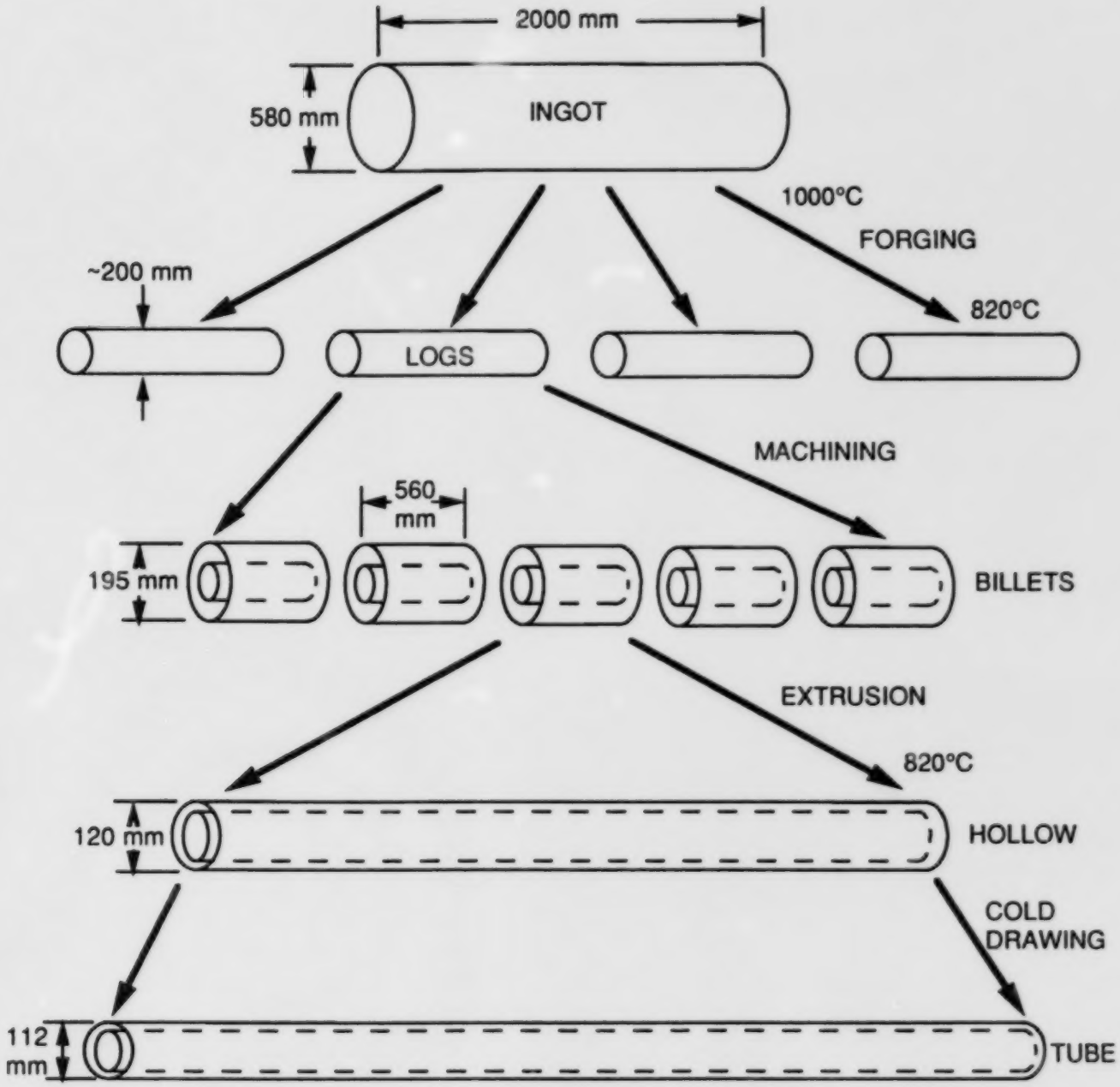

FIGURE 4.4

ILLUSTRATION OF THE BREAK DOWN SEQUENCE OF AN INGOT FOR THE PRODUCTION OF PRESSURE TUBES. WITH THE USE OF A SEQUENTIAL NUMBERING SYSTEM A PRESSURE TUBE CAN BE TRACED BACK TO A SPECIFIC POSITION IN A LOG.

FLECK-14
CAZ-4

89-271

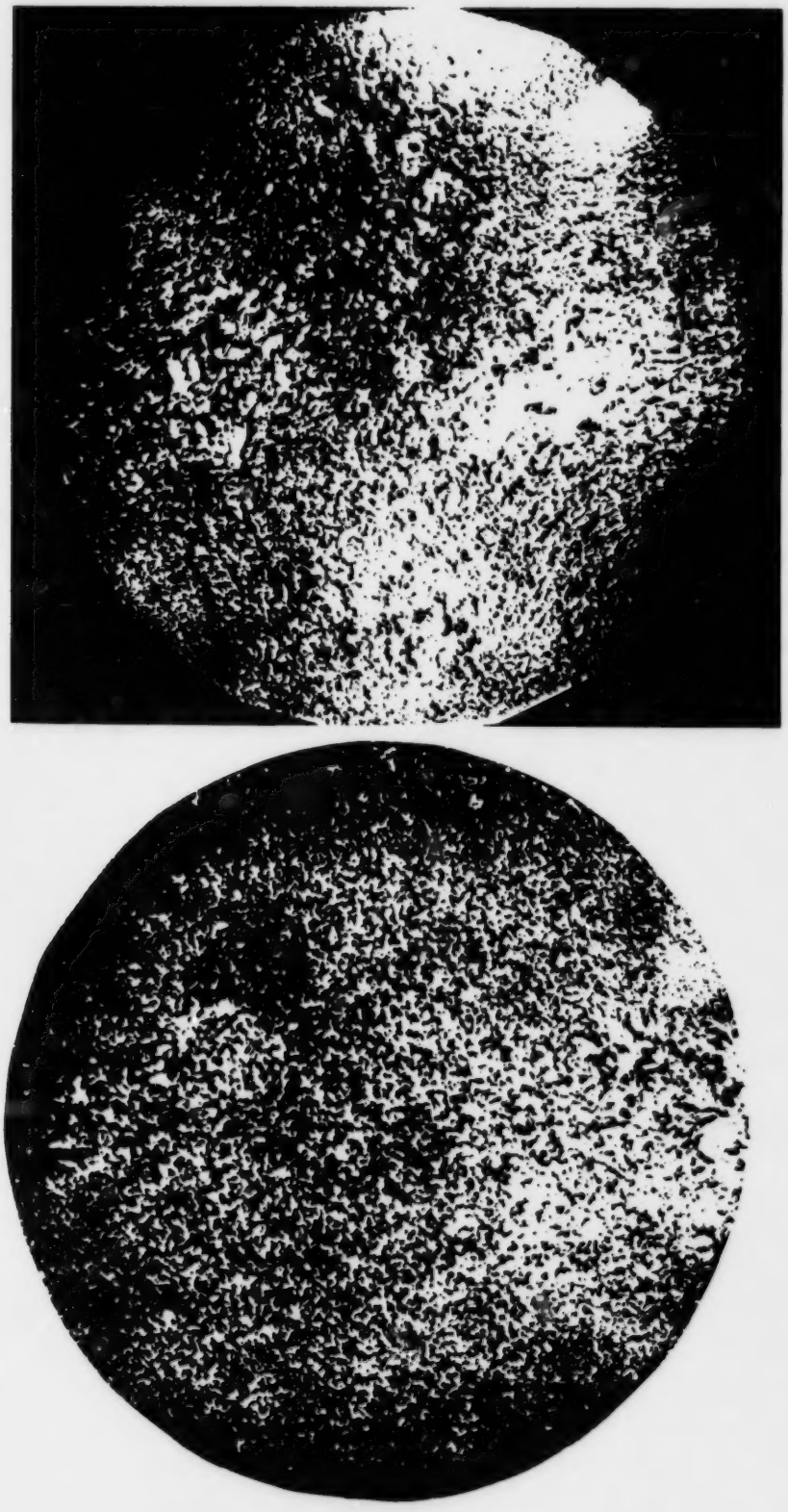

FIGURE 4.5

(A) AND (B) ARE RESPECTIVELY MICROSTRUCTURES FROM A FORGED AND AIR COOLED AND A BETA - QUENCHED Zr-2.5% Nb FORGED BAR (x 0.6). ABOVE MICROGRAPHS ARE FROM CHEADLE IN ZIRCONIUM IN THE NUCLEAR INDUSTRY. ASTM, STP 633, 1977

The as-extruded tube is about 5.8 m long with an outside diameter of 119 mm and a wall thickness of 6 mm. From the above relationship the extrusion ratio is calculated to be about 10.5:1 which is generally rounded up to 11:1.

5. **Cold Reduction**. The as-extruded tube shells are cold reduced to the final tube dimensions. The cold reduction is performed by a plug drawing process, illustrated in Figure 4.7. Prior to drawing the tubes are pickled in order that a conversion coating can be applied. The conversion coating is required to ensure the lubricant sticks to the tube for the drawing process. A two pass cold draw is used to give a wall reduction in the range 25-30%. Each cold draw pass takes about 20 mins to complete.

6. **Final Heat Treatment**. After the cold reduction process the tubes are given a final heat treatment. This process is performed in steam at 400°C for 24 h which stress relieves the tube and also develops a protective oxide layer on the tube.

The above describes the main processes in the production of pressure tubes which will influence their metallurgical structure and hence their in-service performance. No attempt has been made to discuss the various processes for surface finishing and dimensional corrections. Also the quality assurance procedures to ensure tubes are defect free have not been presented. Processes 1 - 3 are performed by Teledyne Wah Chang, Albany, Oregon, USA and all other processes are performed by NuTech Precision Metals (formerly Chase Nuclear) at their plants in Waterbury, Connecticut, USA and Arnprior, Ontario, Canada.

The metallurgical structure of tubes produced by the above process is described in terms of the crystallographic texture, the grain shape and the dislocation density. The preferred orientation of the grains in the tube is such that the basal poles are near the transverse direction, Figures 4.8 (a) and (b), which is referred to as a transverse texture. The grains are elongated in the axial direction and the dislocation density is high with the dislocations arranged in tangles as a result of the cold work process.

Quality assurance procedures require nondestructive examination (NDE) of the material at completion of various stages in the production sequences as shown in Figure 4.1. NDE is performed on the ingot, the billet and the tube in the cold-worked condition and in the autoclaved condition. There is also an inspection of the tube after it is installed in a reactor. The total rejection rate in tube production is about 7% which comprises 3.5% at ingot/billet stage and a further 3.5% at the extrusion/cold drawing stage. Table 4.2 outlines the types of defects that can occur at the various processes in tube production. In practice the quality assurance procedures have resulted in a very low incidence of pressure tube with defects being put into service. In total, four installed pressure tubes have been found to

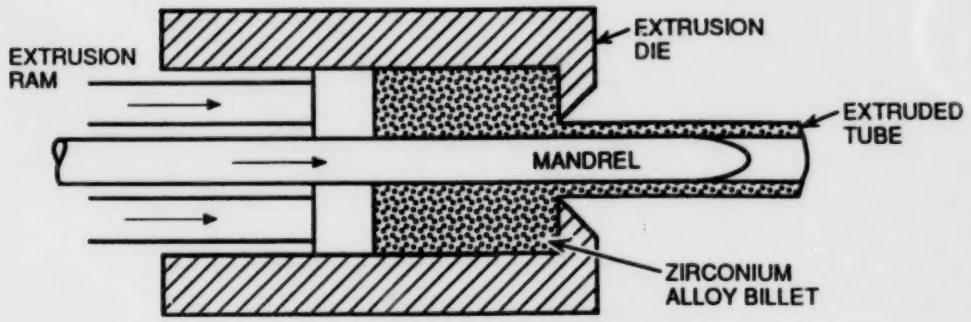

FIGURE 4.6
EXTRUSION PROCESS

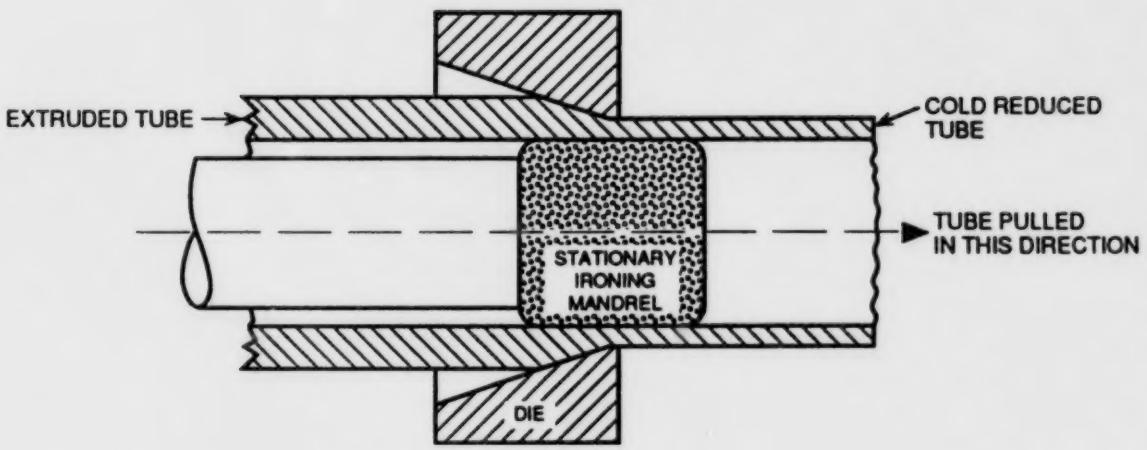

FIGURE 4.7
SCHEMATIC OF PLUG DRAWING PROCESS

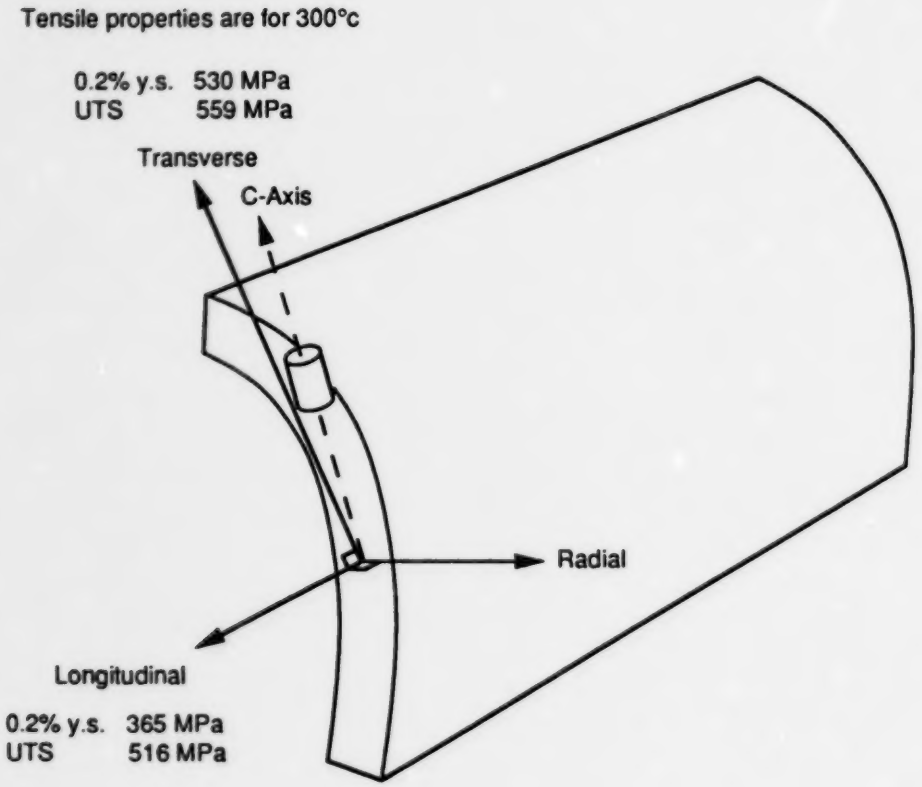

FIGURE 4.8 (a)

SCHEMATIC REPRESENTATION OF THE PREFERRED ORIENTATION OF C-AXIS (BASAL POLES) OF ZIRCONIUM CRYSTALS (GRAINS) IN PRESENT CANDU PRESSURE TUBES. THE FRACTION OF THE BASAL POLES IN THE THREE PRINCIPAL DIRECTIONS ARE DETERMINED

F_T - FRACTION OF BASAL POLES IN TRANSVERSE DIRECTION -0.62

F_R - FRACTION OF BASAL POLES IN RADIAL DIRECTION -0.35

F_L - FRACTION OF BASAL POLES IN LONGITUDINAL DIRECTION -0.03

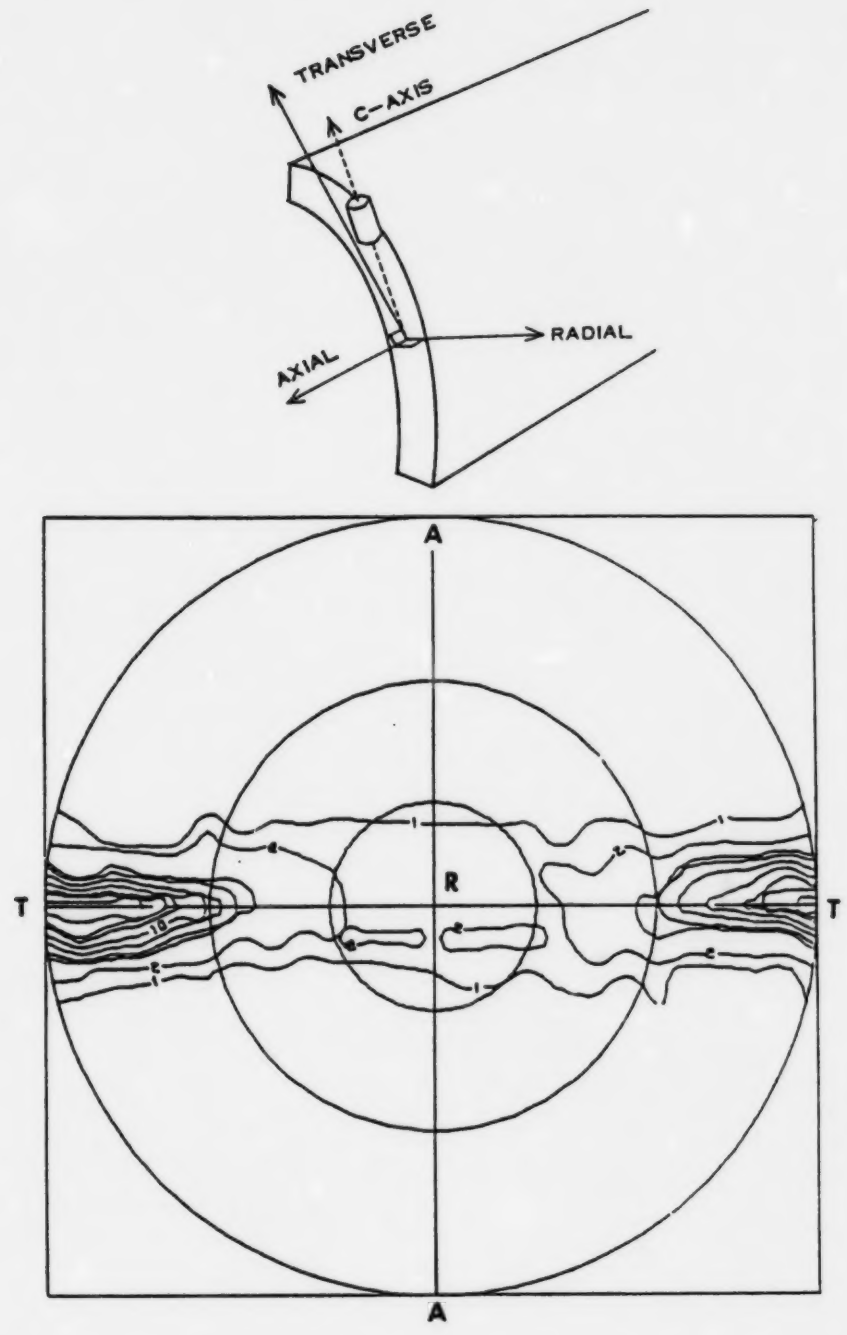

FIGURE 4.8 (b)

SCHEMATIC REPRESENTATION OF BASAL POLES ORIENTED IN THE TRANSVERSE DIRECTION OF A PRESSURE TUBE AND TYPICAL BASAL POLE FIGURE FOR SUCH A TEXTURE

contain manufacturing defects, two of these tubes were removed prior to reactor start-up and the other two resulted in pressure tube leaks. Examination of the defects revealed them to be in the range 100-460 mm long, at a relatively shallow angle to the inside surface of the tube and not always open to the tube surface. Metallography showed the defects to be intermittent in nature over their length (Figure 4.9). Originally the defects were thought to be a result of forging laps but subsequent evaluation indicated that they originated from the pipe defect in the ingot (see Figure 3.2).

TABLE 4.2

Types of Defects found in Tube Manufacture
(Bold Type Signifies Defects that Occur with some Frequency)
[The information in this Table comes from a presentation by E.G. Price August 27, 1986].

PROCESS	TYPE OF DEFECTS
Ingot Melting	- **Porosity** - Nitride and oxide inclusions from contaminated zirconium sponge. - **Piping defects** - Tramp elements - Unmelted alloy additions
Forging	- Surface Cracks resulting from oxide cracking. - **Folds and laps** - Internal cracks from too low a forging temperature
Extrusion	- **Non-uniformity of cross-section** - **Tearing of cladding and galling** - Folding of cladding into the tube - **Pitting**
Cold Drawing	- **Galling and cracking** - Residual lubricant - Sandblasting defects
Autoclaving	- Handling scratches and gouges

The four defected tubes installed in reactors were all found to originate from billets that came from the top of the ingot (see Figure 4.4). Examination of the records of the ingot melt procedures revealed that the hottop process (described in Section 3) had not always been performed to minimize the extent

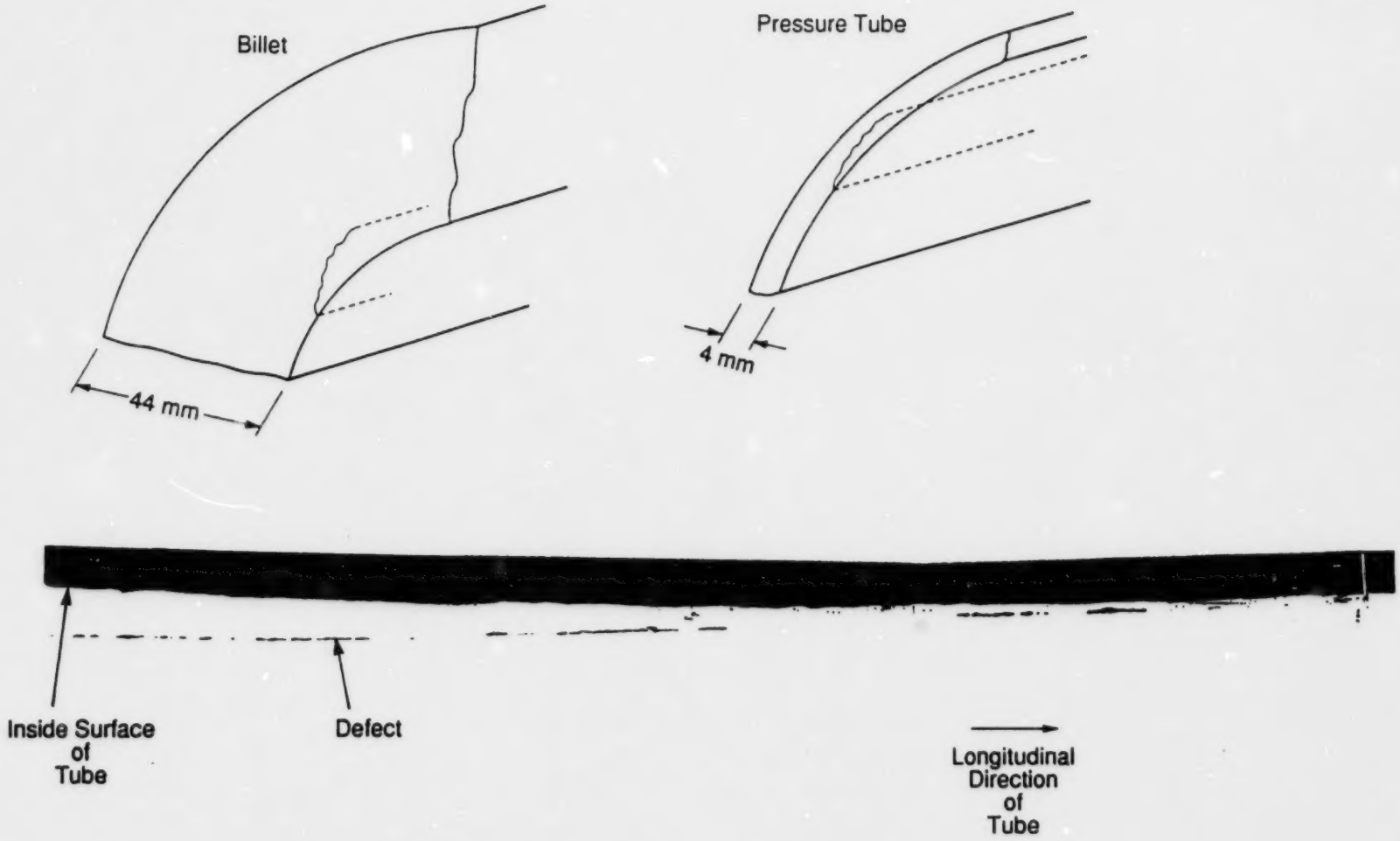

FIGURE 4.9

DEFECT IN PRESSURE TUBE AS A RESULT OF INGOT PIPE REMNANT IN TREPANNED BILLET

of the ingot shrinkage pipe. It was also revealed that the section of the ingot that contained the pipe defect had not been completely removed before forging. Subsequent trepanning of the billets would only remove remnants of the pipe defect if it was centrally located in the billet. This will not always be the real situation and part of the pipe defect could be left on the inside surface of the trepanned billet. Subsequent processing would elongate this defect and also weld the defect under the inside surface of the tube.

To eliminate further incidences of the occurrence of the above type of defects in pressure tubes, some modifications have been implemented. The hottop procedure has been improved to minimize the extent of the shrinkage pipe, the section of the ingot that contains the pipe is machined off prior to forging and an improved ultrasonic NDE technique is now used in final tube inspection which can detect flaws that lie at a shallow angle to the inside surface of the tube.

Pressure tube development programs have been performed where changes in the production process have been introduced. These changes were either to improve the in-service performance of the tubes or to develop an alternative manufacturer. For the former three alternative production routes have been investigated (Figure 4.10) whereas for the latter a pilgering (Figure 4.11(a) and (b)) process has been evaluated as an alternative to the cold drawing procedure.

Metallurgical studies on sections of Zircaloy pressure tubes manufactured by a variety of different routes indicated that the extrusion process controlled the texture. Based on these findings a development program for Zr-2.5 wt% Nb tubes was initiated. Changes were made to the production route to determine if the metallurgical structure could be modified such that the tubes would have lower elongation rates. Three production routes were proposed as shown in Figure 4.10. The extrusion ratio was decreased from 11:1 to 8.5:1 in an attempt to change the crystallographic texture from transverse towards radial. The subsequent process changes were aimed at a reduction of the dislocation density (Route 1); a development of an equiaxed grain shape (Route 2) and a combination of a low dislocation density and an equiaxed grain shape (Route 3). A total of 30 pressure tubes were made under the development program. There are three tubes manufactured from each of the three routes installed in Bruce Unit 8. Further developments of pressure tubes have considered the reduction of the extrusion ratio down to 4:1. Three billets were extruded under these conditions but on subsequent cold drawing shear cracks formed because the intermediate stress relieving temperatures were too low. Some further development of this route is on-going because if the desired texture change occurs the tubes will have a greater resistance to delayed hydride cracking than current tubes. This will be discussed later.

5.0 MECHANICAL PROPERTIES

Pressure tubes have to meet certain minimum longitudinal tensile properties for use in CANDU reactors. The specified tensile properties, measured at 300°C are:

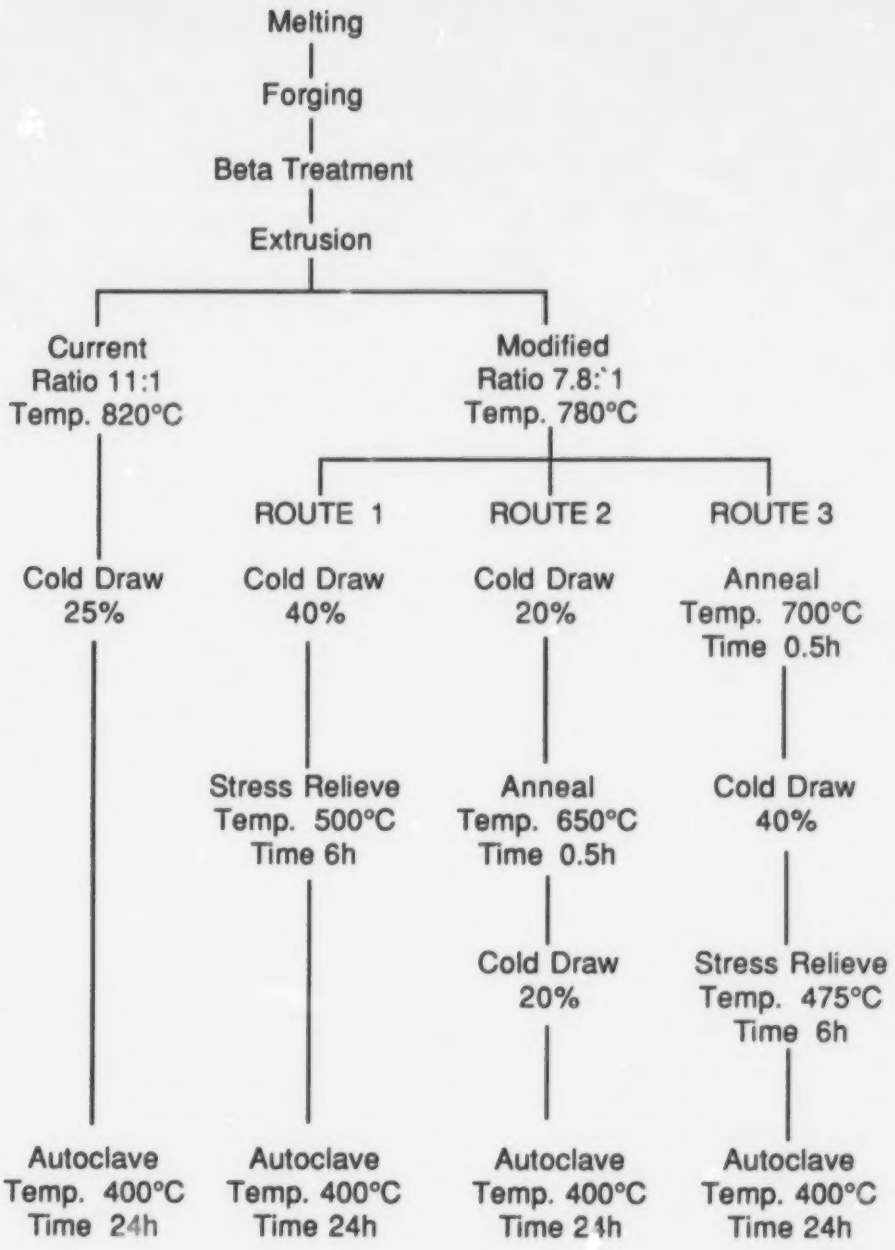

FIGURE 4.10

PRODUCTION ROUTES FOR THE FABRICATION OF COLD WORKED Zr 2.5 wt% Nb TUBES

89-271
FLECK 17
CAZ-4

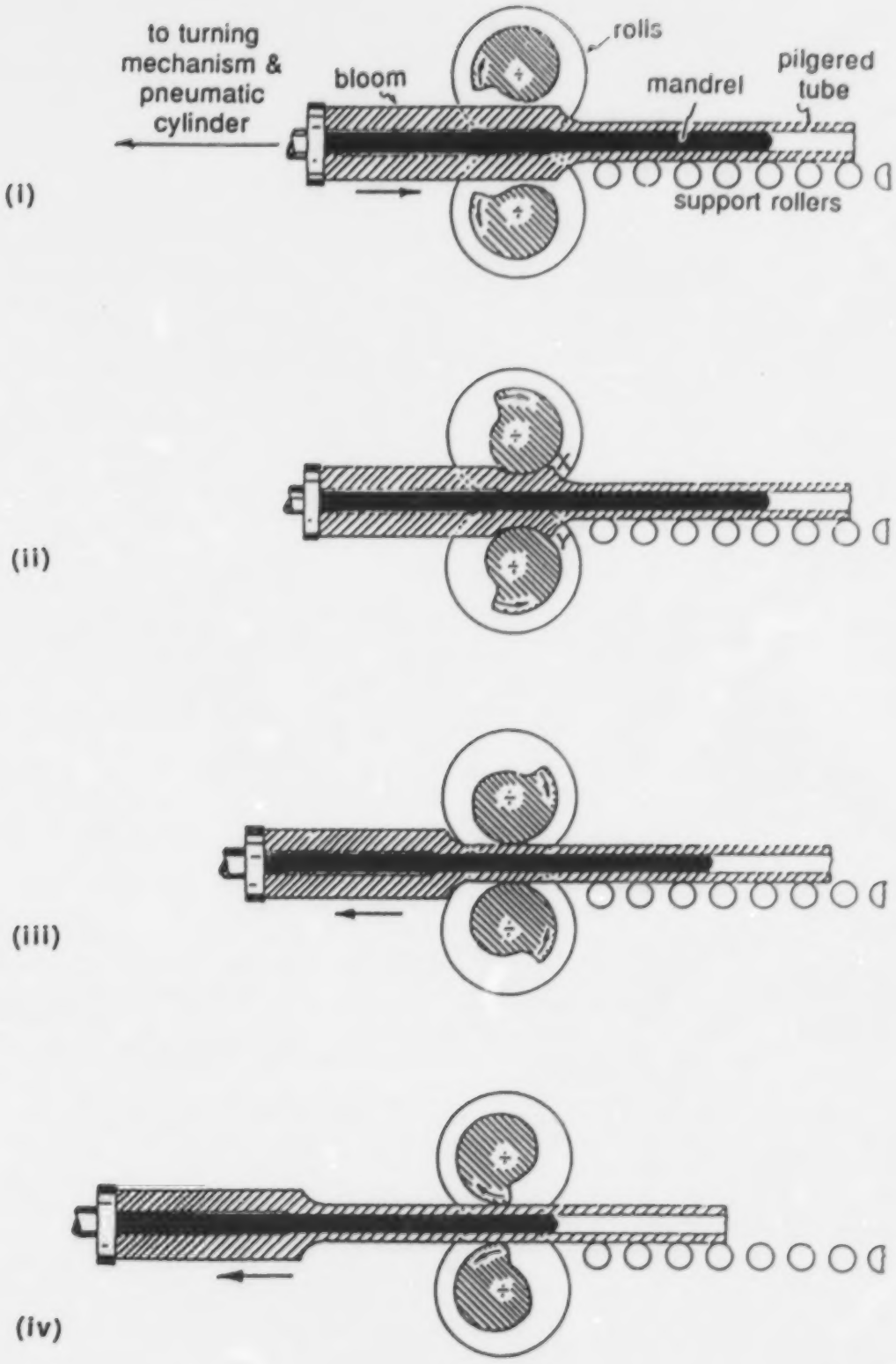

FIGURE 4.11 (a)
PRINCIPLES OF THE PILGER PROGRESS

89-271
180701-RD

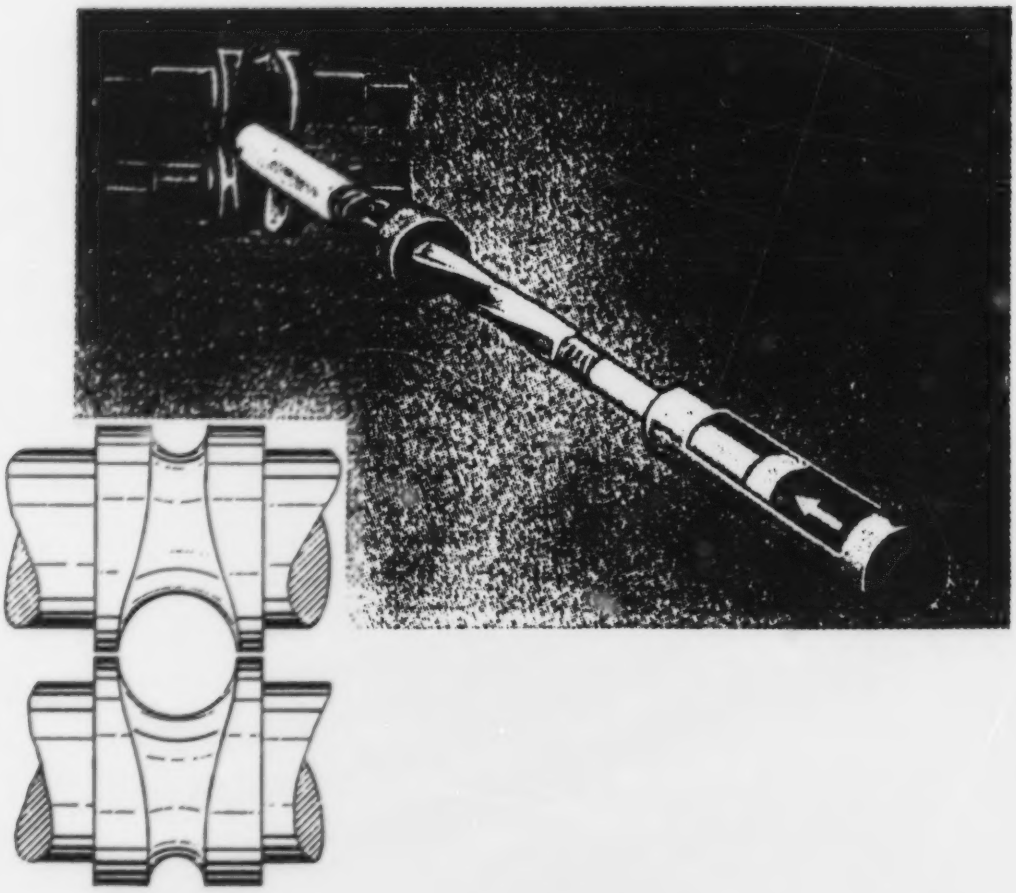

FIGURE 4.11 (b)
PILGER ROLES IN THE 'OPEN' POSITION

Ultimate Tensile Strength (UTS)	480 MPa (69 500 psi)
0.2 % Yield Strength	330 MPa (48 000 psi)
Elongation	12%

Gauge Length = 4.5 [Cross-Sectional Area]$^{0.5}$

The dimensions (in inches) of the tensile specimen used to establish the tensile properties are shown in Figure 5.1. The tests are performed in a tensile test machine at a strain rate of 0.005 mm/mm per minute.

Pressure tubes are designed to meet the intent of Section III of the ASME Boiler and Pressure Vessel Code for Nuclear Power Plant Components. The tensile strength requirements used for design purposes are 0.33 UTS or 0.66 Yield Strength, whichever is the lowest. For pressure tube alloys the UTS criteria is the lowest value.

In the production of pressure tubes the tubes after extrusion are always processed in the same direction i.e. the end of the tube that is first out of the extrusion press is also the first end out of the cold draw die. This end of the tube is referred to as the "front end". Tensile tests on specimens from the front and back ends of pressure tubes illustrate a difference in strength, the front ends tend to have the lowest tensile strengths (Table 5.1). For design purposes the tensile properties are measured on specimens from the front end. Figure 5.2 illustrates the stress/strain curves for longitudinal specimens from the back and front ends of pressure tubes.

The tensile properties of pressure tube material are also affected by the grain size. Figure 5.3 shows the grain size effect on Yield Stress, where the grain dimension measured was the width in the radial direction in the radial/axial plane. As the grain size is reduced the Yield Stress is increased. The grain size effect is considered to be the reason for the end-to-end variation in tensile strength. The back end will be extruded at a lower temperature than the front end due to cooling effects on the billet in the extrusion press. This effect may also result in an increase in dislocation density which would also increase the tensile strength.

TABLE 5.1

TENSILE PROPERTIES OF FRONT (F)
AND BACK (B) ENDS OF PRESSURE TUBES AT 300°C

PRESSURE TUBE ID	0.2% YS (MPa)	UTS (MPa)
TG016F	327 ± 11	476 ± 4
TG016B	355 ± 10	490 ± 2
TG026F	400 ± 14	538 ± 7
TG026B	435 ± 8	586 ± 1

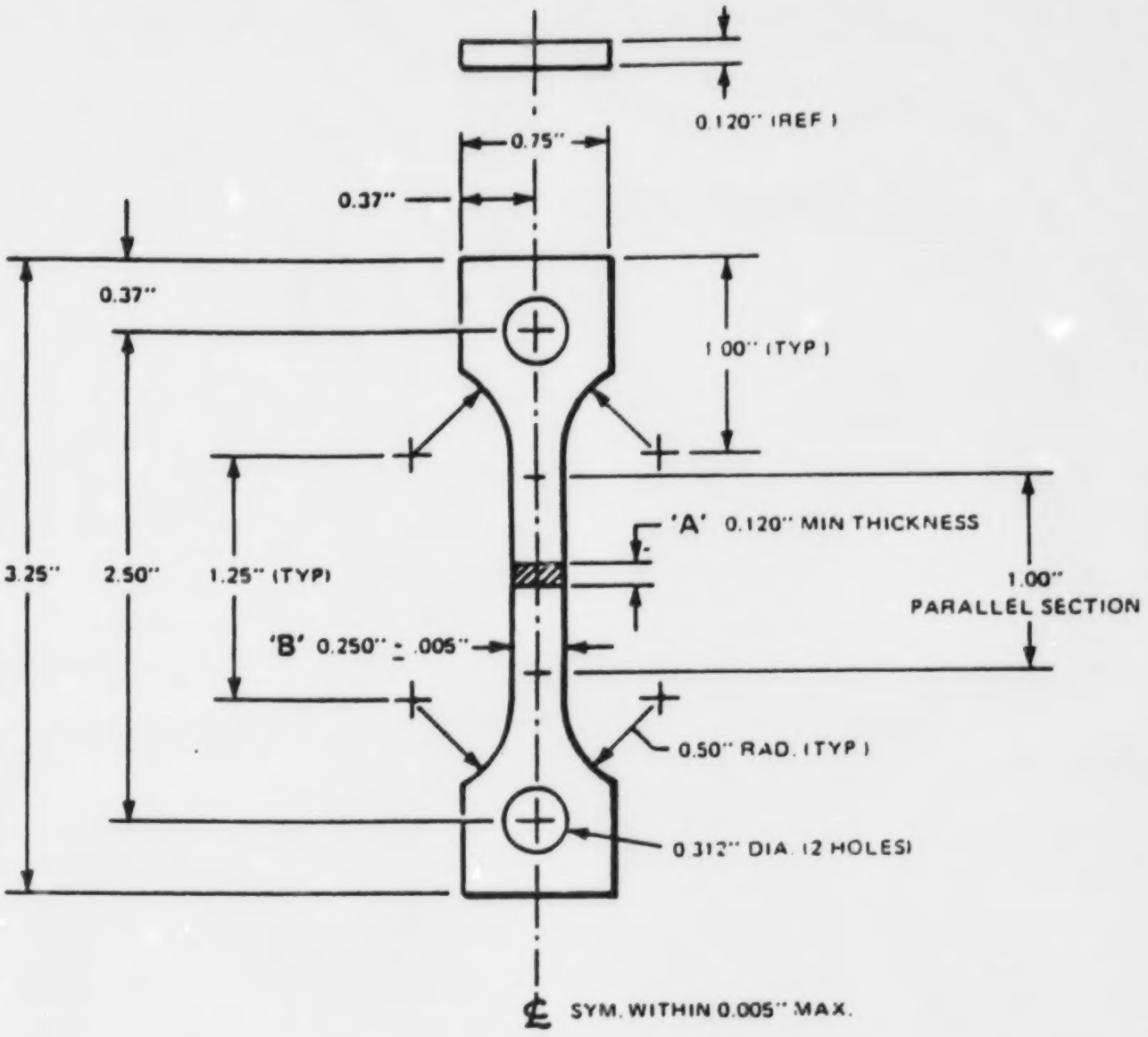

FIGURE 5.1

SCHEMATIC DIAGRAM OF THE TENSILE SPECIMEN
USED TO DETERMINE THE TENSILE PROPERTIES
TO QUALIFY PRESSURE TUBES

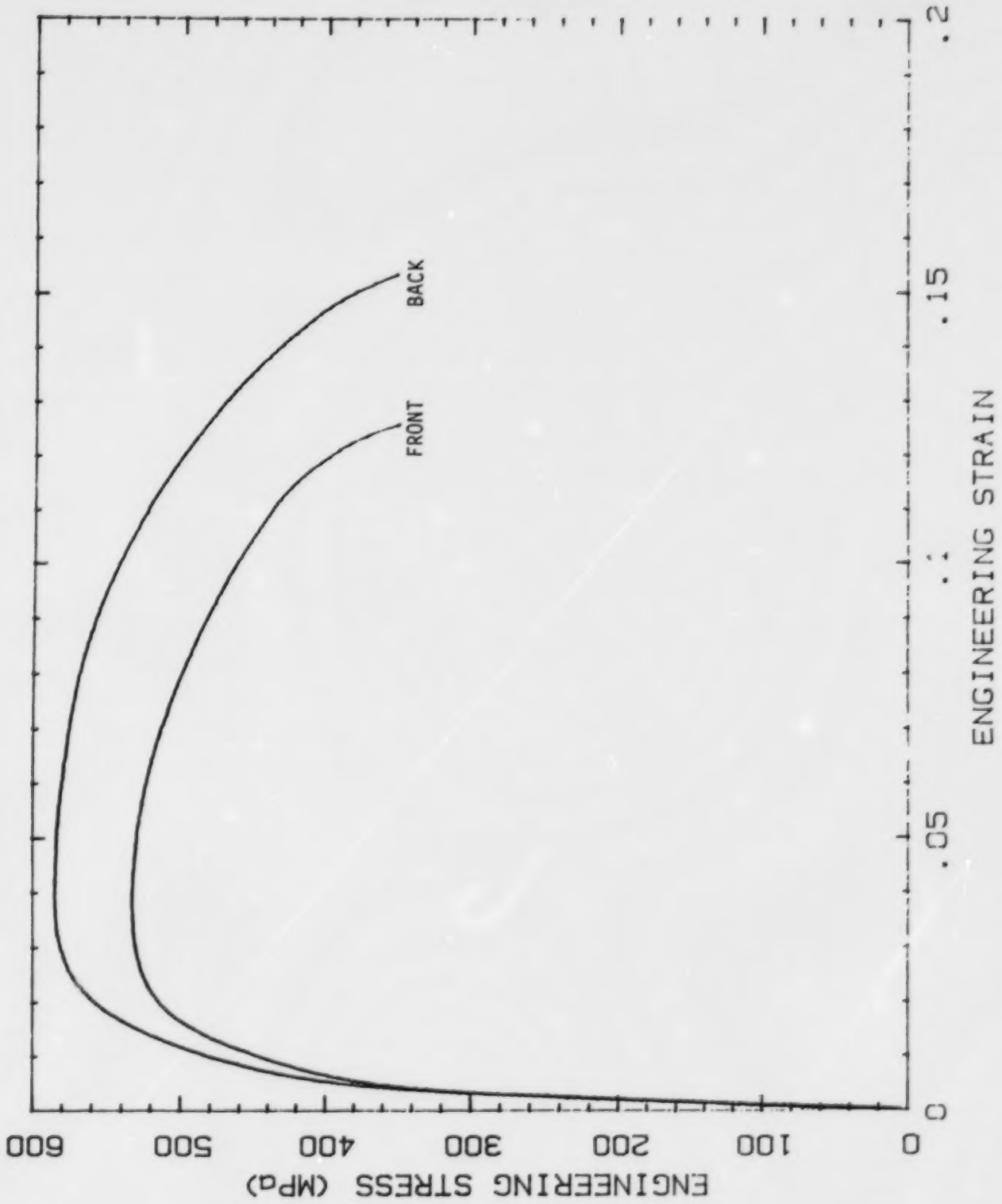

FIGURE 5.2

REPRESENTATIVE ENGINEERING STRESS VS ENGINEERING STRAIN PLOTS FOR LONGITUDINAL SPECIMENS FROM THE FRONT AND BACK ENDS OF A Zr-2.5 Nb PRESSURE TUBE (E.T.C.Ho OHRD)

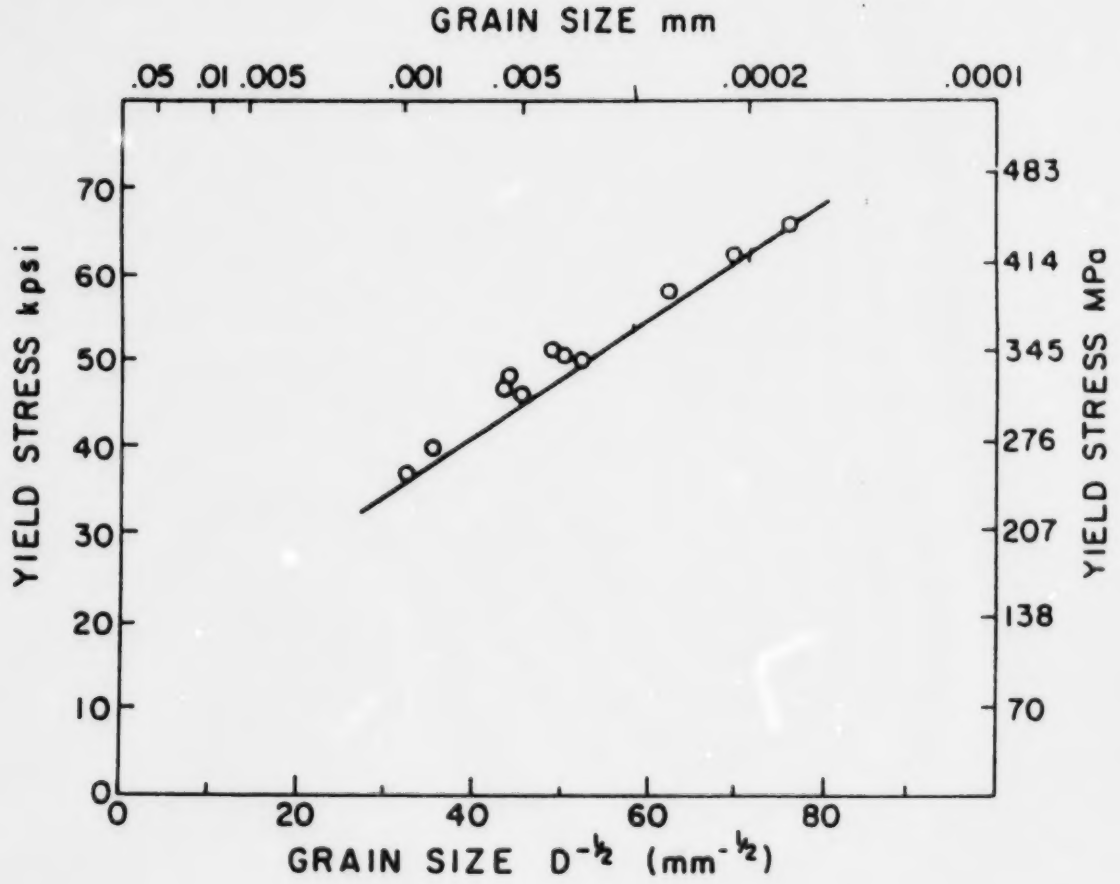

FIGURE 5.3

THE EFFECT OF GRAIN THICKNESS ON THE YIELD STRENGTH OF Zr-2.5 Nb EXTRUSIONS
(From B.A. Cheadle - Bibliography 4.0)

The anisotropy of the pressure tubes is reflected in the difference in mechanical properties in the longitudinal and transverse directions. Figure 5.4 illustrates that the transverse direction is stronger than the longitudinal direction. From Figure 2.3 it is shown that the Youngs modulus is higher in the c - direction than in the a - direction. In pressure tubes the c - direction is preferentially aligned in the transverse direction (Figure 4.8).

In the development of the pressure tubes fabrication routes, Figure 4.10, the effect of cold work and stress relieving temperature on the tensile properties was investigated. The results of UTS are presented in Figure 5.5. Only the effect of temperature above the final autoclave temperature of 400°C was considered. As the temperature is increased the UTS decreases and a similar decrease in Yield Stress occurs, as shown in Table 5.2. In general terms an increase in stress relieving temperature increases the ductility as shown by the elongation results in Table 5.3. The level of cold work is also shown to affect the tensile properties of pressure tube material, where higher levels of cold work result in higher strength.

TABLE 5.2

VARIATIONS OF 0.2% YIELD STRENGTH AND
TENSILE STRENGTH WITH STRESS RELIEVING TEMPERATURE

HEAT TREATMENT	0.2% YS (MPa)	UTS (MPa)
as cold-worked	502 ± 4	558 ± 1
450°C - 6 h	369 ± 8	518 ± 3
475°C - 6 h	366 ± 1	504 ± 1
500°C - 6 h	331 ± 6	476 ± 4

TABLE 5.3

VARIATION OF % ELONGATION WITH STRESS RELIEVING TEMPERATURE

HEAT TREATMENT	% ELONGATION (4.5 A)
as cold-worked	13.0 ± 3.5
450°C - 6 h	17.5 ± 3.4
475°C - 6 h	20.3 ± 1.8
500°C - 6 h	24.3 ± 3.1

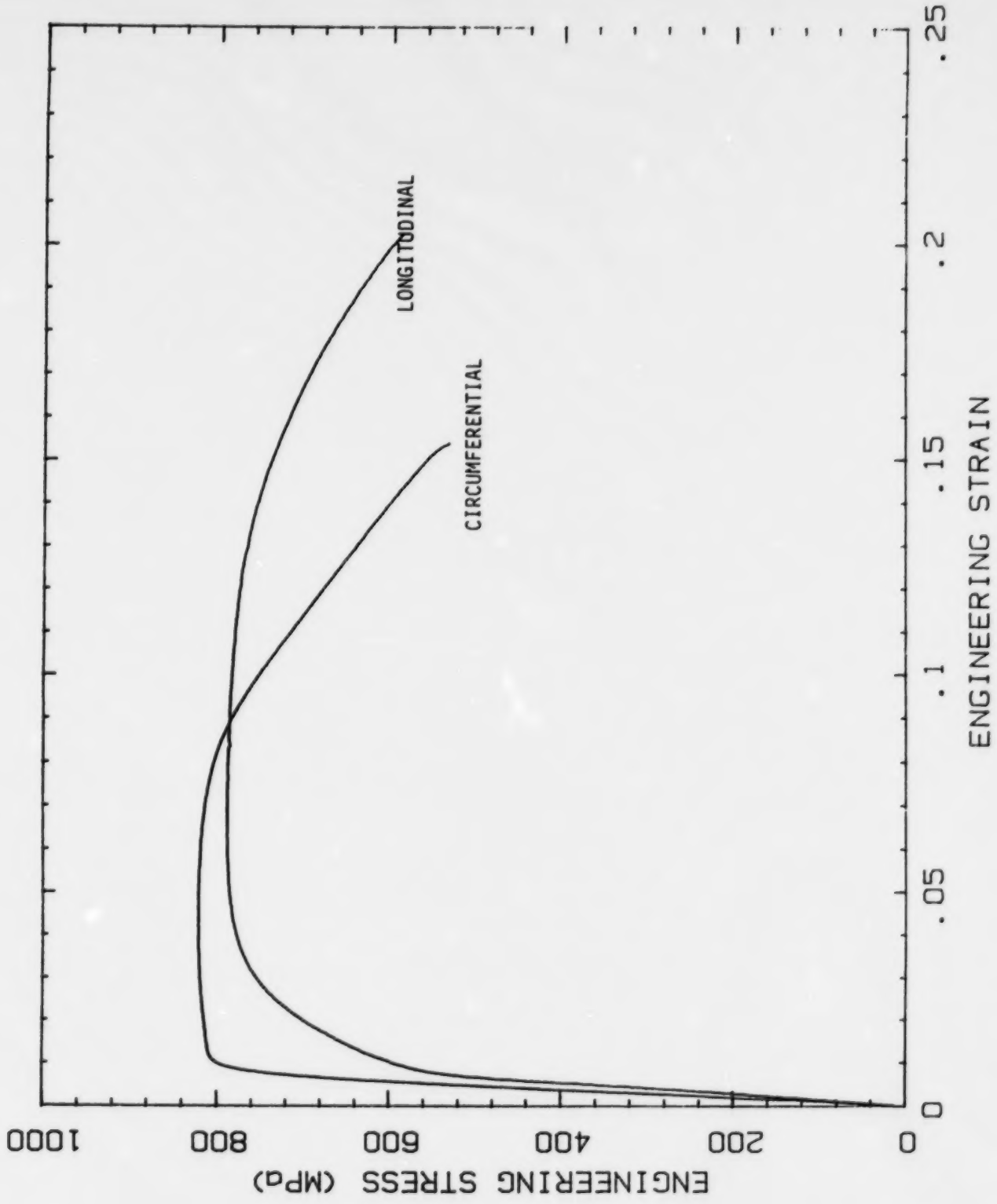

FIGURE 5.4

ENGINEERING STRESS VS ENGINEERING STRAIN PLOTS ILLUSTRATING THE LARGE DIFFERENCES IN TENSILE PROPERTIES BETWEEN LONGITUDINAL AND CIRCUMFERENTIAL SPECIMENS AT AMBIENT TEMPERATURE
(E.T.C. Ho OHRD)

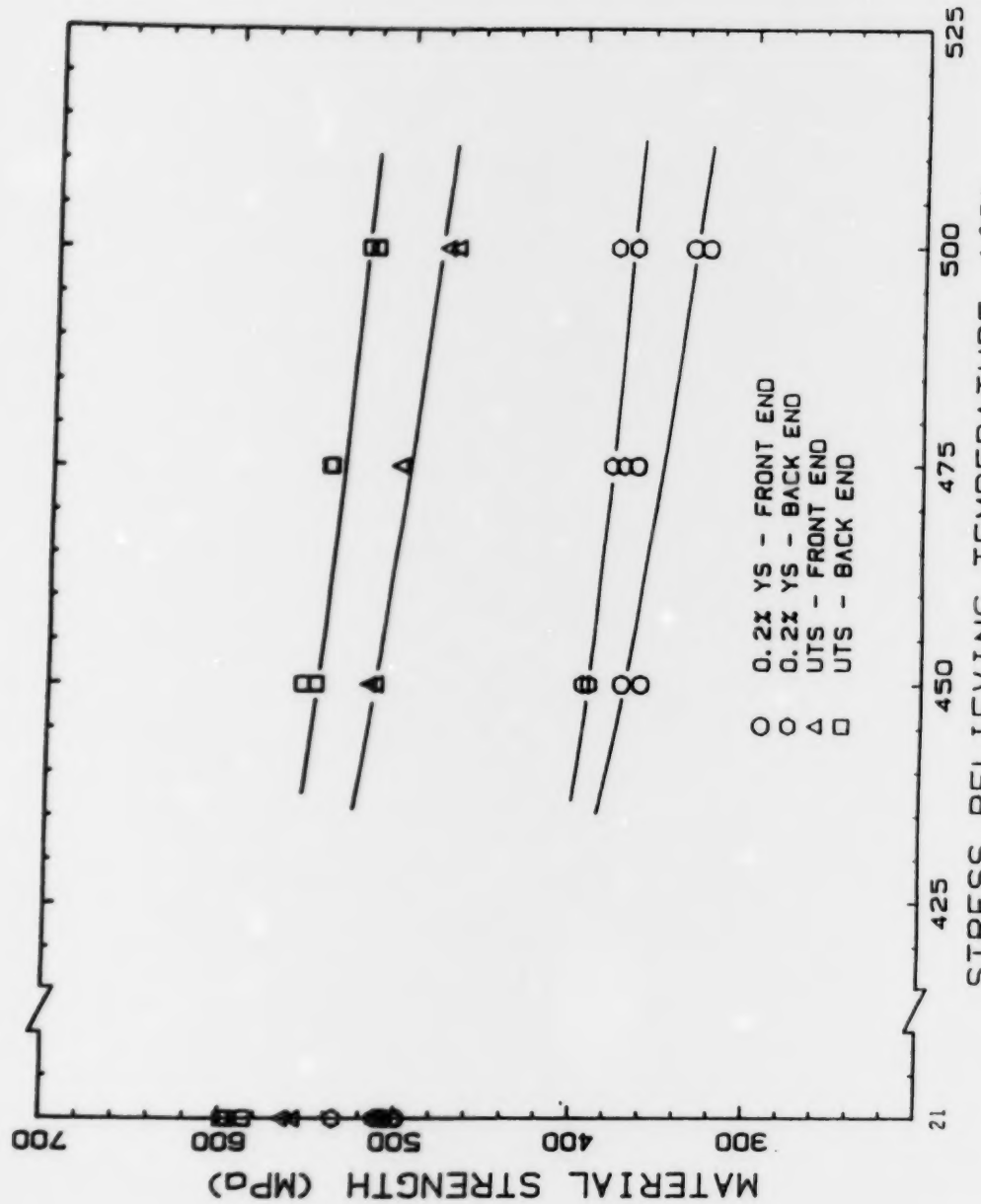

FIGURE 5.5
PLOTS ILLUSTRATING THE DECREASE IN 0.2% YIELD STRENGTH AND TENSILE STRENGTH WITH INCREASING STRESS REVIEVING TEMPERATURES (E.T.C.Ho OHRD)

Exposure of pressure tubes to neutron irradiation at 300°C results in an increase in the tensile strength and a decrease in ductility.

6.0 OPERATING EXPERIENCE

The start of the reactors at Pickering A in 1972 was the start of Ontario Hydro's experience with large (540 MW) power generating CANDU reactors. Prior to the start of Pickering experience had been gained with the NPD (25 MW) and Douglas Point (250 MW) reactors.

The initial concern with pressure tubes in Pickering were related to the deformation rates for diametral expansion and elongation. Design had allowed for about 25.4 mm of total elongation throughout the 30 year life of the reactor. However, elongation rates of about 4 mm/year were measured on the reactors. There were also indications of a tube-to-tube variation in the elongation rates (+/- 25%) that would eventually result in interaction between adjacent feeder pipes.

Deformation concerns were overshadowed by cracks in pressure tubes in the rolled joint region. The cracks occurred in Pickering Units 3 & 4 in 1974-75. Extensive investigation and tube replacement were carried out at this time and the reason for the cracks was determined to be delayed hydride cracking (DHC). The basic reason why the cracks occurred was high circumferential residual stresses developed in the pressure tube wall by an incorrect installation procedure (Figure 6.1). At this time the Bruce Units 1 & 2 had been tubed and the same installation error had been made. To rectify the situation at Bruce the rolled joint regions were stress relieved at about 520°C for 0.5 h. However, for Bruce 2 a few sporadic tube cracks occurred over the period 1982-86 which were attributed to crack nucleation in the time period between installation and stress relieving. In the process of locating one of these leaks the reactor was pressurized cold which resulted in the rupture of the pressure tube and the calandria tube. Subsequent to Bruce 1 & 2 rolled joints were designed to reduce the circumferential residual stresses in the pressure tube wall with zero clearance joints being used on Bruce 4 and all subsequent reactors.

In 1983 a pressure tube rupture occurred in Pickering Unit 2. Unlike previous tube cracks this incident occurred at power and without an initial leak to indicate the presence of a crack. Also, this was the first cracking incident which involved Zircaloy pressure tubes. The reason for the pressure tube rupture was the formation of hydride blisters on the outside surface of the tube in a region where the pressure tube had contacted the calandria tube. Also noted in the Zircaloy tube was a very much higher than predicted hydrogen (throughout this report hydrogen will be used to refer to all hydrogen isotopes) concentration occurred as a result of faster than anticipated corrosion.

In 1987 a Zr-2.5 Wt% Nb tube removed from Pickering 3 for surveillance purposes was found to contain higher than expected levels of hydrogen. A series of tubes was then examined for hydrogen concentration, in Pickering 4,

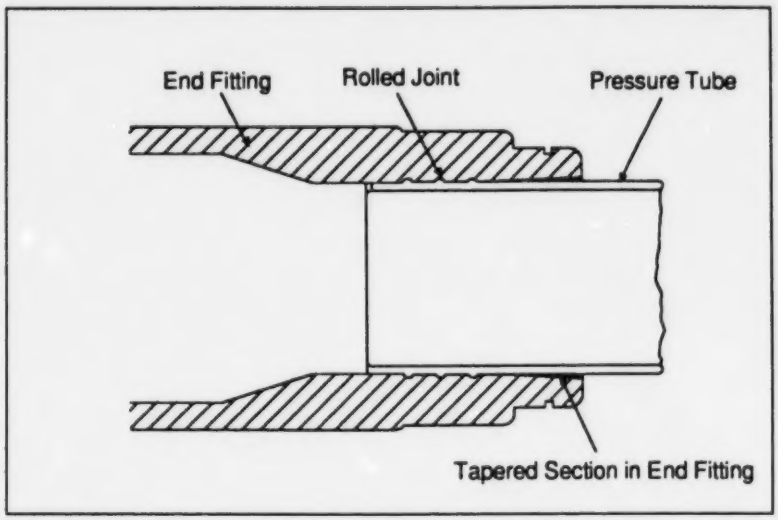

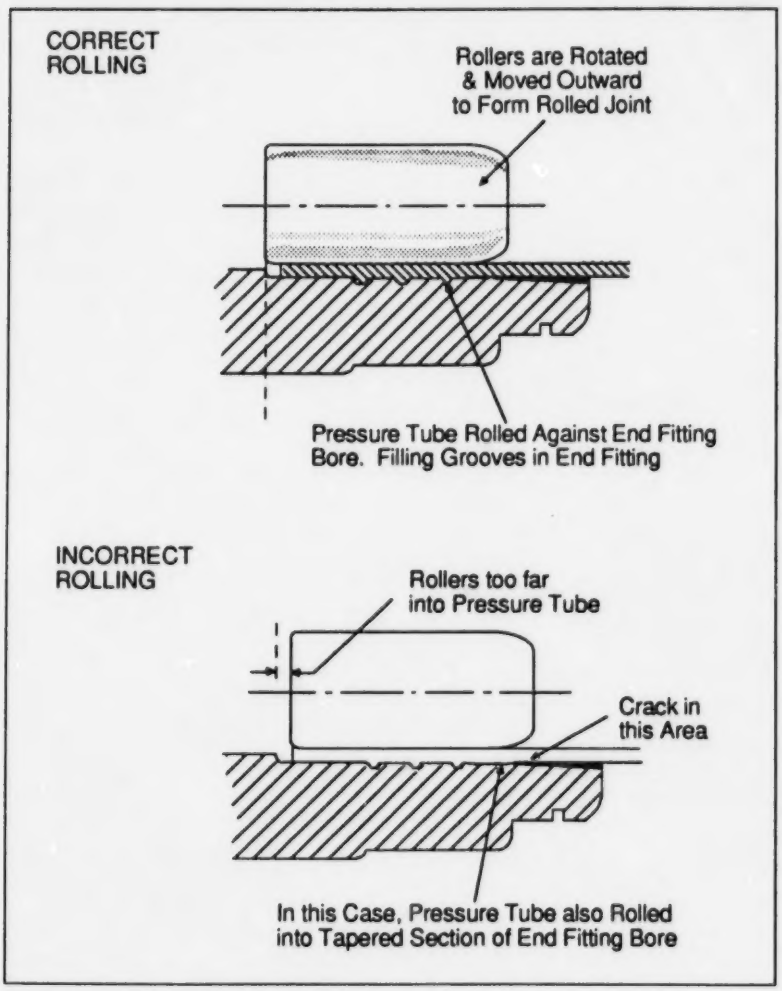

FIGURE 6.1
SCHEMATIC DRAWING TO ILLUSTRATE CORRECT AND INCORRECT ROLLING OF PRESSURE TUBE INTO THE END FITTING

FLECK 10
CAZ-4

by taking shallow scrapings from the inside surface of twenty tubes at the outlet ends. The results of the hydrogen analyses indicated that the hydrogen levels were higher than would have been predicted. A chronology of pressure tube cracking incidents is presented in Table 6.1.

TABLE 6.1
Chronology of Pressure Tube Events

Year	Unit	No. Tubes Replaced	Event
1974	Pickering 3	17	R/J Crack
1975	Pickering 4	52	R/J Crack
1982	Bruce 2	3	R/J Crack
1983	Pickering 2	390	One pressure tube ruptured at power.
1985	Pickering 3	1	R/J Crack
1986	Bruce 2	1	Pressure tube ruptured on cold pressurization to find R/J crack

7.0 DISCUSSION

This section will describe the reasons for the various operational problems with pressure tubes and also give an overview of the research programs which are in place to address these problems. Although the basic concerns with pressure tube operation have been identified since the start of the Pickering A reactors in the early 1970's, the detail and understanding required to answer questions about pressure tube safety and operational life have increased in complexity. There is now a need to develop an understanding of the basic mechanisms of irradiation damage and deformation, DHC and corrosion and hydrogen ingress. Only from such an understanding will long-term solutions to the problems be developed. Pressure tube research is primarily aimed at the development of predictive models to establish when the end-of-life conditions for a given degradation process will be reached. However, the studies will also identify if a particular degradation process can be slowed down by a minor change in operating conditions or if a change to the material would result in tubes with improved service characteristics.

In the development of a new pressure tube material all aspects must be considered. It is not sufficient to improve one property at the expense of another. For example a pressure tube with improved resistance to DHC would also have to demonstrate that corrosion and hydrogen ingress and deformation properties have not been degraded. The economics of the modified routes and the capability of the supplier to meet quality assurance standards must also be evaluated.

7.1 Irradiation Damage and Deformation

Irradiation Damage

This discussion is primarily concerned with the production of defects in the metal crystal as a result of exposure to fast neutrons (neutrons with energies > 25 - 40 eV). The production of the defects is only the initial stage in the irradiation damage process. Subsequent stages include the migration of the defects through the crystal lattice, their interaction with metallurgical features and their effect on the microstructure which then impacts on the properties of the metal e.g. deformation, strength, ductility etc.

When a fast neutron interacts with a metal atom it imparts energy to the atom with the result that the atom is displaced from its' lattice position. This process results in the formation of a vacancy (a lattice position from which the atom has been displaced) and a self interstitial (an atom of the parent metal at a location intermediate between normal lattice positions). This pair of defects is called a Frenkel pair. The atom that moves through the lattice after the neutron collision is called the Primary Knock On Atom (PKA). The extent of displacement damage caused by the PKA depends on the energy of the neutron. Figure 7.1.1 provides a schematic explanation of the displacement damage that results from a PKA in a face centred cubic metal. The various collisions and displacements result in the generation of heat with the result that recombination of some Frenkel pairs occurs. The total time to form the damage presented in Figure 7.1.1 is in the range of 10^{-12} s. The defects which escape the recombination mentioned above are the ones that influence the behaviour and properties of irradiated metals.

The above describes the situation of the interaction of one neutron to form one PKA. In reality the neutron flux is of the order of 3×10^{18} n/m2/s for neutrons with energies > 1MeV. In a given neutron irradiation facility there is also a wide distribution of neutron energy levels. To compare the amount of displacement damage generated in different irradiation facilities reactor physics calculations are performed to determine the number of displacements per atom (dpa). Important to these calculations is knowledge of the neutron energy spectra of the various facilities. In conjunction with the calculations an experimental program is underway. Damage monitors and test specimens, with well characterized and consistent metallurgical structures, are irradiated in various test facilities. Mechanical tests will be performed on the specimens to determine if the same change in properties occurs for the same calculated dpa for the different facilities. Measurement of the damage monitors will also provide checks on the dpa calculations. From the total study of dpa a correlation will be established between the irradiation test facilities and the actual power reactor situation. If the flux spectra are similar it is reasonable to describe the extent of damage in terms of a neutron fluence for a given neutron energy. For the pressure tube studies the most common measure of neutron damage is n/m^2 for neutrons > 1MeV.

The diffusion of the point defects in the metal crystal lattice and their interaction with microstructural features is of fundamental importance to

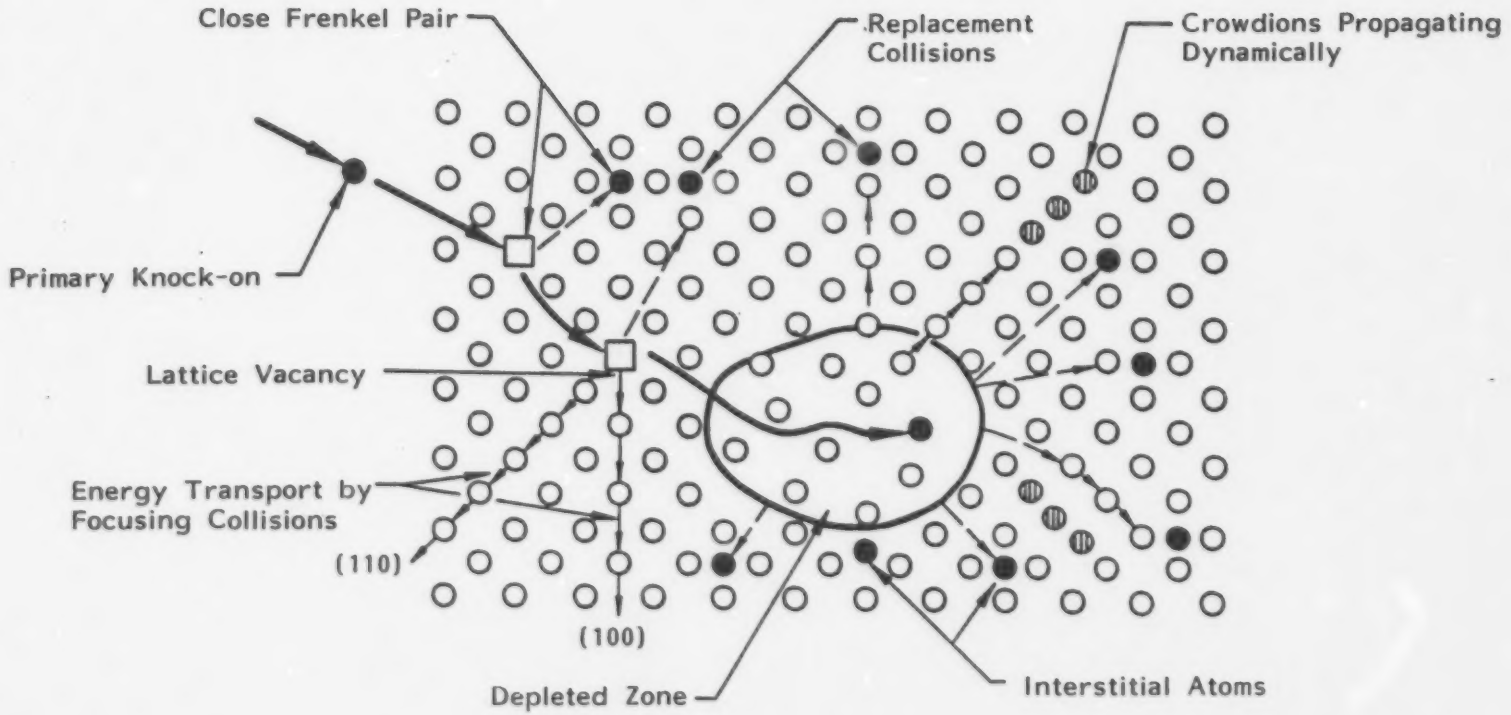

FIGURE 7.1.1

SCHEMATIC DIAGRAM OF A DISPLACEMENT OR SEEGER ZONE.
(AFTER SEEGER PROC SYMP RADIATION DAMAGE IN SOLID REACTION MATERIALS, 1, 1962)

understanding the impact of neutron irradiation on the development of the microstructure which then dictates the behaviour and properties of the metal.

Along with formation of point defects, irradiation damage also results in phase changes. The second phase in the pressure tubes is changed to the equilibrium β Nb (Figure 4.2) phase and also precipitation occurs within the grains. This latter precipitation cannot be reproduced in the absence of a fast neutron flux. In general exposure to a fast neutron flux results in an increase in strength, decrease in ductility, increase in deformation rates and a reduction in fracture toughness.

In-Reactor Deformation

Two mechanisms, namely irradiation growth and irradiation enhanced creep, have been identified as responsible for the faster than anticipated in-service deformation of pressure tubes. Both mechanisms occur as a result of exposure of the tubes to a fast neutron flux.

Irradiation Growth: This deformation mechanism occurs without the application of an external stress and is generally confined to anisotropic metals i.e metals with a hexagonal close packed crystal structure (Figure 2.1). For isotropic metals there has been a report of growth in cold worked material. The shape change, as a result of growth occurs without an increase in volume in contrast to the swelling observed in stainless steels irradiated in fast reactors.

Irradiation Enhanced Creep: Creep deformation is common in many industrial situations where metallic components are exposed to an external load or stress at elevated temperatures for prolonged periods of time. For zirconium alloys out reactor creep tests at normal operating stresses and temperatures show very low creep rates. However, for similar stress and temperature conditions, in-reactor tests show very much faster creep rates (Figure 7.1.2).

Total Deformation = Irradiation Creep + Irradiation Growth

There are basically two aspects of the research studies on irradiation deformation: 1) develop a model that can predict the deformation behaviour of pressure tubes throughout the design life of the reactor and 2) develop pressure tubes that have improved in - reactor deformation properties.

As an example of how irradiation induced point defects enhance deformation their interaction with a dislocation is described. As illustrated previously, Figure 2.5, metals deform as a result of the motion of dislocations. The motion illustrated in Figure 2.5 is dislocation glide. Motion perpendicular to the glide direction is called climb. The stress required to deform a metal increases if dislocation motion is restricted, for example by a particle. Irradiation induced point defects can increase the mobility of a dislocation by enabling the dislocation to climb away from a barrier, Figure 7.1.3(a) and (b). Once away from the barrier the dislocation can then glide and cause

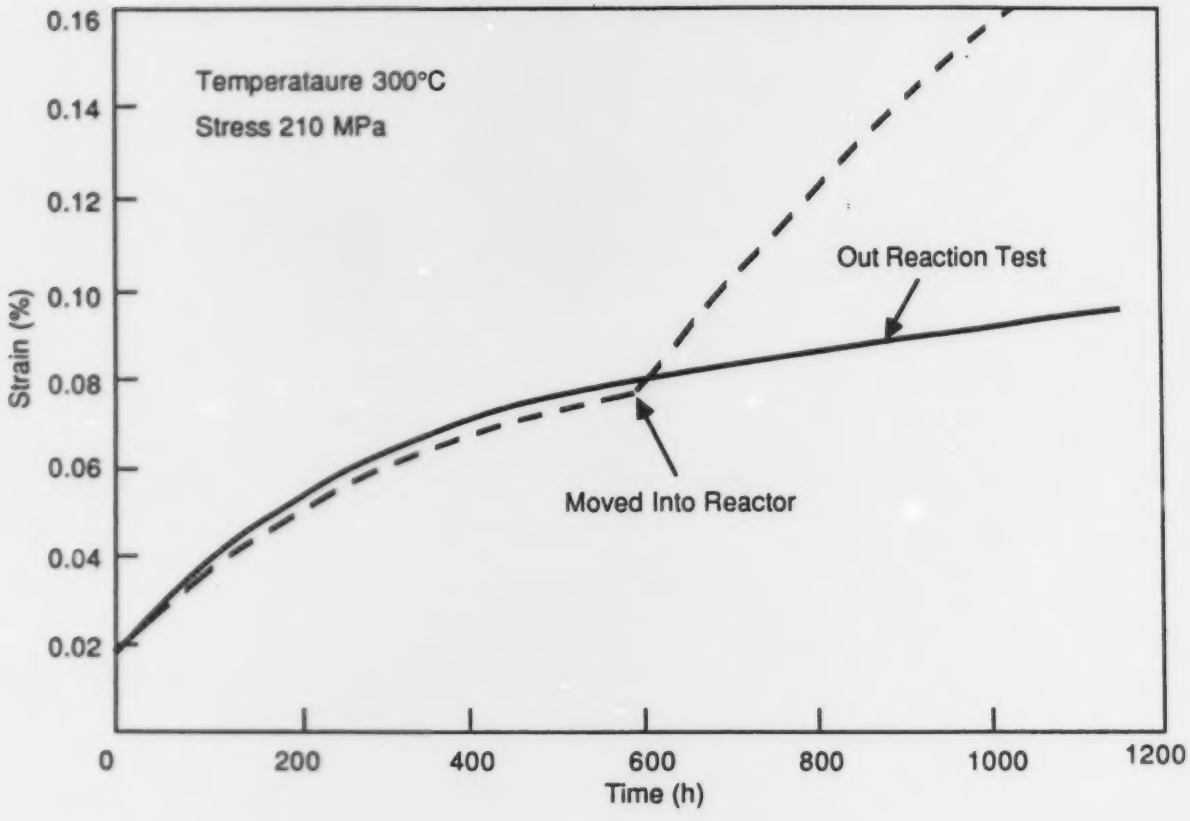

FIGURE 7.1.2

AN ILLUSTRATION OF THE INFLUENCE OF A FAST NEUTRON FLUX ON THE THERMAL (OUT REACTOR) CREEP RATE (INFORMATION OBTAINED FROM FIDLERIS ASME PUBLICATION 62 - WA - 325)

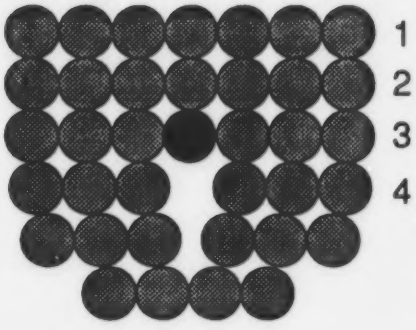

EDGE DISLOCATION WITH IT'S CORE AT POSITION 4

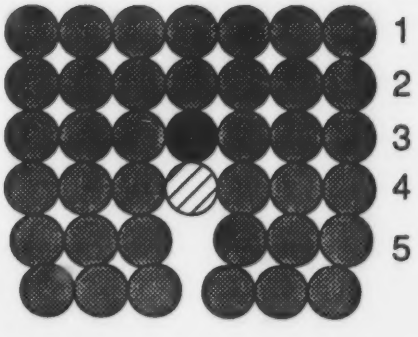

INTERSTITIAL ATOM ARRIVES AT THE CORE OF THE EDGE DISLOCATION. THE CORE IS NOW AT POSITION 5. THE DISLOCATION IS SAID TO HAVE CLIMBED IN THE NEGATIVE DIRECTION

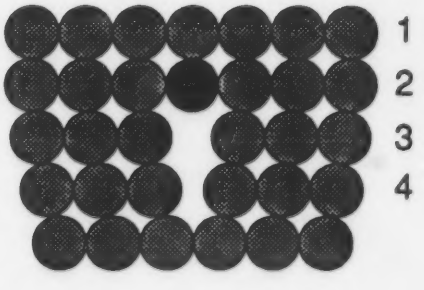

VACANCY ARRIVES AT THE EDGE DISLOCATION. THE CORE IS NOW AT POSITION 3. THE DISLOCATION IS SAID TO HAVE CLIMBED IN THE POSITIVE DIRECTION

FIGURE 7.1.3 (a)

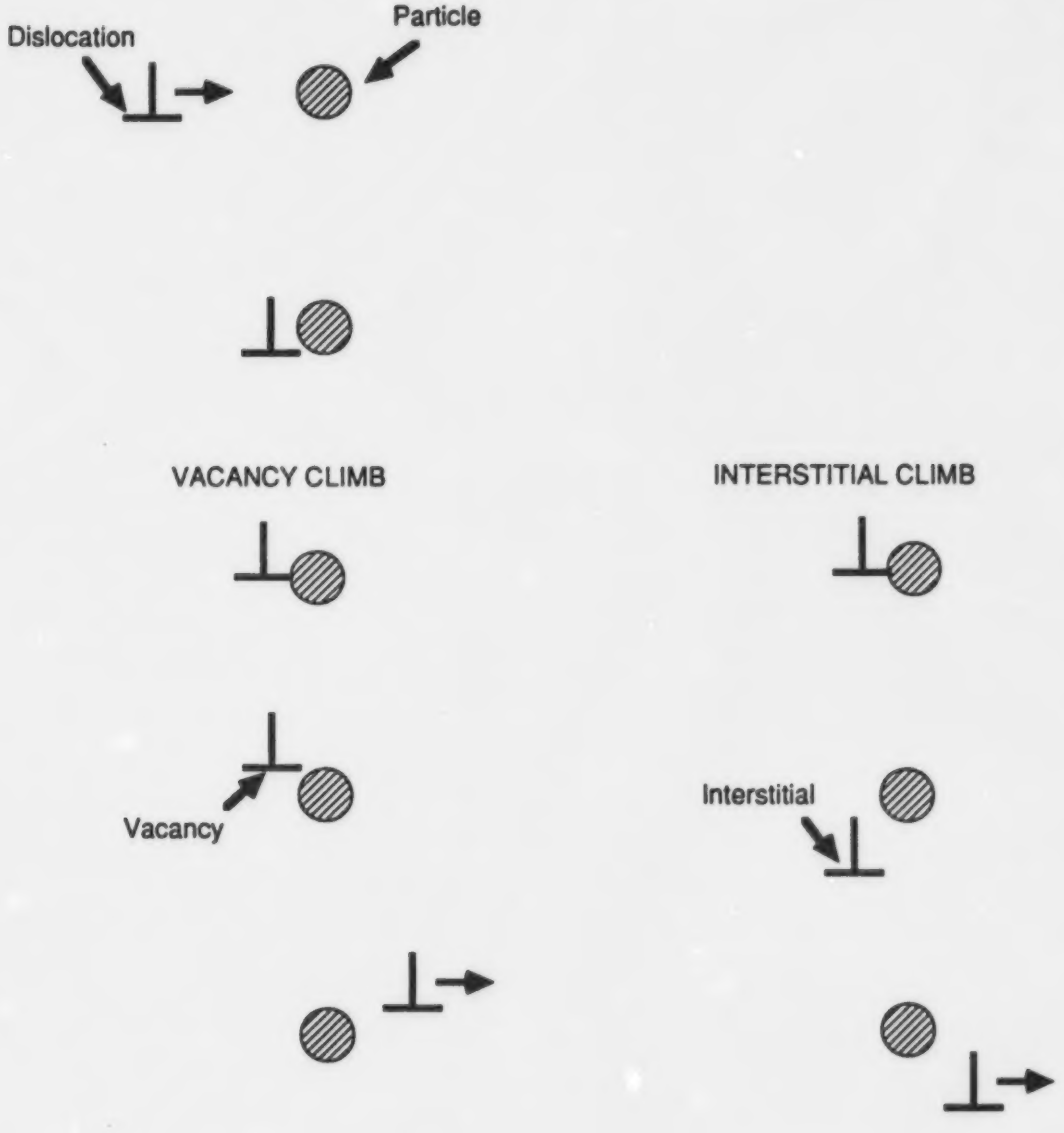

FIGURE 7.1.3 (b)

DISLOCATION MOTION: AS THE DISLOCATION MOVES, THE METAL DEFORMS. DISLOCATION MOTION CAN BE STOPPED BY A BARRIER, IN THIS CASE A PARTICLE. A FLOW OF INTERSTITIALS OR VACANCIES TO THE DISLOCATION RESULTS IN CLIMB UNTIL THE DISLOCATION IS FREE OF THE BARRIER AND CAN CONTINUE TO MOVE AND THEREFORE RESULT IN FURTHER DEFORMATION OF THE METAL

further deformation. Without the irradiation produced point defects the dislocation would remain pinned at the barrier and deformation would only occur if higher stresses were applied. There are other metallurgical features that the irradiation induced defects can interact with that will result in deformation e.g. boundaries. If the grain boundaries, for example, preferentially absorb vacancies and if the boundaries are not isotropically oriented then a shape change would occur, Figure 7.1.4.

In the initial design stages of the CANDU reactor only diametral creep was expected to occur. A test program on pressure tubes was initiated to establish the extent of diametral expansion that could be expected. The data from the test program was used to develop an empirical design equation. This equation did not account for irradiation growth and could not predict elongation. However, there was an indication that elongation could occur and this resulted in a program of in-service measurements. These measurements on Pickering Units 1 - 4 confirmed that elongation was occurring and at a much higher rate than anticipated. This necessitated further work on the development of a design equation that could explain the in-service behaviour.

The development of a predictive model initially concentrated on the analysis of in-service deformation measurements and the metallurgical analysis of various pressure tube materials, mainly Zircaloy, as used in several different types of reactors e.g. Douglas Point, Pickering 1 & 2, Hanford N reactor (USA) and SGHWR (UK). From these studies a correlation of elongation rate with crystallographic texture and dislocation density was identified. On the analysis of fast and slow elongating tubes in Pickering Unit 2 grain shape was also identified as a metallurgical parameter with a possible influence on the elongation behaviour. From this information an equation was developed to describe pressure tube deformation. Further developments of the design equation were based on improved understanding of the deformation mechanism. Table 7.1 records the various design equations developed to date.

The design equation evolves as new information becomes available. The end point of the evolution will be the development of a predictive mechanistic model. As described above and in Table 7.1 the original empirical equation has been updated. Further developments will include results from the studies on irradiation damage and on the actual deformation mechanism. The additive nature of creep and growth has formed the basis of the models to date but these two processes may not be strictly additive. This is another aspect of the deformation process that has to be positively established if a good predictive mechanistic model is to be developed. Once the mechanism has been established the influence of operating parameters, stress, temperature and damage rate will have to be established so that pressure tube deformation can be predicted for a variety of possible operating conditions.

The difficulties in developing a predictive model are the complexities of understanding the irradiation damage process and in performing in-reactor deformation tests. Deformation data at fluences in excess of the power reactors is important for predictive purposes. High fluence irradiations are performed in offshore facilities (until Canada develops a reliable facility)

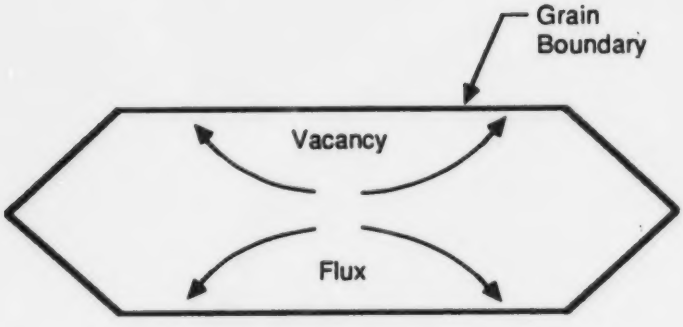

Anisotropic Vacancy Flux in an
Elongated Grain

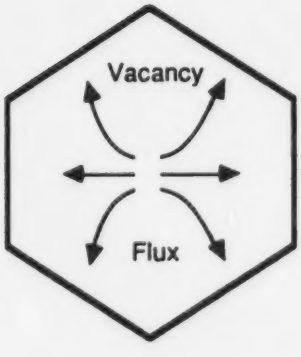

Isotropic Vacancy Flux in an
Equiaxed Grain

FIGURE 7.1.4
INFLUENCE OF GRAIN SHAPE ON
IRRADIATION INDUCED VACANCY FLUX

TABLE 7.1
Development of the Pressure Tube Deformation Design Equations

Equation	Comment	Reference
$\dot{\epsilon}_t = k \phi \sigma_t (T-160)$	Diametral Creep only	AECL 4626 (1973)
$\dot{\epsilon}_d = k_1 \sigma_F^3 C_d \exp(-25{,}000/T) + k_2 \phi \sigma_F C_d [\exp(-9{,}000/T) + 1.1 \times 10^{-7} + k_3 \phi G_d \exp(-7{,}000/T)/[1 + 8.9 \times 10^{16} \exp(-25{,}000/T)]$	Contains growth and anisotropy and explains elongation as well as diametral deformations	CRNL 1993 (Oct 1979)
$\dot{\epsilon}_d = [A_1 C_d + A_2 C'_d \sigma'^2] \exp(-Q_1/T) + A_3 (x) C_d \sigma \exp(-Q_2/T) + A_4 C_d \sigma\phi \exp(-Q_3/T) + A_5 G_d \phi \exp(-Q_4/T)$	Explains elongation and diametral deformation and gives correct diametral profile along the length of the tube. Contains a growth term which is negative in transverse direction which is in agreement with experimental results.	CRNL 4000 (Sept 1986)

which are expensive and this restricts the type of tests and the number of specimens that can be studied. The Dido reactor at AERE, Harwell has been used, since 1978, to evaluate the growth behaviour of pressure tube materials. The fast neutron flux in Dido is approximately three times that in a Pickering reactor. This facility has been used to evaluate the influence of metallurgical structure and operating temperature on irradiation growth. The effects of metallurgical structure were investigated in relation to the previously mentioned pressure tube development program. The results of the influence of temperature show that a relatively small change has a significant effect on the growth characteristics. Tests at Pickering and Darlington outlet temperatures, 280 and 310°C respectively, show that the direction of growth can be completely changed to relatively high neutron fluences, Figure 7.1.5. This result illustrates that pressure tube deformation for a given set of operating conditions cannot be used to predict deformation for different operating conditions. Also for load maneuvering (i.e when the reactor power is varied to meet the demands for electricity) there will be temperature changes that may impact on the pressure tube deformation

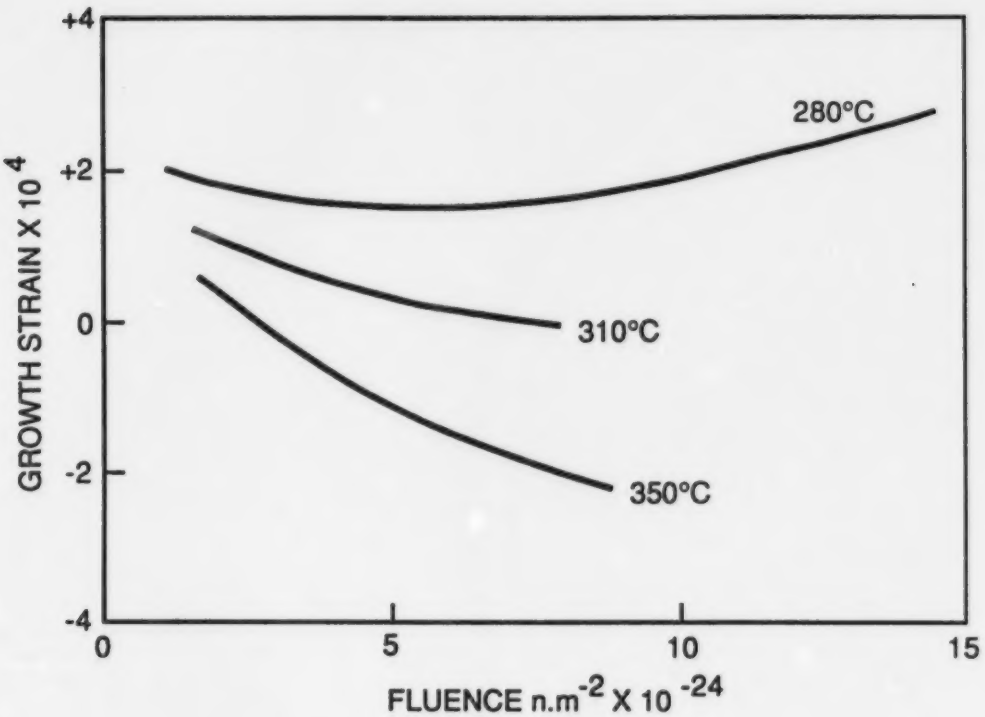

FIGURE 7.1.5

IRRADIATION GROWTH BEHAVIOUR OF DARLINGTON PRESSURE TUBE MATERIAL AT 280, 310 AND 350°C SAMPLES CUT LONGITUDINALLY. (Holt and Fleck OHRD)

FLECK-37
CAZ-4
89-271

behaviour. To date only preliminary tests have been performed under thermal and flux cycling conditions to establish if there are any effects on deformation.

Detailed metallurgical tests were performed to compare the properties of tubes manufactured by the modified routes with those manufactured by the standard process. The development tubes had similar or better properties than the standard tubes and in-reactor growth tests indicate that the desired improvements to the in-service deformation properties of pressure tubes could be achieved by the Route 1 tubes, Figure 4.10.

The detailed microstructural analysis required for the pressure tube development program has resulted in a better understanding of the metallurgical factors which control the in-reactor deformation. The crystallographic texture and dislocation density have been measured by X-ray diffraction. Grain shape has been measured by scanning electron microscopy and detailed transmission electron microscopy has been performed to establish the dislocation type and distribution as well as the phase content of the different materials. More recent studies have used neutron diffraction to determine the residual stresses in the different materials as well as provide further information on the phase content.

To date, the results indicate that no single metallurgical parameter can be considered as controlling. The original thoughts were that the texture would dictate the direction of irradiation growth and that dislocation density would control the rate. However, there is now information which illustrates that texture does not always control the direction of growth, Figure 7.1.6 (a) and (b) are growth data for Zr-2.5 Nb materials which have essentially the same textures. Transmission electron microscopy (TEM) studies show a difference in the metallurgical substructure of the various materials, Figure 7.1.7. Model development has included the TEM observations and theoretical calculations on anisotropic point defect diffusion to explain why texture does not always control the direction of growth.

7.2 Pressure Tube Fracture

All pressure tube leaks that have occurred to date, have been associated with the presence of hydrides and the cracks have propagated by Delayed Hydride Cracking (DHC). The DHC process requires the presence of hydrides and sufficient stress. Pressure tubes in the as received condition can contain up to 20 ppm of hydrogen (typical values are in the range of 6 - 9 ppm) and this limits DHC to temperatures below about 175°C. Under service conditions the tubes pick up hydrogen which increases the temperature at which DHC can occur. For a hydrogen content of 40 ppm hydrides will be present at operating temperatures and potentially DHC could occur at these temperatures.

The occurrence of the rolled joint leaks in Pickering Units 3 & 4 highlighted the problems associated with the use of a material that has a high affinity and low solubility for hydrogen as shown in the hydrogen/zirconium phase diagram, Figure 2.7. The initial rolled joint cracks occurred at cold

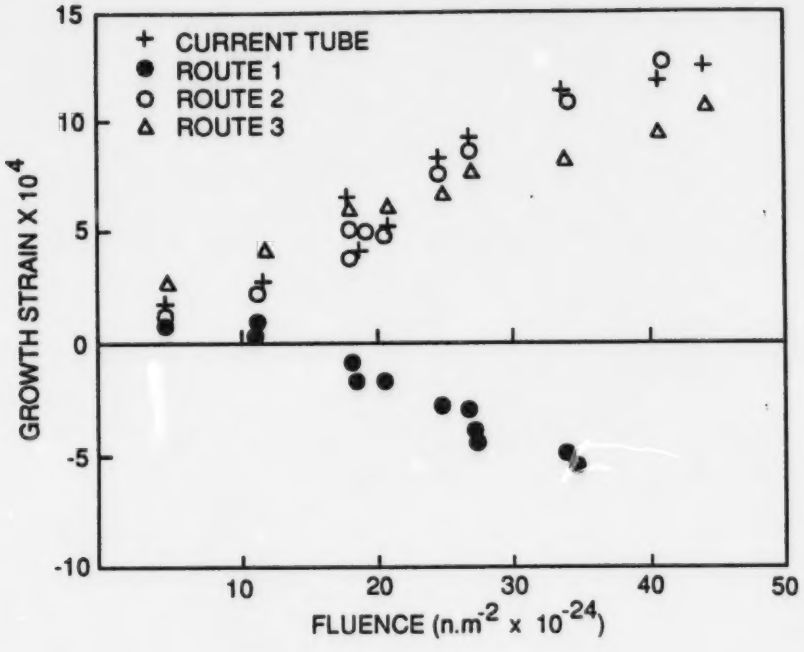

FIGURE 7.1.6 (a)

IRRADIATION GROWTH BEHAVIOUR OF Zr/2.5 WT% Nb MATERIAL
AT ~ 280°C. SAMPLES CUT LONGITUDINALLY FROM THE PRESSURE TUBE.

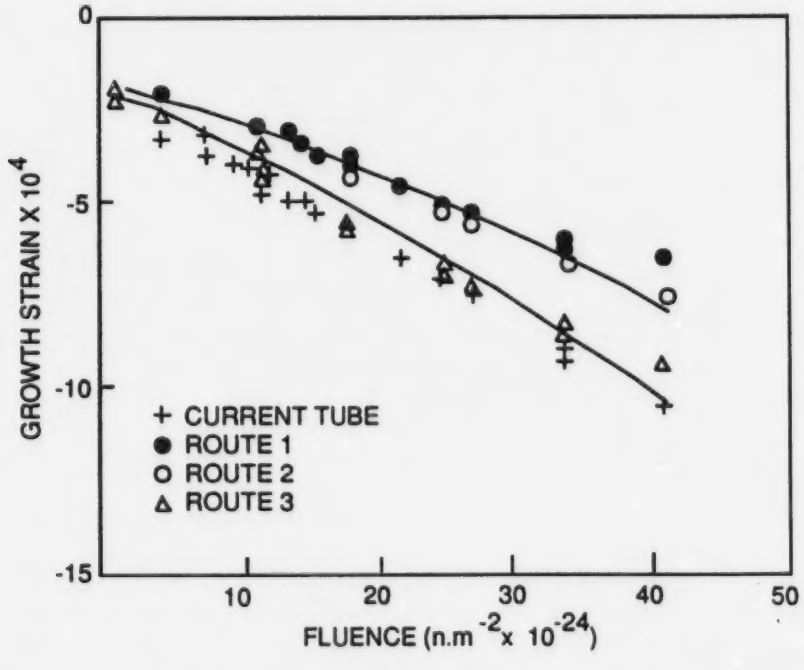

FIGURE 7.1.6 (b)

IRRADIATION GROWTH BEHAVIOUR OF Zr/2.5 WT% Nb MATERIAL
AT ~ 280°C. SAMPLES CUT TRANSVERSELY FROM THE PRESSURE TUBE.
(Holt and Fleck OHRD)

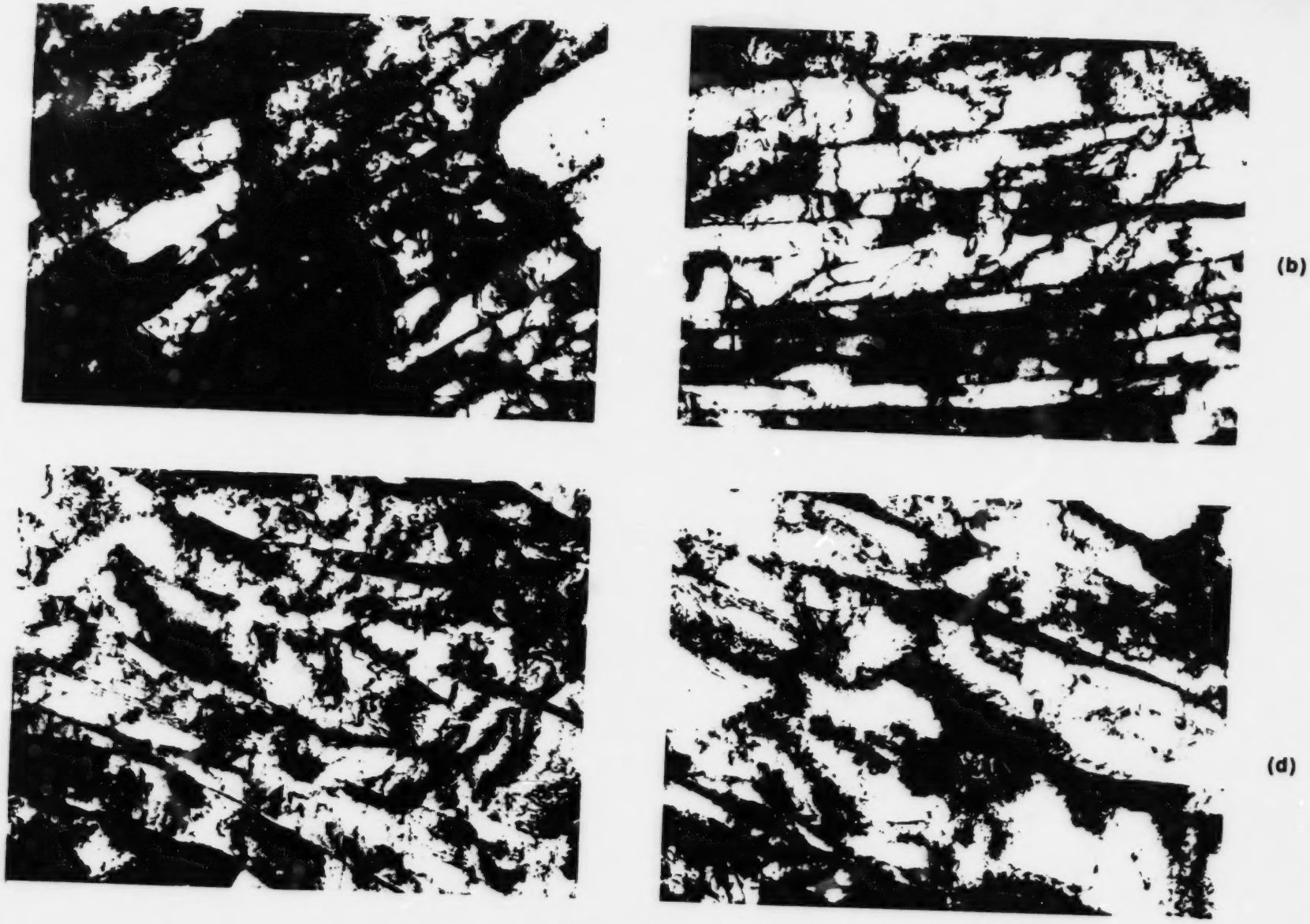

FIGURE 7.1.7

MICROSTRUCTURE OF A CURRENT Zr-2.5 Nb & TG3 PRESSURE TUBE IN THE LONGITUDINAL SECTION
(a) CURRENT, (b) ROUTE 1, (c) ROUTE 2, (d) ROUTE 3
(Fleck, Price and Cheadle - Bibliography 4.0)

7 Fleck
Marj Disk
89-271

shutdown conditions after short operating time so the pressure tubes contained the as-received hydrogen concentrations. When hydrides precipitate perpendicular to the principal stress (Figure 7.2.1) they have a negative impact on the ductility of zirconium alloys. The DHC process occurs as a result of the formation of a hydride at the tip of a flaw which subsequently cracks resulting in crack extension. Hydrogen in solid solution in the matrix diffuses to the high stress region at the crack tip, Figure 7.2.2, which results in precipitation of a hydride at the tip of the extended crack. This process repeats until a through wall crack is formed, Figure 7.2.3.

An important aspect in fracture is the relationship between stress intensity and flaw size. A schematic representation of how a flaw concentrates stress at its' tip is shown in Figure 7.2.4. The larger the flaw then the higher the stress concentration. Mathematically the relationship is represented as follows:

$$K = 1.12\ Q\ \alpha^{0.5}$$

where K is the stress intensity factor.
Q is the stress.
α is half the flaw length.

For a crack to propagate the value of K has to exceed a critical value, K_{1c} which is the Fracture Toughness of the material. The discussions on pressure tube fracture will refer to a parameter K_{1H} which is the critical stress intensity factor for DHC to occur.

Figure 7.2.5 describes the relationship between DHC and the stress intensity factor, K_1. DHC does not occur until a K_{1H} of about 4.5 MPa $m^{0.5}$ is exceeded. In Stage 1 the crack growth rate is strongly dependent on the K value. A plateau region is reached, Stage 11, where the crack growth rate is independent of the K_1 value until the crack reaches a critical size and K_{1C} is reached, which is the onset of Stage 111 and unstable crack growth, ie, a critical size is reached.

For pressure tubes, the assurance of Leak-Before-Break (LBB) is an important operating criterion. To maintain this criterion a crack has to penetrate the pressure tube wall and the leak detected before the crack reaches a critical length. After the crack penetrates the wall the leak of PHT water into the gas annulus will be detected and the reactor shut down. The ideal situation would be to prevent Stage 1 cracking. However, if it is assumed that crack initiation can occur then to maintain LBB it is desirable to have a slow crack growth rate in Stage 2 and to have as long a critical crack length as possible along with short detection times for leaks into the gas annulus system.

In the as-received condition the hydrides in the tubes are oriented in the axial - circumferential plane which is parallel to the principal stress in the operating condition. In the Pickering situation the problems were a result of

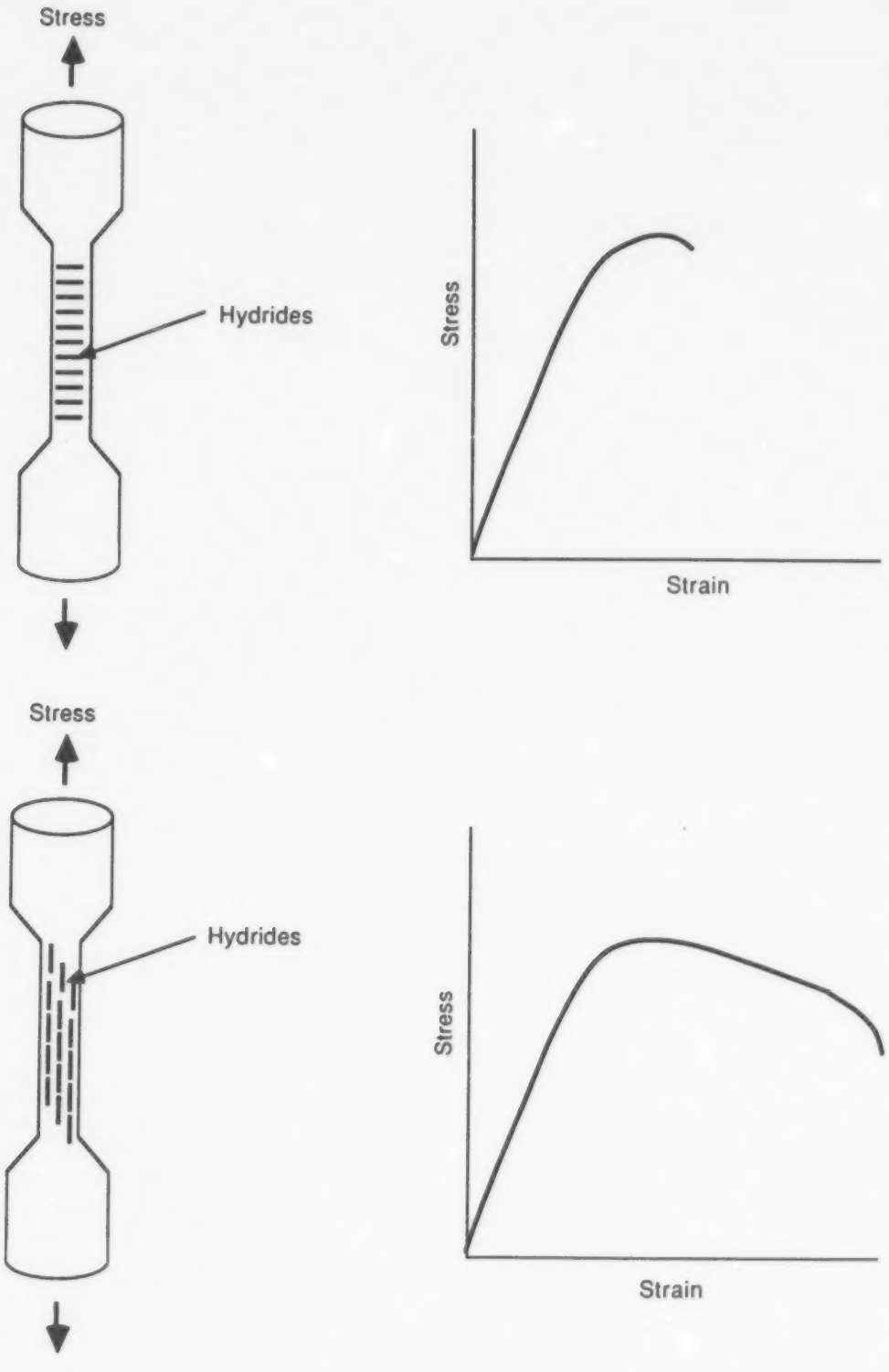

FIGURE 7.2.1

A SCHEMATIC ILLUSTRATION OF HOW THE ORIENTATION OF HYDRIDES IN RELATION TO THE APPLIED STRESS INFLUENCES THE DUCTILITY OF ZIRCONIUM

FLECK 18
CAZ-4

FIGURE 7.2.2

LARGE HYDRIDE PRECIPITATED AT THE ROOT OF A NOTCH (MAG 160 X) (W.K. Lee OHRD)

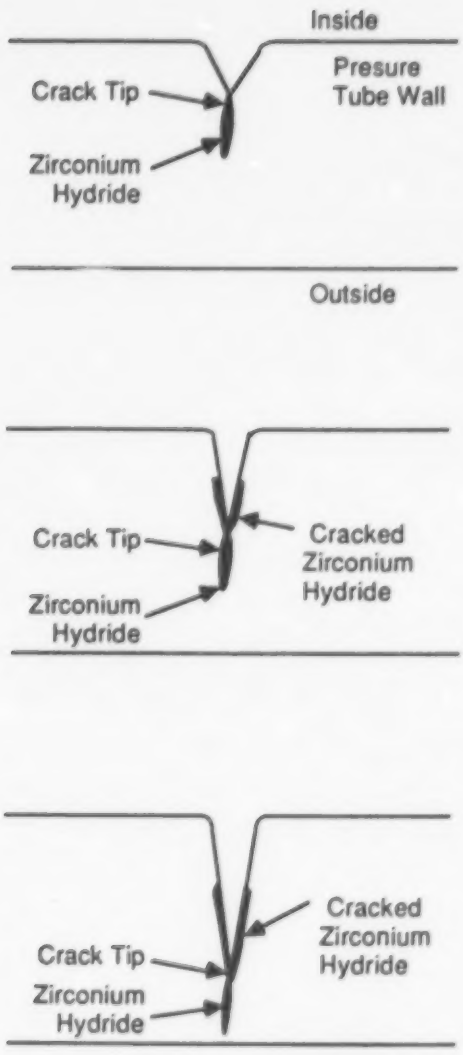

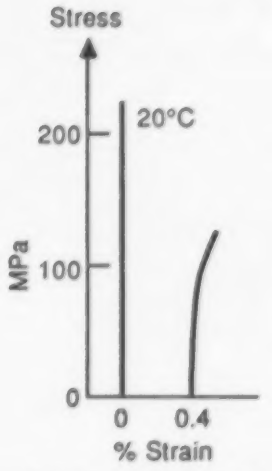

Stress-Strain Curves
for Zirconium Hydride

FIGURE 7.2.3

SCHEMATIC ILLUSTRATION OF DELAYED HYDRIDE CRACKING

FIGURE 7.2.4
SCHEMATIC DIAGRAM TO ILLUSTRATE THE RELATIONSHIP BETWEEN NOTCH SIZE AND STRESS CONCENTRATION

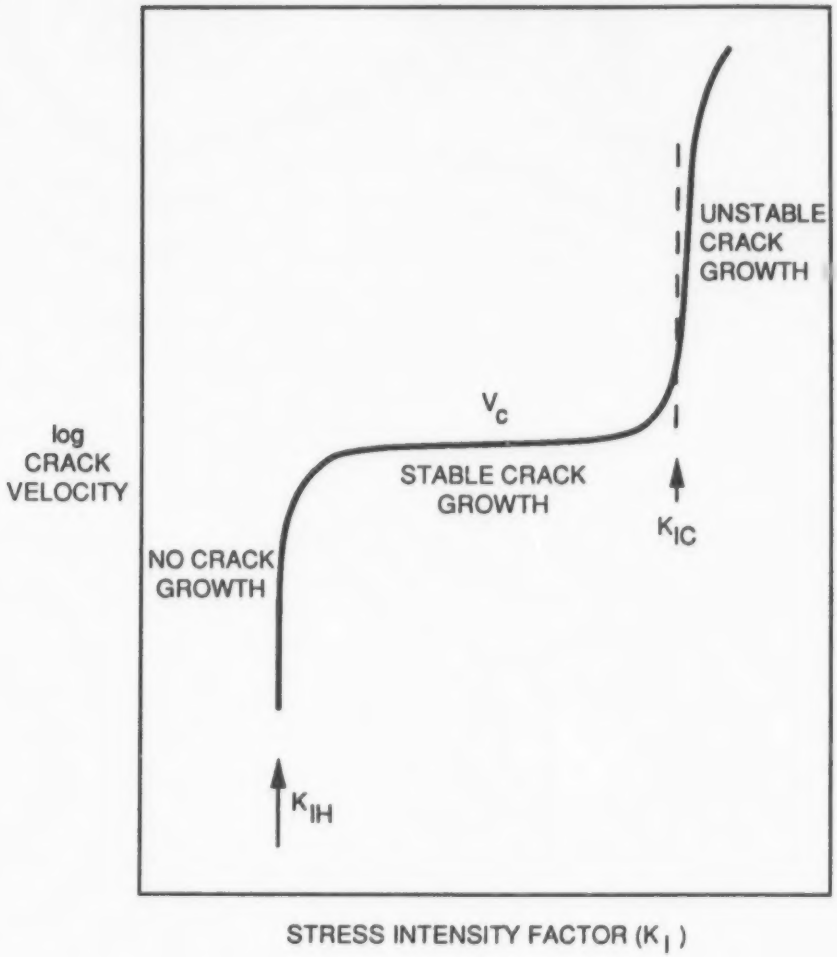

FIGURE 7.2.5

SCHEMATIC DIAGRAM OF THE DEPENDENCE OF CRACK VELOCITY ON STRESS INTENSITY FACTOR

reorientation of the hydrides in the rolled joint region. The reorientation was caused by the high residual stresses developed in the pressure tube due to the incorrect installation procedure, as shown in Figure 6.1. The resultant stresses developed in the tube wall caused the hydrides to orient in the radial - axial plane as opposed to the circumferential - axial plane i.e. locally the hydrides were perpendicular to the operating hoop stress. Cracks initiated in this region, which is just inboard from the rolled joint, either by the fracture of a hydride or from a small surface defect. It is interesting to note that the Zircaloy tubes in Pickering Units 1 & 2 were also installed by the incorrect procedure but the cracking problem did not occur in these tubes. This is attributed to the lower tensile strength of Zircaloy as compared to Zr-2.5 wt% Nb which resulted in a lower residual stress in the Zircaloy tubes.

The analysis of the cracked joints in the Pickering units indicated that the residual stresses were highest in rolled joints where the clearance, before rolling, between the OD of the pressure tubes and the ID of the end fitting were largest. To overcome the potential for DHC in rolled joints in subsequent reactors i.e. after Bruce 1 & 2, a modified rolled joint design was developed where the clearance between the OD of the tube and the ID of the end-fitting, before rolling, is zero. To install the pressure tube, for the assembly of the zero clearance rolled joint, the end fitting has to be heated to increase its' inside diameter. This reduces the extent of plastic deformation of the tube required to make the rolled joint and so reduces the circumferential residual stresses in the tube. Also procedures were modified to eliminate the risk of over rolling the joints.

Delayed Hydride Cracking

In discussing the DHC process there are several factors that have to be considered.

1. hydride distribution
2. crack nucleation
3. crack growth
4. critical crack size

The studies on the influence of hydrides on the fracture characteristics of pressure tubes consider metallurgical and operating parameters which influence hydride precipitation and orientation and their impact on crack initiation and growth and fracture toughness.

Fundamental to all the programs to study the effects of hydrides on pressure tube integrity is the development of material with different hydride distributions. A key step in this process was the decision to hydride material while under stress. This technique provided a more realistic simulation of the situation of an operating pressure tube. The results indicated that the stress to re-orient the hydrides was in fact lower than previously thought. It was this test that predicted that the operating hoop

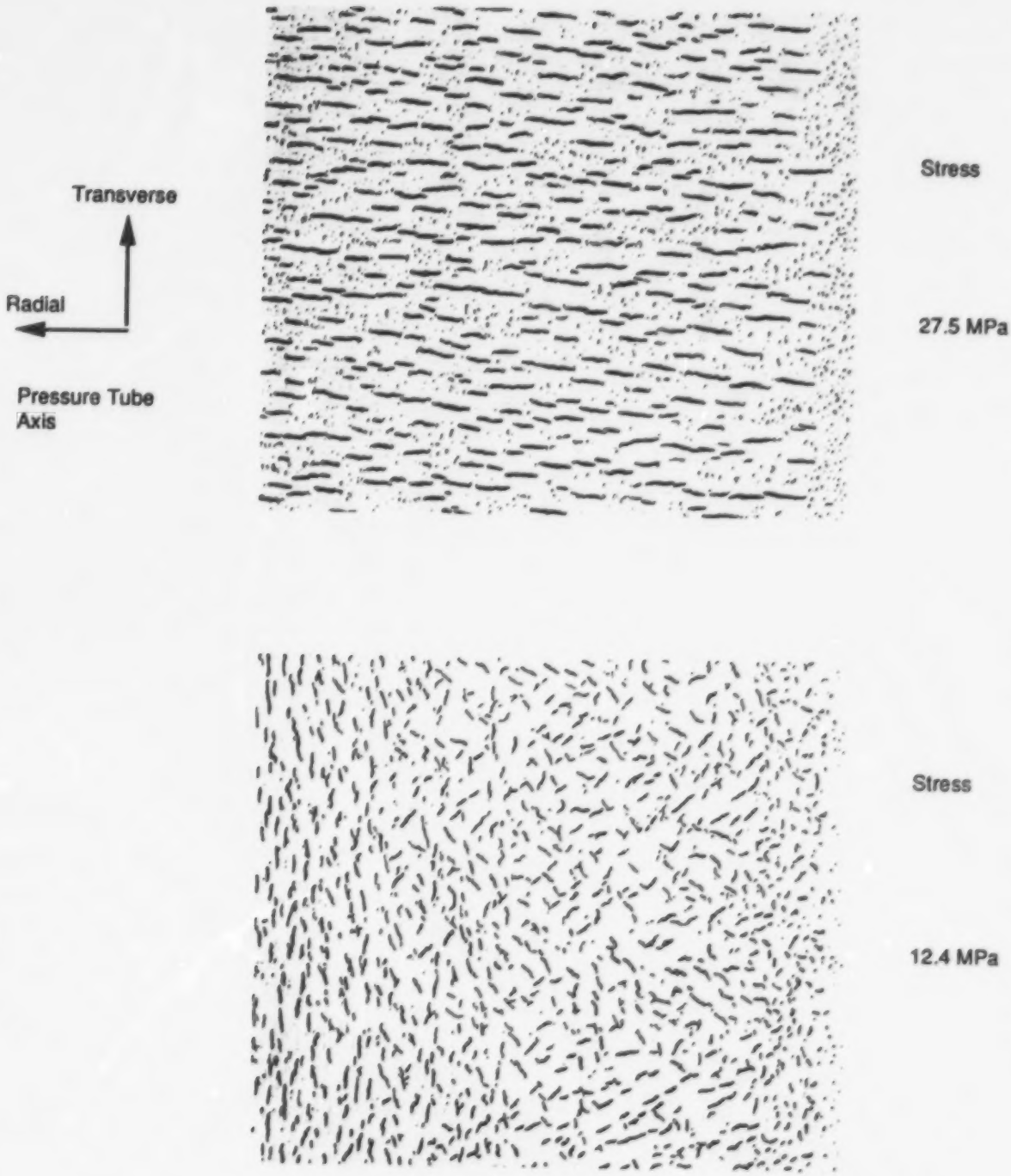

FIGURE 7.2.6
THE INFLUENCE OF APPLIED STRESS DURING HYDRIDING ON THE DISTRIBUTION OF HYDRIDES (G.K. Shek OHRD)

Fleck 1-K6

89-271

stress would re-orient the hydrides in Zircaloy tubes. By control of the applied stress and thermal cycles, during hydriding, it is possible to produce various hydride distributions in pressure tube sections, Figure 7.2.6.

Specimens are hydrided by first depositing a hydride layer on the surface of the specimen. This is accomplished by the electrolysis of water with the hydrogen ions migrating to the specimen which is the cathode in the electrolytic cell. When a hydride layer is formed the specimen is then annealed at the appropriate temperature that corresponds to the terminal solid solubility of the desired hydrogen concentration. From the phase diagram, Figure 2.7, the annealing temperature to give a specific concentration can be established. Difficulties arise when the desired hydrogen concentration would require anneals at temperatures above 400°C which would result in changes to the metallurgical structure of the tube as the last process in tube production is the 400°C autoclave (Figure 4.1).

Hydride Distribution

Transmission Electron Microscopy (TEM) has played an important role in the development of the understanding of parameters which influence hydride precipitation and distribution. On an optical scale the hydrides appear as single precipitates, Figure 7.2.7, but TEM shows that these hydrides are actually stacks of small individual platelets, Figure 7.2.8. The hydrides preferentially precipitate on crystallographic planes close to the basal plane of zirconium, Figure 2.2. From the texture consideration this would suggest that the hydrides should be preferentially oriented in the radial - axial plane of the tube. Also a study based on TEM and neutron diffraction indicates that the residual stress pattern in the pressure tube controls the hydride orientation. The hydrides precipitate to relieve the residual stresses which results in the observed circumferential/axial orientation of the hydrides in the as received tubes. Hydride distribution can also be influenced by the morphology of the phase boundary. If the boundary is smooth the hydrides will grow along the boundary, Figure 7.2.9(a), but if there are irregularities on the boundary the hydrides will grow into the alpha grains, Figure 7.2.9(b).

The TEM studies have provided important input to the understanding of hydride precipitation and also give some insight on how pressure tube microstructure could be modified to minimize the effect of hydride precipitation on the mechanical properties of pressure tubes.

Crack Initiation

To nucleate a delayed hydride crack both hydride and stress have to be present. The stress can either be the operating stress plus any residual stresses in the tube or else it can be the applied stress locally concentrated at a defect. Although some rolled joint cracks have been attributed to nucleation at manufacturing defects the quality assurance procedures in manufacture generally ensure that the tubes are defect free. The hydrides themselves are brittle and if the overall stress on the tube is high enough

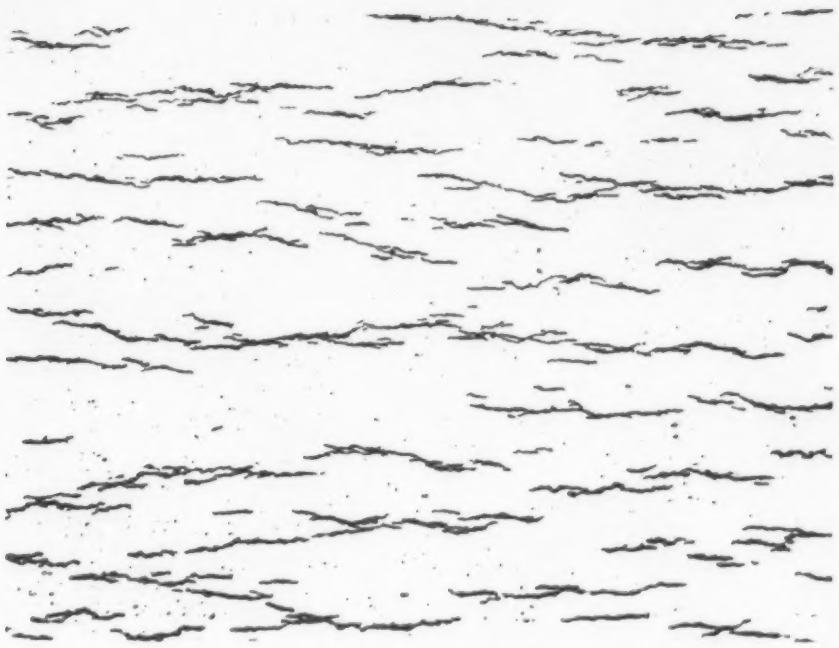

FIGURE 7.2.7

OPTICAL MICROGRAPH (MAG 115 X) OF
HYDRIDES IN Zr-2.5 wt % NB
(G.K. Shek OHRD)

4 Fleck
Marj Disk
89-271

TRANSMISSION ELECTRON MICROGRAPH (MAG 44,000 X) OF
A HYDRIDE IN Zr-2.5 wt % Nb

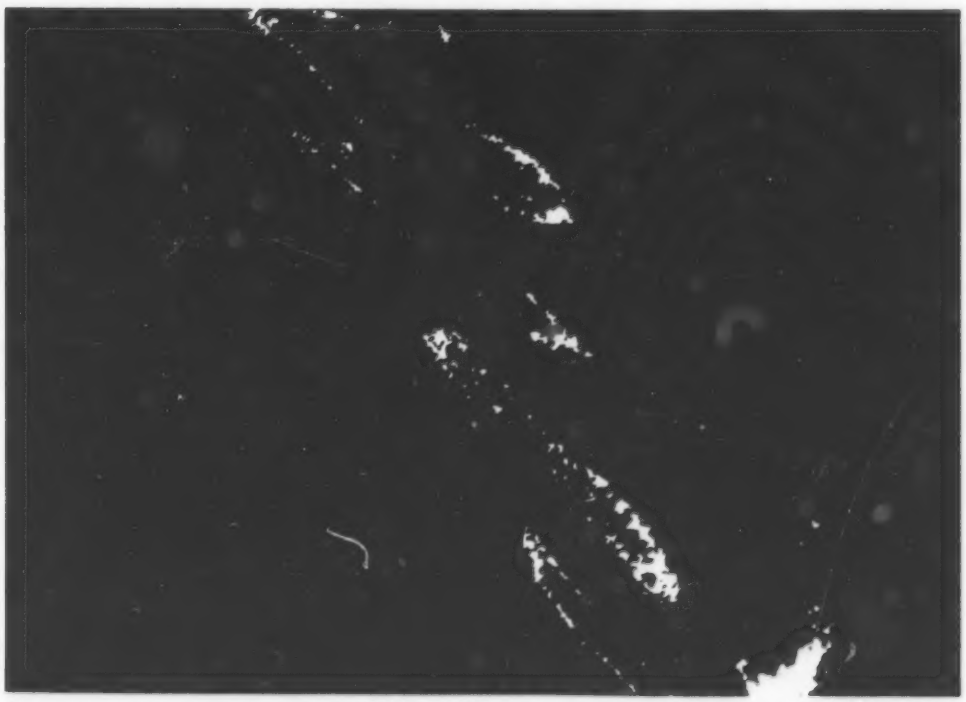

FIGURE 7.2.8
A TRANSMISSION ELECTRON MICROGRAPH (MAG 122,000 X) WHICH SHOWS
STACKING OF SMALL HYDRIDES THAT FORM A "SINGLE" HYDRIDE
AS SHOWN IN FIGURE
(V. Perovic OHRD)

6 Flock
Marj Disk

89-271

FIGURE 7.2.9 (a)
TRANSMISSION ELECTRON MICROGRAPH (MAG 85,000 X) OF
A HYDRIDE (A) LYING ALONG A SMOOTH BETA BOUNDARY

FIGURE 7.2.9 (b)
A TRANSMISSION ELECTRON MICROGRAPH (MAG 105,000 X) OF A HYDRIDE
(A) LYING AT AN ANGLE TO AN IRREGULAR BETA BOUNDARY
(V. Perovic OHRD)

5 Fleck
Marj Disk
89-271

and the hydrides are oriented perpendicular to the principal stress then they will fracture within the metal matrix. Once the hydride has fractured then that location will act as a stress concentrator within the metal.

The parameters which control DHC initiation have not been positively identified. One approach to the study has been to use cantilever beam specimens machined from pressure tubes, Figure 7.2.10. Both notched and unnotched specimens have been used with different hydrogen concentrations and held at different stress levels. The tests, in general, last for several years and there is a large variation in the times to failure between specimens of similar metallurgical structure. The reason for the difference in initiation times between apparently identical specimens is not understood. The time factor in initiation is a result of the need to diffuse hydrogen to the defect and for the hydrides to precipitate. The time required for crack nucleation to occur is the least understood aspect of the DHC process. To explain variations in time to nucleate between apparently identical specimens requires detailed studies on a local level to establish if there are variations in metallurgical structure or stress distribution.

The programs to study DHC initiation address the situation that for similar conditions and metallurgical structure cracking does not occur in all specimens. This was illustrated in the cracking of the Pickering 3 & 4 tubes and with cantilever beam specimens where the onset of cracking occurs at different times in similar specimens. A detailed study using four point bend specimens, Figure 7.2.11, has been initiated to establish the factors that govern the initiation of DHC. The four point bend specimens are larger than the cantilever beam specimens and they also provide a constant deflection test which is more representative of the rolled joint situation than the cantilever beam test. Specimens with different hydrogen concentrations and hydride distributions will be subjected to a variety of test condition. Tests have also been performed to establish if scratches on the pressure tube as a result of fuel bundle movement could initiate delayed hydride cracking. The results of these tests indicate that fuel bundle scratches do not act as crack initiation sites.

To establish if the driving force for initiation would be increased by hydrogen supersaturation (ie, hydrogen levels in solution that are greater than the levels that occur by dissolution of hydrides) a test technique was developed to determine crack initiation under conditions of a continuous increase in hydrogen concentration. This condition can be achieved by setting up temperature gradients in the specimen such that the crack tip is in a uniform temperature zone which is at a lower temperature than the rest of the specimen, Figure 7.2.12. This temperature gradient results in the hydrogen diffusing to the crack tip region.

Crack Growth

Crack growth studies have received more attention than initiation. The determination of the influence of metallurgical variables and operating parameters on the crack growth rate is important for the development of a

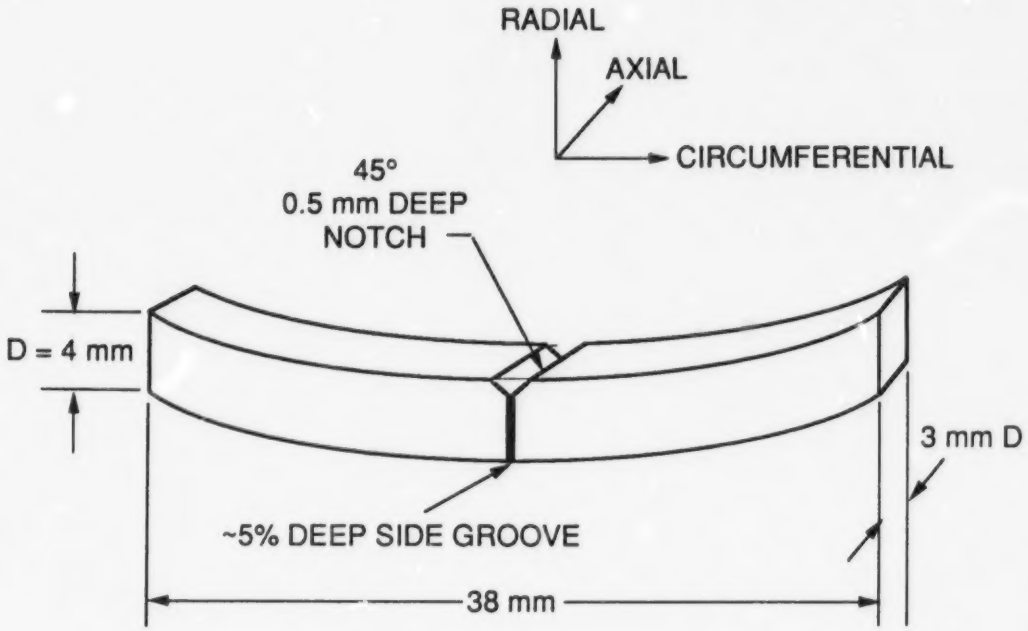

FIGURE 7.2.10

CANTILEVER BEAM TEST SPECIMEN USED TO STUDY THE DELAYED HYDROGEN CRACKING BEHAVIOUR OF Zr-2.5 Nb SHOWING ORIENTATION RELATIVE TO THE PRESSURE TUBE FROM WHICH IT WAS CUT

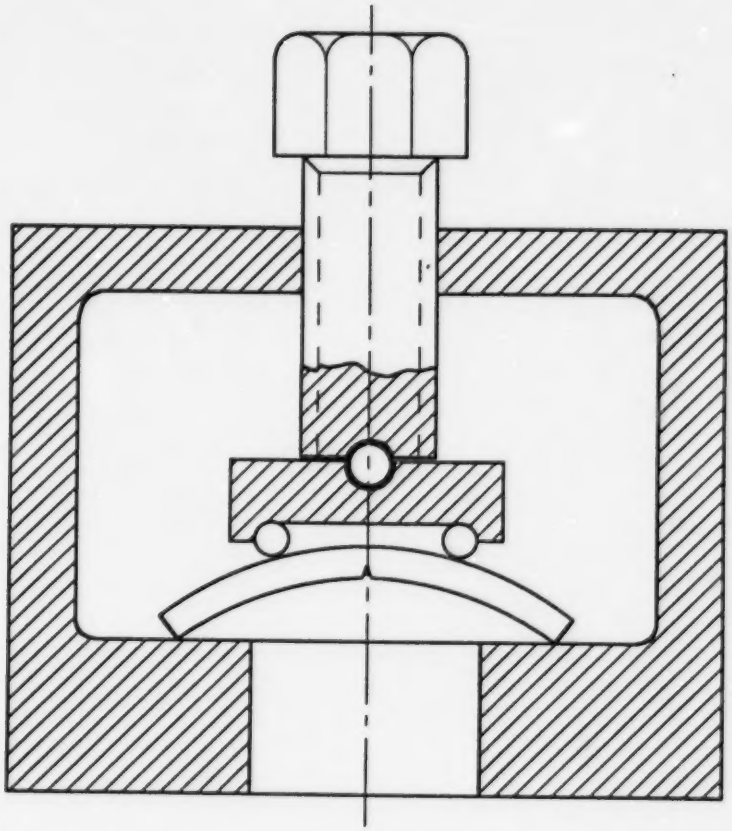

FIGURE 7.2.11

SCHEMATIC DIAGRAM FOR THE 4 POINT BEND LOADING
(W.K. Lee OHRD)

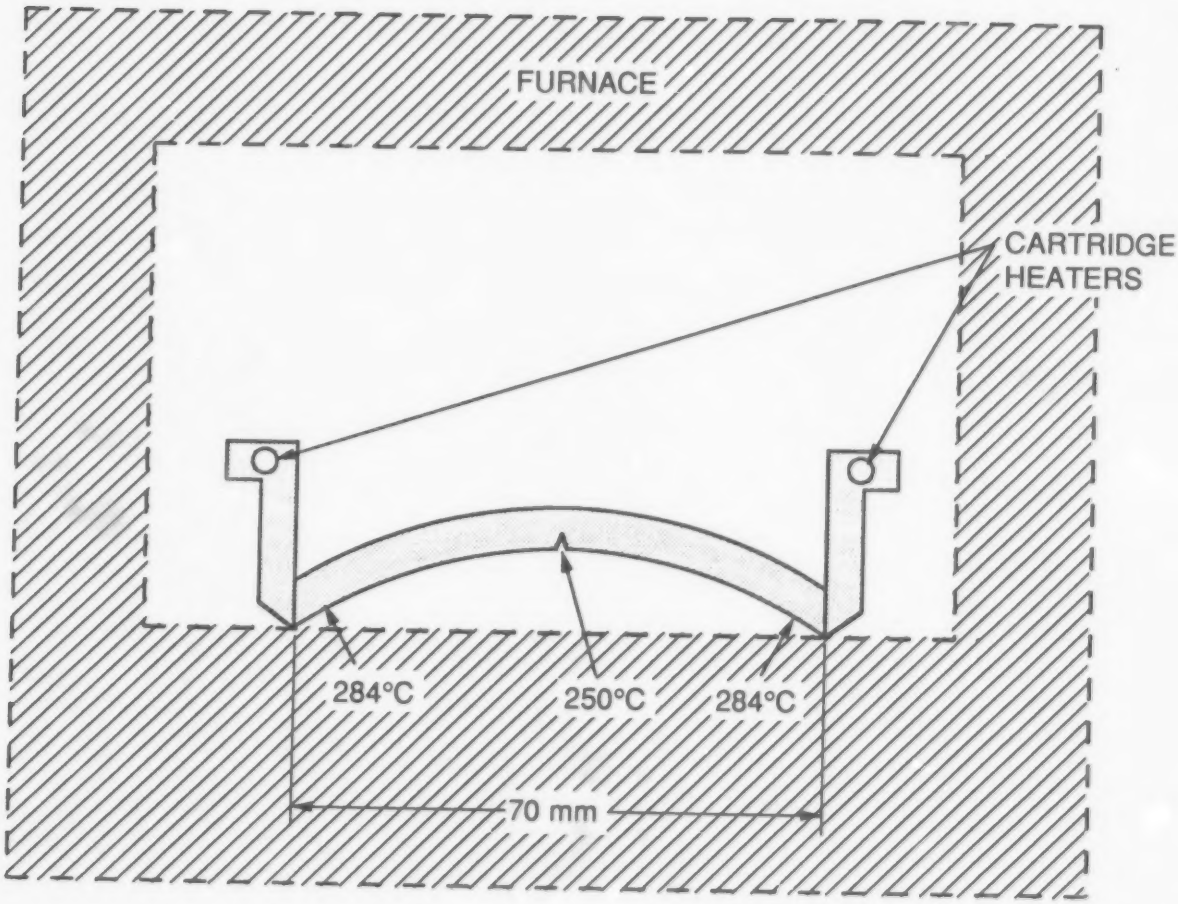

FIGURE 7.2.12

SPECIMEN USED TO INVESTIGATE CRACK INITIATION INTO A REGION OF CONTINUOUS INCREASE IN HYDROGEN CONCENTRATION (W.K. Lee OHRD)

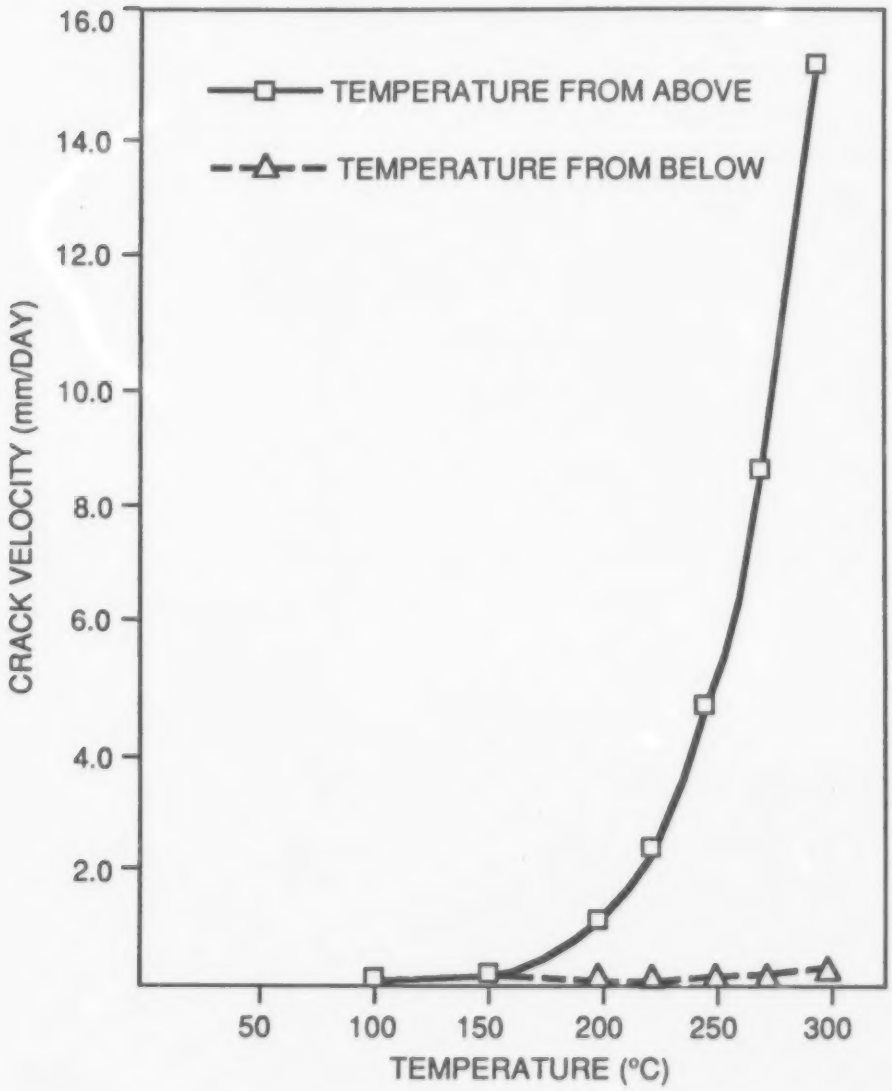

FIGURE 7.2.13

THE EFFECT OF DIRECTION OF APROACH TO TEST TEMPERATURE ON THE SUBSEQUENT VELOCITY OF DELAYED HYDRIDE CRACKS (G.K. Shek OHRD)

predictive model. The initial rolled joint failures, in the early 1970's, occurred at low temperatures with the reactors in a cold shut down condition. However, with time the hydrogen concentration in the critical rolled joint region is increased and crack growth at operating temperatures could occur. Figure 7.2.13 illustrates the influence of temperature on the crack growth rate. Further tests are underway to establish the actual crack growth rate under operating conditions in order to determine the time available to detect a leaking crack before it grows to a critical size. Along with the increase in hydrogen concentration with time the hydride distribution will also change and the role of the hydride size and orientation on the growth rate must be established.

To reduce the incidence of crack growth on reactor shut down a modified cool down procedure was put in place based on results from laboratory tests. These tests demonstrated that crack growth could be significantly reduced if the designated hold temperature was approached from below as opposed to a straight cool down to the final hold temperature, Figure 7.2.13. If a pressure tube leak has been detected, by annulus gas dew point rise it is often necessary to use a temperature maneuver in the depressurized condition to increase the leak rate in order to locate the defected pressure tube. Laboratory tests have shown that for the depressurized shut down condition an incubation time is required before DHC will resume, Figure 7.2.14.

To study the influence of microstructure and reactor operating parameters on the growth rate compact tension specimens are used (Figure 7.2.15). The crack extension is monitored by measuring the change in an electrical potential across the crack due to an applied current or by acoustic emission.

Critical Crack Size

Typically cracks grown by the DHC process in pressure tubes penetrate the tube wall when their length is about four times their width ie, penetration of the 4 mm wall occurs when the cracks are 16 mm long, Figure 7.2.16. When the Bruce 2 pressure tube ruptured in attempts to find a DHC, the reactor was pressurized cold. Under these conditions the crack was of the critical size and fast fracture occurred.

The tube rupture in Pickering Unit 2 was an example of "break-before-leak" as the crack initiated and reached a critical size before penetration of the tube wall occurred. There is now a need to identify the parameters that can influence the growth rate of delayed hydride cracks and the fracture toughness of pressure tube material. If the DHC growth rate is too fast then a critical size could be reached before a leak can be detected and if the fracture toughness is decreased then the critical crack length is reduced. Both these effects could result in the loss of "leak-before-break" assurance.

Fracture toughness is a measure of the resistance of a material to fast fracture. The concern is to determine at what size (length) a crack becomes unstable. Two techniques are used to measure the fracture toughness in pressure tubes i) sections of pressure tube have a known crack machined into

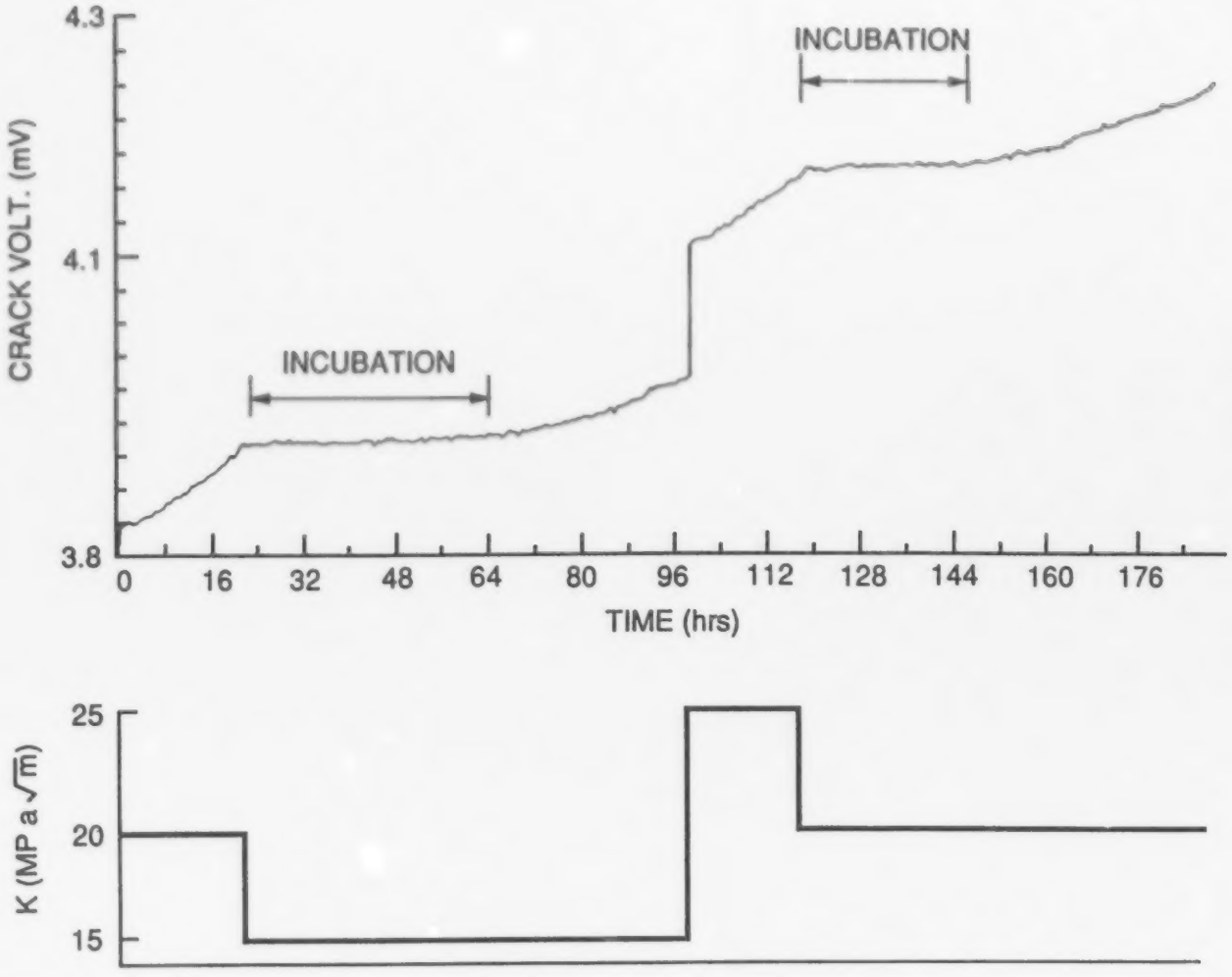

FIGURE 7.2.14

CRACK GROWTH DEPENDENCE ON STRESS CONCENTRATION, K. AFTER A DECREASE IN K THERE IS AN INCUBATION PERIOD BEFORE CRACKING OCCURS AT THE LOWER K VALUE.

89-271
FLECK 29
CAZ-4

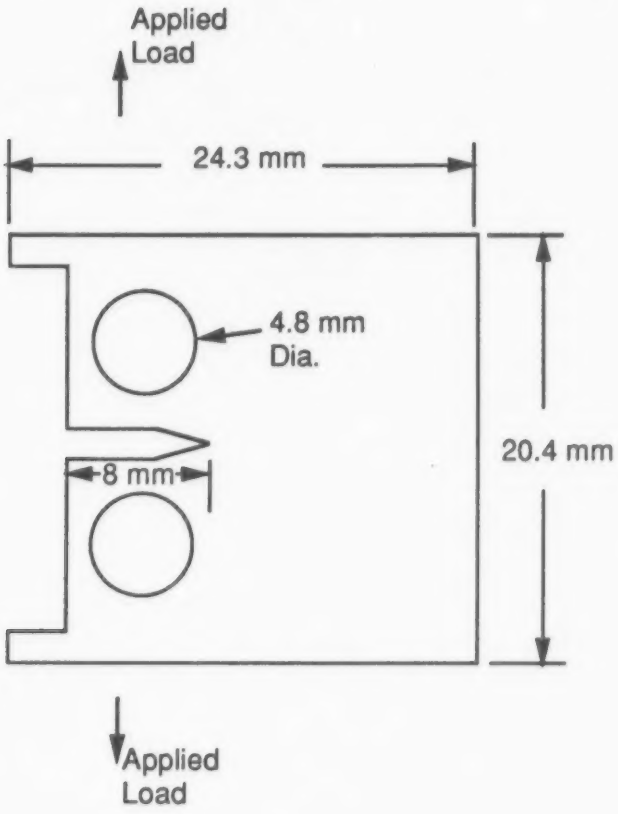

FIGURE 7.2.15

SCHEMATIC DRAWING OF A COMPACT TENSION SPECIMEN

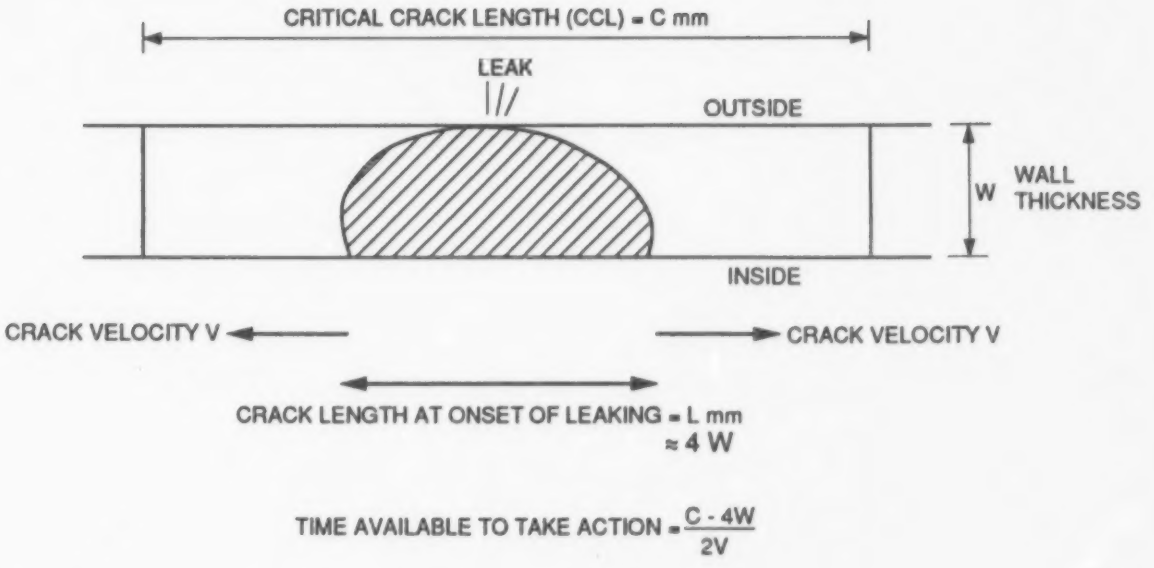

FIGURE 7.2.16

SCHEMATIC DIAGRAM TO SHOW CRACK DIMENSIONS AT ONSET OF LEAKAGE

them and ii) small specimens are machined from a pressure tube and a known flaw introduced into the specimen. In both cases the specimens are loaded until fast fracture occurs and the fracture toughness is calculated from the length of the crack and the stress required to cause fracture.

If the fracture toughness of the material is decreased with time in service there is the possibility that innocuous flaws for an "as manufactured tube" could become a source of concern for tubes late in life. The fracture toughness can change as a result of irradiation damage and hydrogen pick up, through the subsequent distribution of the hydrides.

Blisters

The rupture of the Zircaloy tube in Pickering Unit 2 in 1983 was a result of a number of contributing factors: i) the hydrogen levels were much higher than anticipated and hydrides were present at operating temperatures; ii) the operating hoop stress in the Zircaloy tubes resulted in hydride re-orientation along the length of the tube; iii) the pressure tube had sagged into contact with the calandria tube, Figure 7.2.17, which resulted in a steep, through wall, temperature gradient in the pressure tube. Hydrogen diffused down the temperature gradient and subsequently solid hydride blisters formed on the outside wall of the pressure tube, Figure 7.2.18. The time required for sag to contact had been less than anticipated due to the garter springs not being in their design locations. A crack initiated from a blister. The crack grew apparently by DHC (perhaps accelerated by the presence of large quantities of radial hydride) but took on an elongated shape partly due to the temperature gradient through the wall of the pressure tube. Unstable crack growth occurred before the crack penetrated the wall. Examination of the failed tube indicated the region of crack growth but the precise nucleation site or mechanism could not be identified.

A comprehensive study on hydride blisters in pressure tubes was put in place after the tube ruptured in Pickering Unit 2. The studies considered the factors which influence blister growth and the parameters which result in crack formation from the blisters. Initially the most important aspect of the studies was to establish whether or not blisters could be formed in Zr-2.5 wt% Nb pressure tubes similar to those which were found in the Zircaloy tubes. It was quickly demonstrated that hydride blisters could be formed on Zr-2.5 wt% Nb.

Blister growth studies have concentrated on Zr-2.5 wt% Nb. Two techniques to grow blisters on a laboratory scale have been used: 1) an air jet impinging on the surface of a hot section of pressure tube and 2) contact of a hot section of pressure tube with a cold surface. A loop test was also used where a section of pressure tube was put in contact with a section of calandria tube and the pressure tube was removed for periodic inspection. Blisters have been grown under a variety of conditions to try and reproduce the morphologies and shapes as detected in the pressure tubes and to test the predictive capabilities of the blister growth model as developed by OHRD.

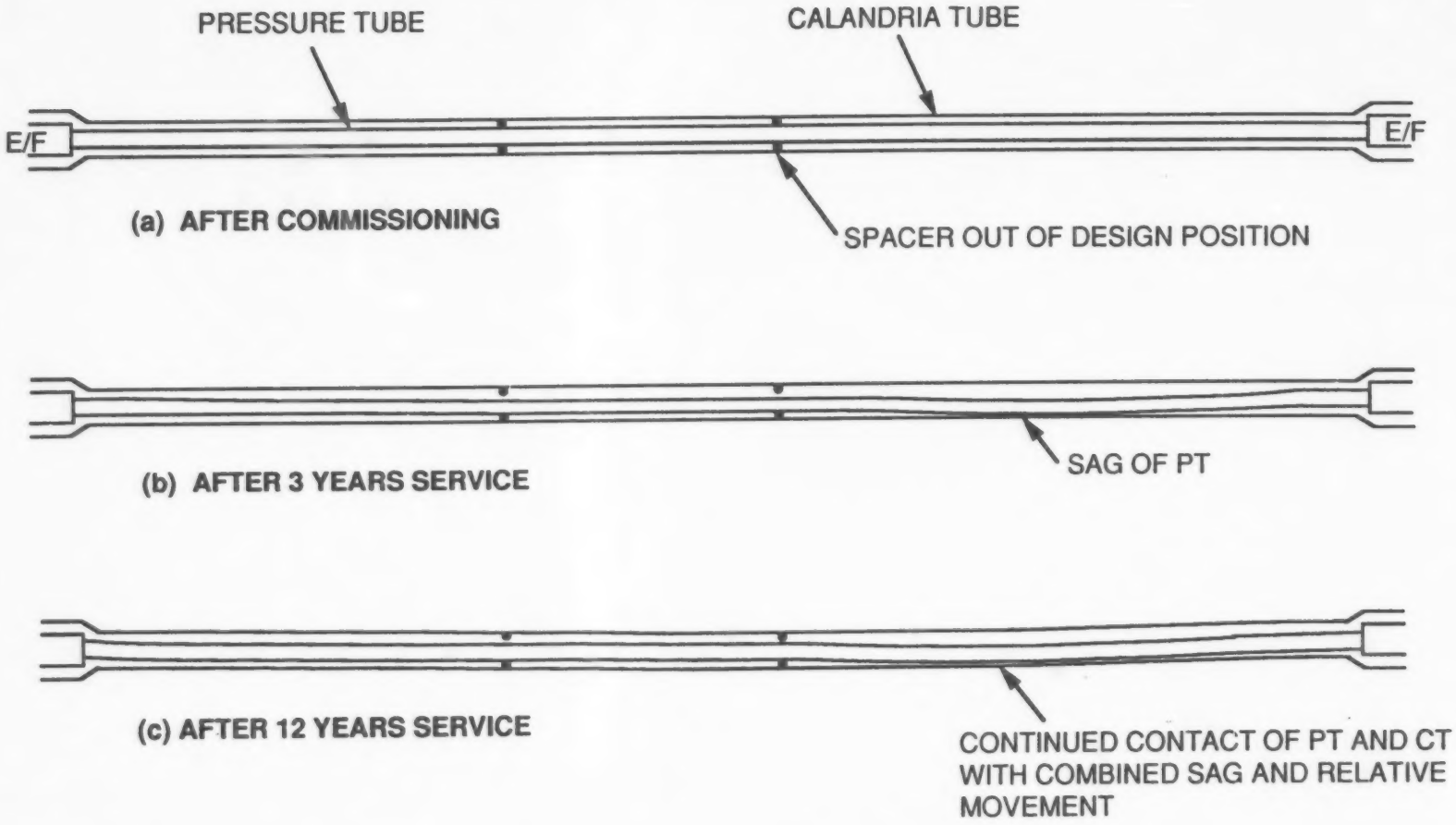

FIGURE 7.2.17

PRESSURE TUBE SAG INTO CONTACT WITH CALANDRIA TUBE AS A RESULT OF A SPACER MOVED OUT OF DESIGN POSITION AS A RESULT OF VIBRATION DURING INSTALLATION AND COMMISSIONING
(From Price - Bibliography 6.0)

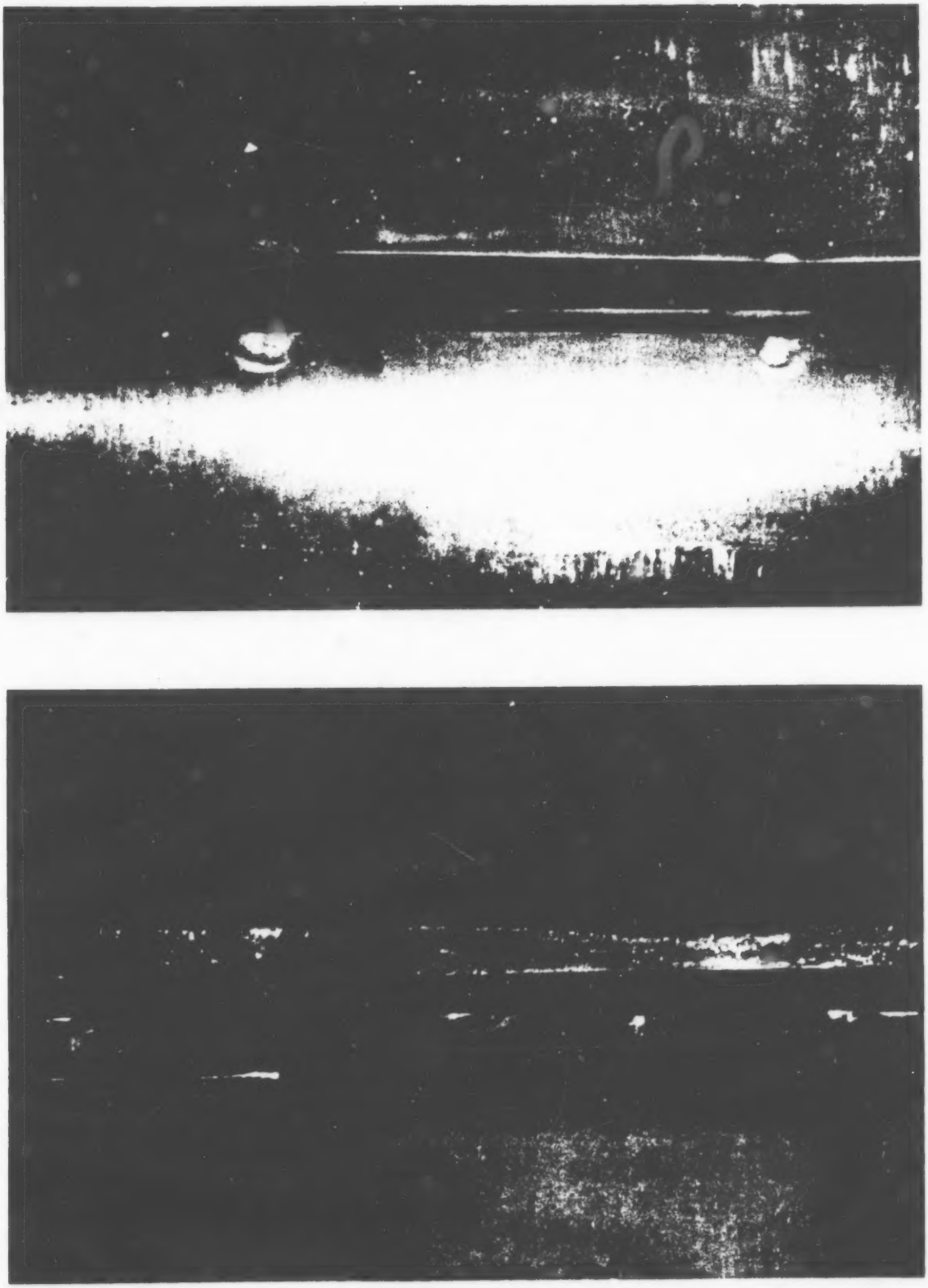

FIGURE 7.2.18
HYDRIDE BLISTERS ON A PRESSURE TUBE

The model has proved to be successful in predicting the size, shape and concentration gradients within the blister. The concentration gradients were measured at Queen's University by an ion irradiation using He_3 ions at 1.3 MeV which results in the emission of protons when the helium ions interact with the deuterium atoms. Figure 7.2.19 illustrates the agreement with the predictions of the model with the actual concentration gradients measured at Queen's.

The actual sequence of events which led to the pressure tube rupture in channel G16 of Pickering Unit 2 have not been clearly established i.e. the mechanism of initiation of the crack which resulted in the failure has not been determined. There are two possibilities: i) a delayed hydride crack was initiated in the matrix as a result of the stress distribution associated with the blister or ii) a crack grew from a blister into the matrix and then propagated by a delayed hydride crack mechanism. Observations of blisters on G16 and other tubes showed that only in G16 were there blisters that had cracks extending into the matrix. In the other tubes the cracks were contained within the blisters. From laboratory tests it has been established that the larger the blister, the lower the stress required to crack the blisters, Figure 7.2.20.

In the Zircaloy pressure tubes, the hydrides were reoriented which would make the material brittle. From tests on Zr-2.5 wt% Nb material, it is observed that in the immediate vicinity of the blister there is hydride reorientation but this does not extend through the tube wall. The stress to reorient the hydrides in the Zr-2.5 wt% Nb is higher than for Zircaloy, but the formation of blisters generates stress that must locally exceed the reorientation stress in Zr-2.5 wt% Nb.

7.3 Hydrogen (Deuterium) Ingress and Corrosion

There are two areas of the pressure tube where hydrogen ingress occurs: 1) the rolled joint and 2) along the length of the tube. Each area will be discussed separately.

Rolled Joint

There is a high rate of hydrogen ingress into the rolled joint region of the pressure tube. This could be of concern for crack initiation late in life even if the residual stresses due to rolling are significantly reduced by creep processes. The solutions to the rolled joint cracking problem were aimed at elimination of the Pickering 3 & 4 type cracks which occurred early in the life of the reactor as a result of high residual stresses from the rolling operation. With time any residual stresses in the rolled joint will decrease by stress relaxation due to the temperature of operation and to some extent the fast neutron flux. However, a concern for operation, late in life, is the local build up of hydrogen in the pressure tube in the rolled joint region. The possibility is that rolled joint cracks could occur, even at the lower stress levels present late in reactor life, as a result of high hydrogen concentrations. Figure 7.3.1 illustrates the increase in hydrogen

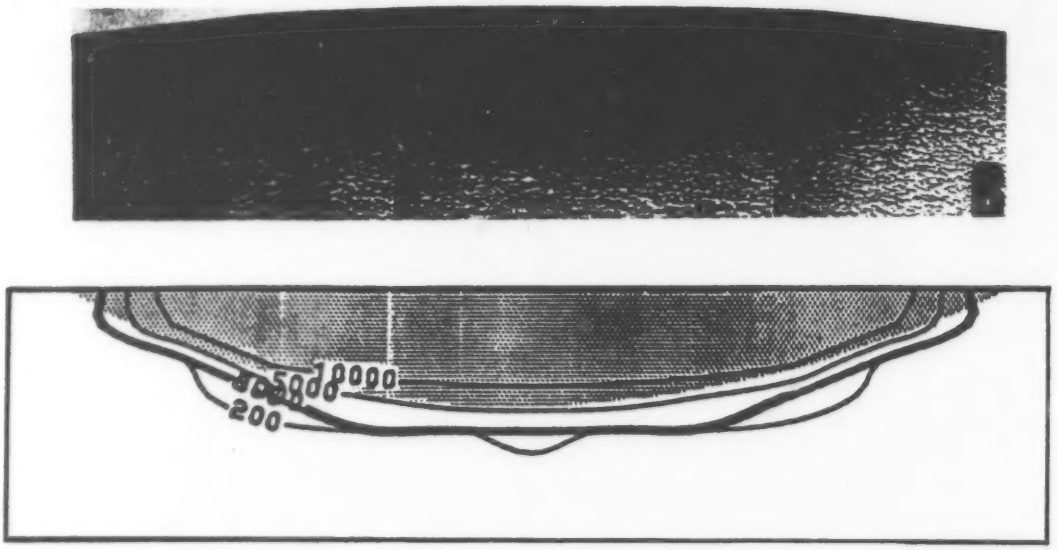

THE TOP FIGURE IS A MICROGRAPH (40X) OF A DEUTRIDE BLISTER AFTER 42 DAYS GROWTH
THE BOTTOM FIGURE ILLUSTRATES THE ABOVE BLISTER AS THE SHADED AREA WITH
ISO-CONCENTRATION (ppm) LINES CALCULATED FROM THE GROWTH MODEL SUPERIMPOSED

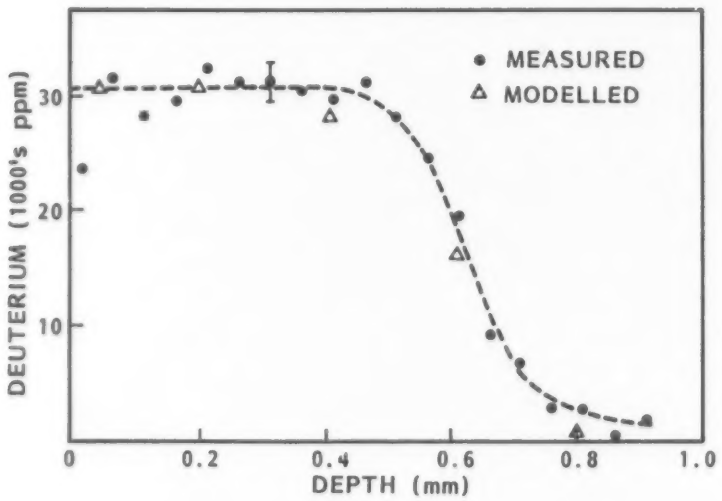

FIGURE 7.2.19

COMPARISON OF MEASURED AND CALCULATED DEUTERIUM PROFILES THROUGH THE BLISTER SHOWN IN THE ABOVE MICROGRAPH (M. LEGER OHRD)

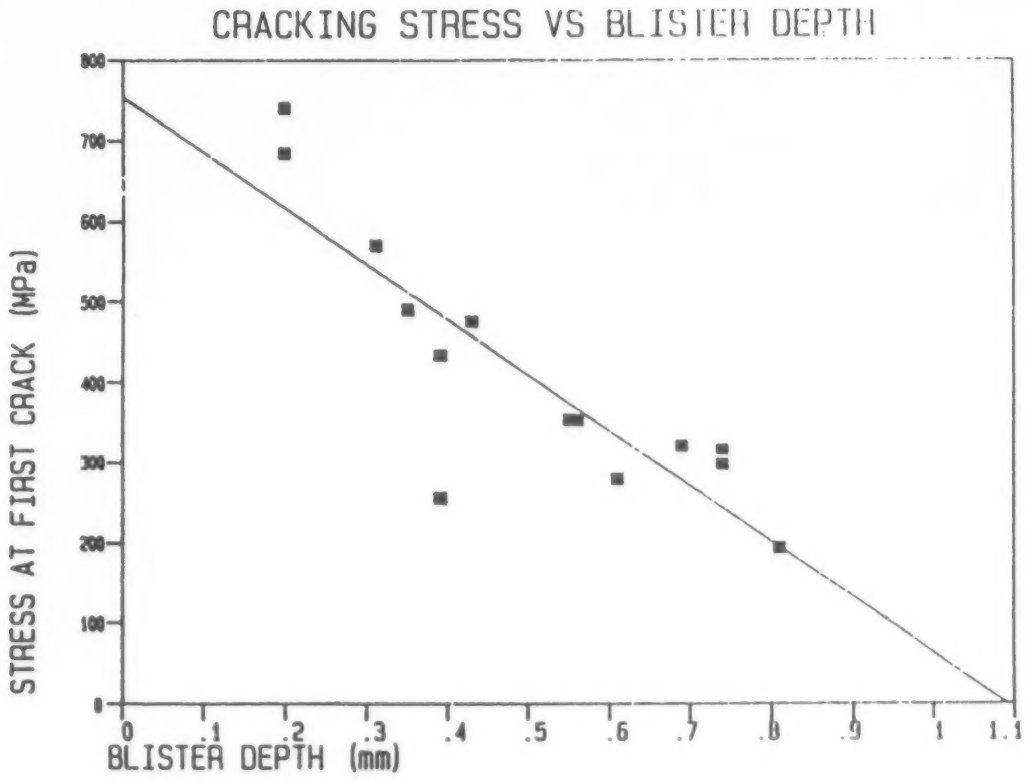

FIGURE 7.2.20

APPLIED TENSILE STRESS TO CAUSE CRACKING PLOTTED AGAINST BLISTER DEPTH FOR ALL BLISTERS
(A.C. Wallace - OHRD)

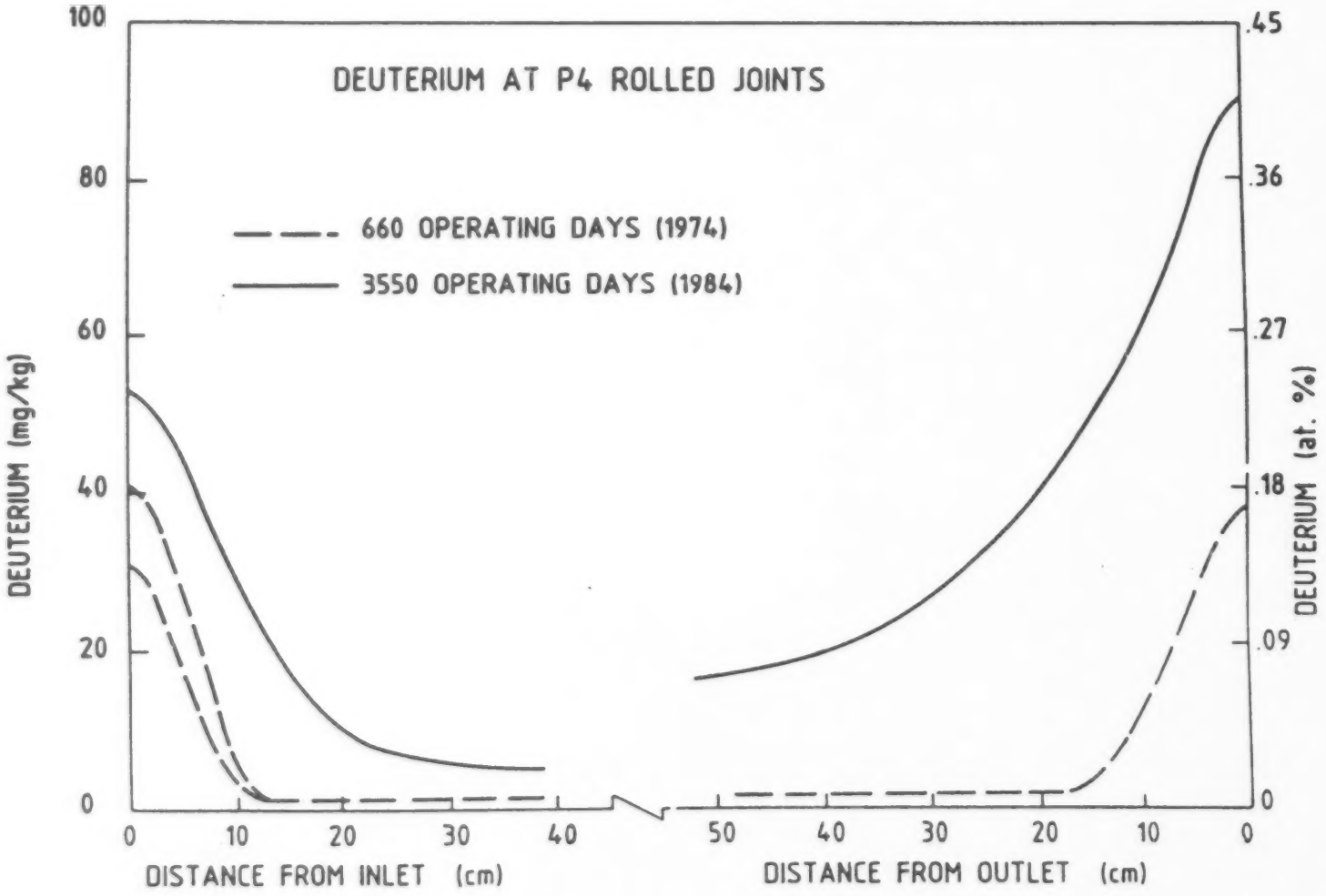

FIGURE 7.3.1

DEUTERIUM BUILDUP AT PRESSURE TUBE ENDS OF PNGS UNIT 4 FUEL CHANNELS
(From Urbanic - Bibliography 9.0)

concentration, as a function of operating time, in the rolled joint region. In considering the hydrogen build up in the rolled joint region of the pressure tube there are two aspects: i) the source of the hydrogen and ii) the ingress route.

i) The source of hydrogen could be from the hydrogen added to the PHT coolant, to prevent corrosion, or from galvanic corrosion as a result of the electrochemical potential differences between the stainless steel end fitting and the pressure tube. Out reactor tests of rolled joint assemblies in loops with water chemistries in the range 0-30 cm^3/L of hydrogen (operating levels are in the range 3-10 cm^3/L) are underway to establish if the dissolved hydrogen is the source of the rolled joint hydrogen. To establish if galvanic corrosion is the source, tests with small diameter titanium end fitting hubs are underway (the electrochemical potentials of titanium and zirconium are similar). The results from these test programs indicate that the galvanic coupling is the source of the hydrogen which enters the rolled joint region of the tube.

ii) A number of routes for the hydrogen to enter the pressure tube have been proposed, Figure 7.3.2.

Route 1. The hydrogen is proposed to preferentially enter the pressure tube at this location as the inside surface oxide will have been damaged by the rolling process. Under normal conditions the oxide on the pressure tube acts as a very effective barrier to hydrogen ingress. To establish if this route is significant for hydrogen ingress strips of pressure tube with a damaged (from rolling) inside surface oxide layer were exposed in the RD5 loop at AECL-RC, Whiteshell. After 50 days the damaged oxide had been repaired and the hydrogen distribution in the strips was uniform. Once the oxide layer has been repaired it will act as a barrier to hydrogen ingress.

Route 2. Data from power reactor and test loop rolled joints indicate that the ingress rate is decreasing with time. This is consistent with Route 2 where the hydrogen diffuses down the crevice and enters the pressure tube in the region where the outside surface oxide, of the pressure tube, has been damaged by the rolling. With time this oxide will be repaired and the ingress rate will decrease as observed.

Route 3. To establish if hydrogen can diffuse through the end fitting to the rolled joint and as in Route 2, enter the pressure tube through the damaged OD oxide, a number of different tests have been performed. From the analysis of zirconium discs embedded in some test end fittings (E/F) the diffusion of hydrogen along the E/F was confirmed. Tests with an Inconel E/F (lower permeability for hydrogen than stainless steel) did not reduce the level of hydrogen entering the pressure tube in the rolled joint when compared to the use of a standard E/F. The implication from these tests is that the hydrogen does diffuse along the E/F but this is not the dominant route for hydrogen to enter the pressure tube. Tests on a chrome plated rolled joint assembly have shown a significant reduction in the hydrogen levels in the pressure tube.

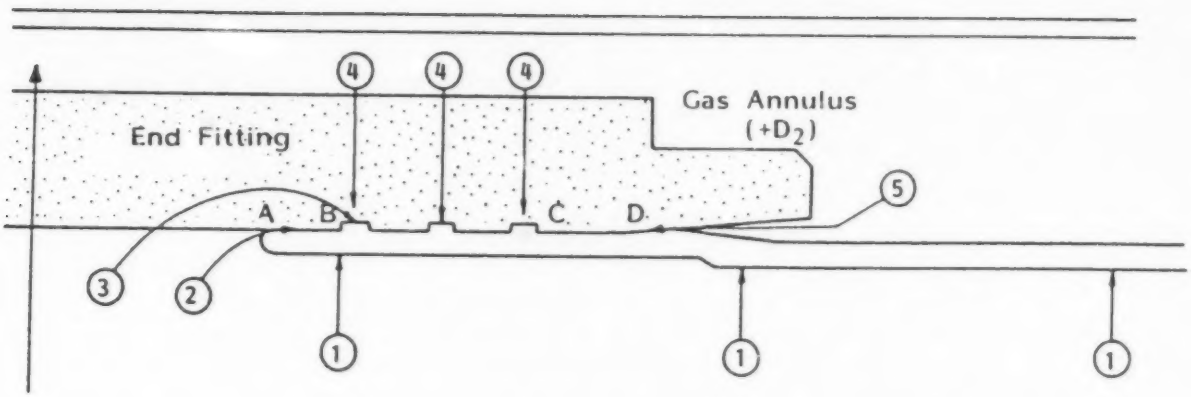

D_2O Coolant (+ Dissolved D_2)

AB = Outboard Crevice CD = Inboard Crevice

FIGURE 7.3.2

POTENTIAL ROUTES FOR DEUTERIUM INGRESS
AT ROLLED JOINTS
(From Urbanic - Bibliography 9.0)

This result could imply that the chrome acts as a barrier for the hydrogen to enter the pressure tube from the rolled joint or that the production of hydrogen has been reduced by a reduction of the electrochemical potential between the pressure tube and the end fitting.

Route 4 & 5. Ingress from the annulus gas either by diffusion through the E/F or down the pressure tube/end fitting crevice has been shown to only account for less than 10% of the hydrogen in the pressure tube. This result comes from tests of rolled joint assemblies on the RD5 loop at AECL-RC, Whiteshell.

From the above studies to investigate the source and ingress route for hydrogen in the rolled joint region of the pressure tube a number of potential techniques to limit the hydrogen build up have been proposed. To date the most practical solution is the use of the chrome plating which is undergoing further development to establish if it can be used in future reactors.

Yttrium has a higher affinity for hydrogen than zirconium and the possibility of combining yttrium with zirconium has been investigated. The proposals have tried to establish if the yttrium could be used as a sink for the hydrogen in the zirconium. At one stage zirconium/yttrium alloys were made but they had very poor corrosion properties. The possibility of an external sink has been investigated such that the yttrium would be attached to the outside surface of the pressure tube. For the rolled joint situation a yttrium sink concept was developed such that the yttrium would be encapsulated in a zirconium alloy and that assembly would be welded onto the end of the pressure tube, Figure 7.3.3. In laboratory trial tests the hydrogen in the rolled joint area diffused to the yttrium sink. Extensive development work was carried out to establish if the sinks could be used in future rolled joints such as in the large scale fuel channel replacement programs for Pickering and Bruce.

In the trial testing of the yttrium sinks it was difficult to hydride the yttrium to the projected end of life hydrogen levels. This type of test is important to establish if the sink will remain intact throughout the service life of the fuel channel. Modelling of the stress distributions in the sink indicated that areas of high local stress could be developed. These stress levels were such that delayed hydride cracking of the Zircaloy encapsulation was predicted to be possible. If the encapsulation failed such that the yttrium became exposed to the primary heat transport water the yttrium would oxidize and swell such that fuel passage would be restricted. As a result of the difficulties in demonstrating that failure of the encapsulation is unlikely the application of the yttrium sinks in future rolled joints has not been accepted. Development work continues at AECL-RC (Whiteshell).

Length of the Tube

The high hydrogen contents found in the Pickering 1 & 2 Zircaloy pressure tubes is considered to be a result of a faster than anticipated corrosion process. The analysis of the Zircaloy tube showed that the hydrogen concentration along the tube followed a similar profile as the oxide thickness, Figure 7.3.4, although the hydrogen peak was generally narrower

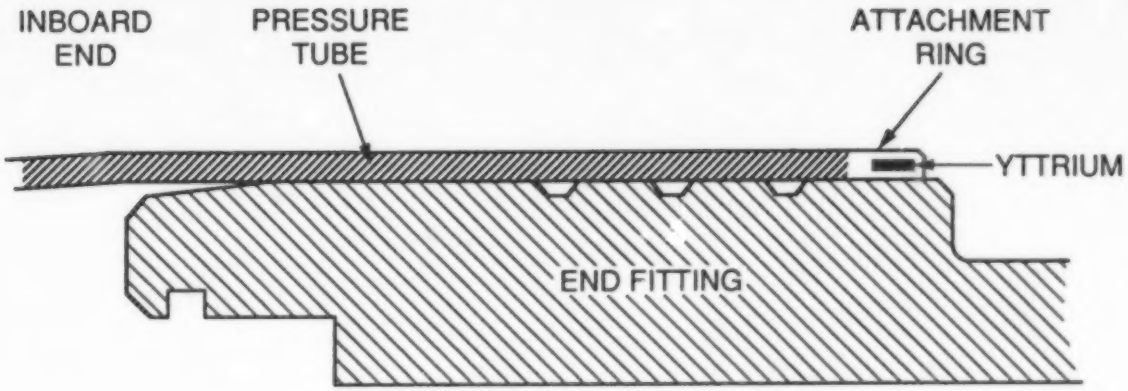

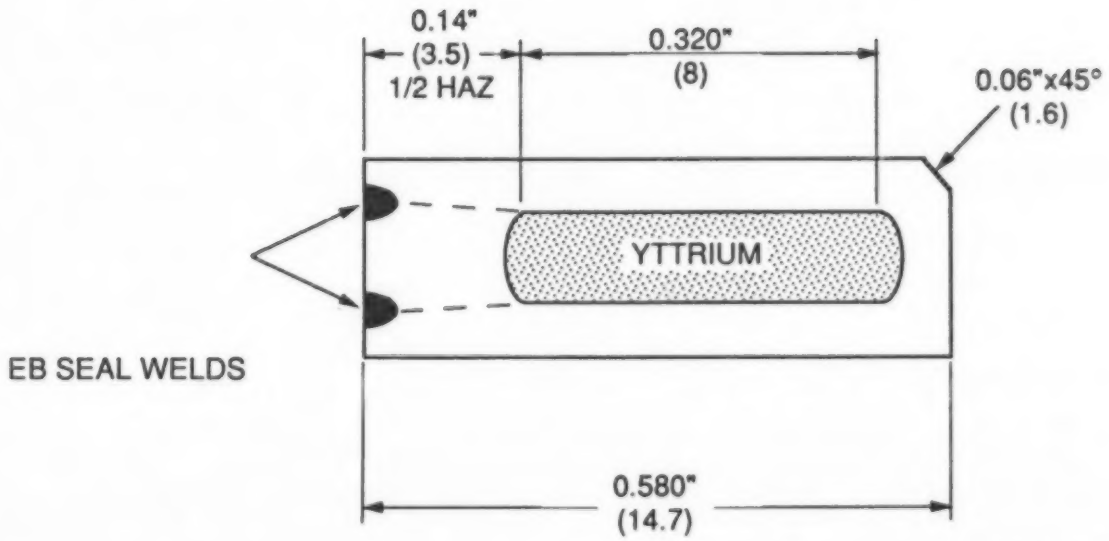

DIMENSIONS SHOWN IN
BRACKETS ARE IN
MILLIMETERS)

FIGURE 7.3.3

LOCATION OF YTTRIUM SINK, ATTACHMENT RING ON PRESSURE TUBE IN RELATION TO ROLLED JOINT

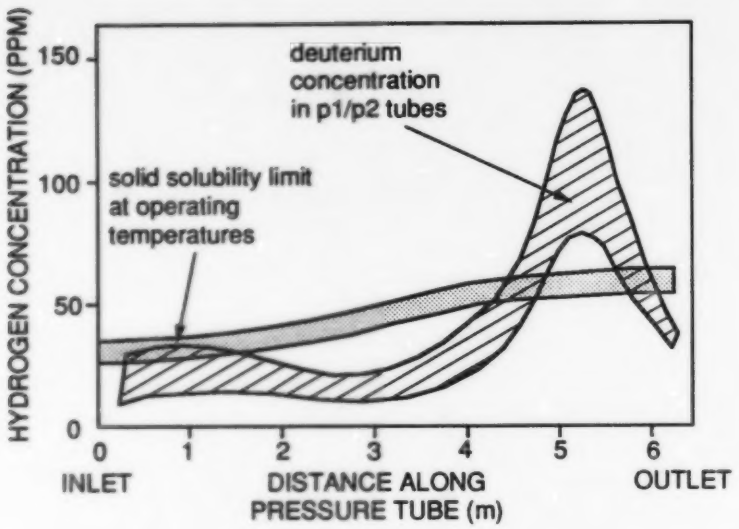

DEUTERIUM CONCENTRATION

The Zircaloy-2 pressure tubes in units 1 and 2 (P1/P2), of Pickering Generating Station, developed a particular deuterium concentration profile in channels in high flux zones. Analysis of the outlet ends of each tube showed an area of tube where hydride was present at operating temperature.

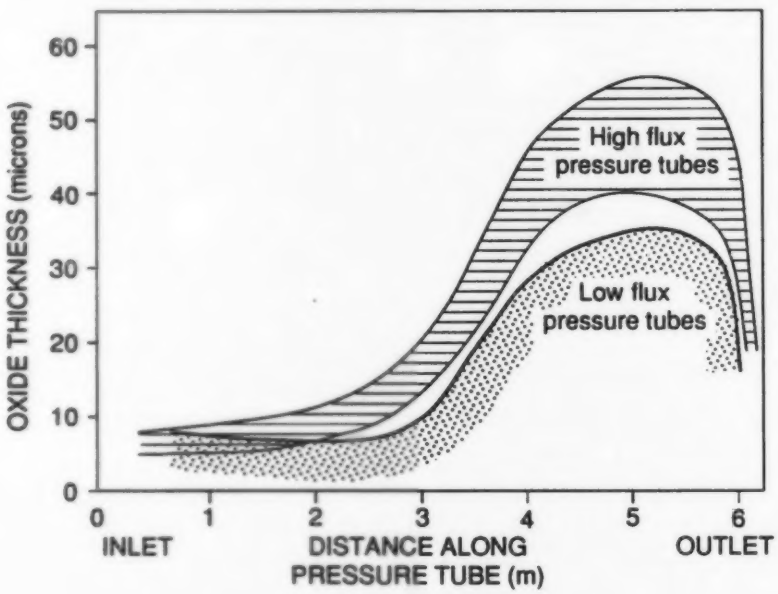

FIGURE 7.3.4

CORROSION OF PICKERING 1 AND 2 ZIRCALOY-2 PRESSURE TUBES

The Zircaloy-2 pressure tubes in Pickering units 1 and 2 had peak oxide thicknesses towards the outlet ends of the tubes where the combination of temperature and fast neutron flux were most severe. At the outlet end, the tube corroded at a faster rate than the rest of the tube, to a threshold oxide thickness of 15 to 20 microns. Oxide thickness greater than the threshold sustained a local water chemistry that was not affected by the bulk water chemistry. This allowed radiolysis within the oxide pores to generate a separate oxidizing water chemistry.

(From Price - Bibliography 6.0)

FLECK-27
CAZ-4

than the oxide peak. As the pressure tube oxidizes some of the liberated hydrogen is absorbed by the tube. For Zircaloy about 90% of the liberated hydrogen from the corrosion process is picked up by the tube. The main problem was the increase in the corrosion rate after about five full power years of operation. The increase in the oxidation rate has been attributed to development of an oxidizing water chemistry, which is independent of the bulk coolant chemistry, within the thick oxides.

Although previous indications were that the hydrogen pick up in Zr-2.5 wt% Nb would be lower than in Zircaloy measurements of the hydrogen concentration in tubes in Pickering 3 & 4 (prior to large scale fuel channel replacement) indicate that the increase in hydrogen concentration is faster than expected but the rate is lower than that observed in the Zircaloy tubes. The concern with the observations in the Zr-2.5 wt% Nb tubes is that the hydrogen levels could reach levels where blister formation would be of concern in the units where the garter springs are displaced from their design locations. Even in units where the garter springs are properly located the effects of high hydrogen levels on the service life of the pressure tubes would have to be established. From measurements of the oxide thickness on the inside surface of the pressure tube it would appear that the source of the hydrogen is not from the corrosion process. The observations indicate that excessive corrosion has not occurred in these tubes. There is also no evidence to indicate that the percentage pick-up of the hydrogen from the corrosion process has increased above the expected 10% level for Zr-2.5 wt% Nb.

An area of investigation is the ingress of hydrogen from the gas annulus. This is a possibility if the oxide on the outside surface of the pressure tube is not maintained due to a lack of oxygen in the gas annulus system. There are some indications that in fact the outside surface oxide is not protective and that hydrogen could therefore enter the tube. The technique used to establish the protective nature of the outside surface oxide is to measure the local resistivity of the oxide. A high resistivity indicates that the oxide is protective whereas a low resistivity suggests that there are open paths through the oxide to the metal surface. The results show that there is a similarity in the profile of the oxide breakdown with the hydrogen concentration profile, Figure 7.3.5. Hydrogen in the gas annulus is present as a result of diffusion through the end fitting and radiolysis of water in the gas annulus.

To prevent the build up of hydrogen along the length of the tube would require detailed knowledge of the source and ingress routes. For a gas annulus source and ingress through the outside surface oxide the solution would be to ensure that the gas annulus is oxidizing. This would keep the outside surface oxide in good repair which would prevent the ingress of hydrogen, in the gas annulus, into the pressure tube. To maintain the outside surface oxide intact it is required to add oxygen to the gas annulus even for the CO_2 systems. If the main source is the hydrogen in the bulk coolant, with ingress through the inside surface oxide, the solution becomes much more difficult. The hydrogen in the bulk coolant is required to prevent oxidation of the materials in the primary heat transport system and it would be

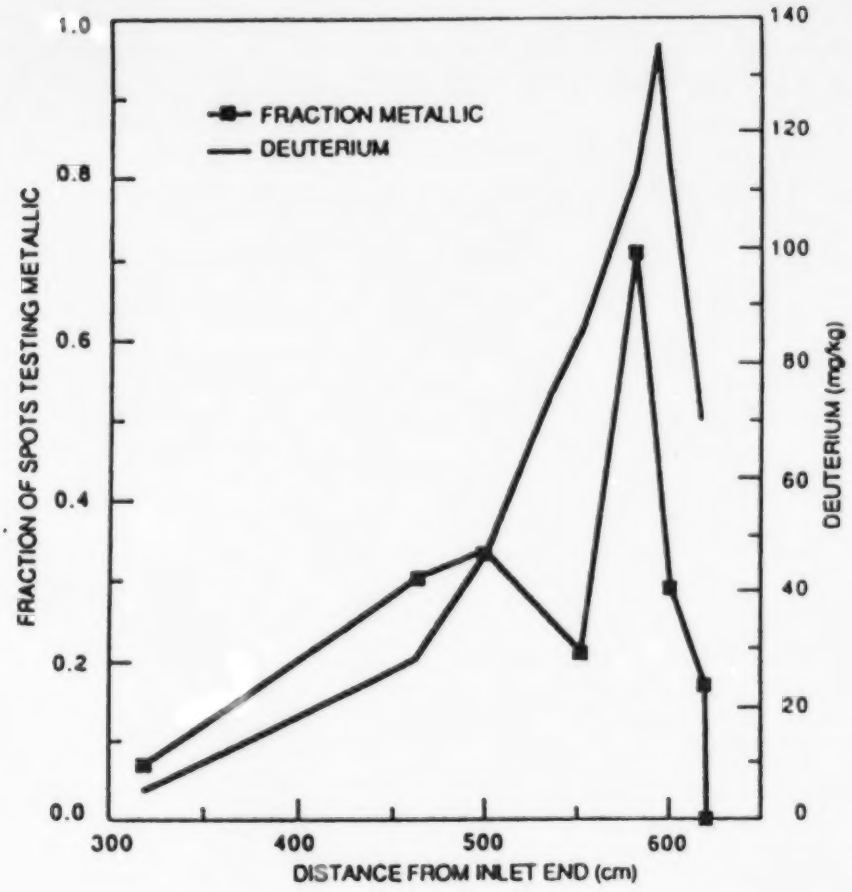

FIGURE 7.3.5

BREAKDOWN OF PROTECTIVE OXIDE ALONG THE OUTSIDE OF P3L09 COMPARED TO DEUTERIUM CONCENTRATION (From Lichtenberger - Bibliography 9.0)

difficult to predict the influence of changes to the coolant chemistry on the performance of the primary coolant materials. Hydrogen pick up as a result of an accelerated corrosion process could also occur as was the case with the Zircaloy tubes. To prevent this mechanism from operating a more reducing bulk chemistry would be desirable which would present the same type of problem as a change to an oxidizing chemistry.

The basic problem with studies on hydrogen pick-up is that accelerated tests are difficult and it is also not well established that out reactor test can give good indications of in reactor behaviour. A detailed research program is in place which covers a wide range of investigations from chemistry effects of the coolant to the role of trace elements in the pressure tube alloy. As with other studies on the effects of irradiation on the performance of pressure tubes an important aspect is the evolution of the microstructure. Effectively the alloy can change from exposure to service conditions such that the distribution of the alloy or trace elements could be substantially different to the initial distribution. Precipitates in the alpha zirconium grains have been observed after exposure to neutron irradiation which are not present in unirradiated material. Such precipitation could change the corrosion and hydrogen pick-up characteristics of the alloy.

8.0 ALLOY DEVELOPMENT

The initial alloy used for pressure tubes was Zircaloy which was a development from the USA nuclear program. There are two types of Zircaloy that have been used: Zircaloy 2 and Zircaloy 4. The composition of these alloys is presented in Table 4.1. For pressure tubes Zircaloy 2 was used and the Zircaloy 4 is used for fuel cladding.

The Russian nuclear program had developed Zr-Nb alloys and reports of the better strength and improved creep properties of Zr-2.5 wt% Nb was of interest to the CANDU reactor. The improved strength would allow the use of a thinner walled pressure tube which would result in a higher fuel burn-up. The Zr-2.5 wt% Nb alloy was used in the CANDU reactors constructed after Pickering Unit 2. From Figure 4.2 it is seen that the alloy is in a eutectoid system similar to that of steels. This suggested that the alloy could be heat treated to further improve it's strength in a similar manner to that used for steels. Pressure tubes have been manufactured and given a heat treatment after extrusion. These heat treated tubes were used in the KANUPP and Gentilly 1 reactors. The Japanese also use heat treated Zr-2.5 wt% Nb pressure tubes in their Fugen reactor. Further use of such pressure tubes was not considered because in comparison to the cold worked Zr-2.5 wt% Nb pressure tubes there was: i) a reduced room temperature critical crack length; ii) lower stress for hydride reorientation and iii) a reduction in the ratio of transverse UTS/ longitudinal UTS. However, results from studies of a heat treated Zr-2.5 Nb pressure tube removed from NPD suggest that some further evaluation of this material should be performed.

An alloy development program at AECL-RC (CRNL) showed that zirconium alloys containing tin, molybdenum and niobium had higher strength than Zr-2.5 wt% Nb. From these studies AECL-RC developed the alloy Excel, the composition of which is shown in Table 8.1. Several pressure tubes have been made with this alloy and a tube has been irradiated in NRU. The fabrication of the tubes has considered the material in the "as extruded" condition as well as tubes cold worked 10-15%. From the in-reactor deformation aspects this alloy has some promise but it's main drawbacks are that it has a faster in-reactor corrosion rate and a faster DHC velocity than cold worked Zr-2.5 wt% Nb. There is the possibility that further studies could be performed on this alloy. If the DHC growth rate could be reduced and information from the corrosion studies on Zr-2.5 wt% Nb indicate how the corrosion resistance could be improved. Some work continues on this material with emphasis on the in-reactor testing of a tube in NRU.

TABLE 8.1

Composition of Alloy Excel

Element	Content
Sn	3.3 - 3.8 wt%
Mo	0.5 - 1.0 wt%
Nb	0.5 - 1.0 wt%
O	800 - 1300 ppm
Zr + imparities	balance

Another approach to alloy development at AECL-RC was to produce a zirconium alloy with an ordered atomic structure, Figure 8.1. This type of structure would make dislocation movement more difficult and would therefore reduce the rate of in-reactor deformation. The alloy developed was $Zr_3A\ell$ which is formed by the peritectoid reaction:

$$Zr + Zr_2A\ell \text{ --------> } Zr_3A\ell$$

A number of laboratory tests were performed on this material and some trial pressure tubes were made. The concept of the ordered alloy to improve in-service deformation worked against the fracture toughness of the material. The tubes were too brittle to be of practical value.

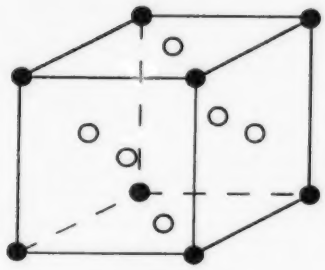

○ = Zr

● = Aℓ

FIGURE 8.1

ATOMIC ARRANGEMENT FOR THE ORDERED ALLOY Zr_3 Aℓ

9.0 SUMMARY

The discussions on the basic metallurgy of zirconium and on the metallurgical structure of Zr-2.5 wt% Nb illustrated the reason for the complexities encountered in the evaluation of the properties of pressure tubes. The anisotropy of the zirconium crystal structure results in the development of crystallographic texture in the pressure tubes which means their mechanical properties are anisotropic. A further complication is that the alloy Zr-2.5 wt% Nb is in a metastable state which results in phase changes occurring in operation. Added to these difficulties is the influence of fast (E>1MeV) neutron irradiation on the metallurgical structure of Zr-2.5 wt% Nb.

To understand the operational problems that have occurred with CANDU pressure tubes a detailed understanding of the points noted above has to be developed. The main concerns with pressure tube operation in CANDU reactors are: irradiation enhanced deformation, delayed hydride cracking and fracture, hydride blisters and corrosion and hydrogen ingress. In each of these areas detailed experimental programs are performed. An overview of these programs has been presented where the main purpose is to identify the factors that will limit the operational life of the pressure tubes. In some cases design modifications can alleviate the problem such as with pressure tube elongation and delayed hydride cracking at rolled joints.

From an understanding of the mechanisms that result in the above mentioned problems it would, in principle be possible to develop improved pressure tubes. The various programs to develop such tubes have been presented. However, the various development programs have been focussed on development of a material to overcome a specific problem. The difficulties that have occurred are that a solution to one problem often results in a decrease in one of the other key properties e.g. irradiation creep resistance may be improved but the resistance to delayed hydride cracking decreased.

The research programs address problems with pressure tubes identified in the operation of CANDU reactors. From the various research studies information is provided to establish the pressure tube life limits. This permits rehabilitation programs to be planned in advance which improves the reliabilty and economics of reactor operation. Another aspect of the research programs is that they provide a capability to quickly address pressure tube concerns. If a problem occurs with pressure tubes operation reactor down time will be minimized and relevant investigative programs established.

10.0 ACKNOWLEDGEMENTS

The information presented in this report has been obtained from written articles, and both formal and informal discussions with staff at AECL-RC, AECL-CO, Ontario Hydro and Ontario Hydro Research Division, particularly the staff of the Materials Integrity Section. Discussions with E.G. Price, B.A. Cheadle, S.R. MacEwen (now at Alcan) and P.C. Lichtenberger have been most informative. E.T.C. Ho, R.A. Holt and M. Leger also contributed through informative discussions as well as comments on draft copies of this report.

Approved by:

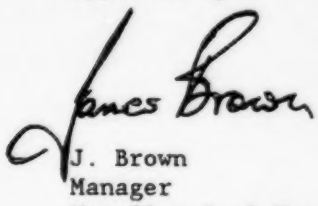

J. Brown
Manager
Metallurgical Research

Prepared by:

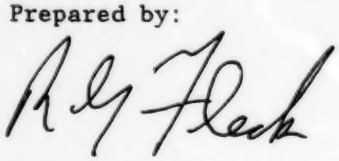

R.G. Fleck
Supervising Engineer
Metallurgical Research

BIBLIOGRAPHY

1.0 INTRODUCTION

Pickering 500, Pickering Generating Station, Hydro Electric Power Commission of Ontario, Atomic Energy Limited Power Projects, 1969.

2.0 BASIC METALLURGY

A.H. Cottrell, An Introduction to Metallurgy, Edward Arnold (Publishers) Ltd., London, 1967.

G.E. Dieter, Mechanical Metallurgy, McGraw- Hill Book Company, Inc., 1976.

A.G. Guy, Elements of Physical Metallurgy, Addison - Wesley Publishing Company, Inc., 1960.

Similar information to that in the above three references can be found in any general text book on Physical Metallurgy.

D.L. Douglas, Atomic Energy Review, The Metallurgy of Zirconium, IAEA, 1971.

3.0 ZIRCONIUM EXTRACTION AND ALLOY PRODUCTION

W.W. Stephens; Extractive Metallurgy of Zirconium - 1945 to the Present; Proceedings of the Sixth Inernational Symposium on Zirconium in the Nuclear Industry; ASTM STP 824, August 1984.

M.E. Hayden and A. Mitchell, Hot-Top Defect Simulation in Zr-2.5 wt% Nb Vacuum Arc Remelted Ingots, University of British Columbia, Final Report to AECL - Ontario Hydro, November 1986.

4.0 TUBE PRODUCTION

C.E. Ells and W. Evans; The Pressure Tubes in the CANDU Power Reactors, CIM Bulletin, July 1981.

B.A. Cheadle; Fabrication of Zirconium Alloys into Components for Nuclear Reactors; Proceedings of the Third International Conference on Zirconium in the Nuclear Industry; ASTM STP 633; December 1977.

R.G. Fleck, E.G. Price and B.A. Cheadle; Pressure Tube Development for CANDU Reactors; Proceedings of the Sixth International Symposium on Zirconium in the Nuclear Industry; ASTM STP 824; August 1984.

E.G. Price, Review of Fabrication Practice for Zr-2.5 wt% Nb Pressure Tubing to the Cold-Worked Condition, Draft Presentation to Task Group 3 of the Creep Engineering Design Plan.

E.G. Price, Fabrication, Inspection and Properties of Current Production Pressure Tubes, TDV1-380, AECL-EC, July 1982.

B. Avitzur, Handbook of Metal - Forming Processes, John Wilely and Sons, 1983.

5.0 MECHANICAL PROPERTIES

R.G. Fleck and G.K. Shek, The Influence of Post-extrusion Thermomechanical Treatments on the Tensile Properties of Zr-2.5 wt% Nb Alloy, Proceedings of the 6th International Conference on the Strength of Metals and Alloys, Melbourne, Australia, August 1982.

B.A. Cheadle, C.E. Ells, J. van der Kuur, Plastic Instability in Irradiated Zr-Sn and Zr-Nb Alloys, Proceedings of Symposium on Zirconium in Nuclear Applications, ASTM STP 551, August 1973.

B.A. Cheadle, Fabrication of Zirconium Alloys into Components for Nuclear Reactors, Proceedings of the Third International Symposium on Zirconium in the Nuclear Industry, ASTM STP 633, August 1976.

6.0 OPERATING EXPERIENCE

E.G. Price, Highlights of the Metallurgical Behaviour of CANDU Pressure Tubes, AECL 8338, October 1984.

J.T. Dunn, Summary of Fuel Channel Design and Operation, Fuel Channel Technology Seminar, CRNL 2950 , OH D&D 85431, November 1985.

J.R. MacEwen, J.T. Dunn, R. Dutton and G.J. Field, Interim Report of Task Force on Pressure Tube Cracking, CRNL 2620, November 1983.

G.J. Field, Problems Caused by Irradiation Deformation in CANDU Reactors, Fundamental Mechanisms of Radiation Induced Creep and Growth, Proceedings of an International Conference, June 1987, Journal of Nuclear Materials, Vol 159.

E.G. Price, G.D. Moan and C.E. Coleman, Leak-Before-Break Experience in CANDU Reactors, AECL - 9609, April 1988.

7.0 IRRADIATION DAMAGE AND DEFORMATION

R.G. Fleck, A Review of Irradiation Creep and growth of Pressure Tube in CANDU Nuclear Reactors, OHRD Report 78-170-K, April 1978.

R. Dutton, An Introduction to radiation Induced Deformation Processes (A "Laymans" Guide), AECL 1989, to be published.

R.A. Holt, A.R. Causey, V. Fidleris, Correlation of Creep and Growth of Pressure Tubes with Operating Variables and Microstructure, Dimensional Stability and Mechanical Behaviour of Irradiated Metals and Alloys, British Nuclear Energy Society, London, 1983, AECL 7931.

W.K. Alexander, V. Fidleris and R.A. Holt, Zircaloy-Pressure Tube Elongation at the Hanford N. Reactor, Proceedings of the Third International Conference on Zirconium in the Nuclear Industry, ASTM STP 633, 1977.

V. Fidleris, R.P. Tucker and R.B. Adamson, An Overview of Microstructural and Experimental Factors that Affect the Irradiation Growth Behaviour of Zirconium Alloys, Proceedings of the Seventh International Conference on Zirconium in the Nuclear Industry, ASTM STP 939, September 1987.

J.D. Parker, V. Perovic, M. Leger and R.G. Fleck, Microstructural Effects on the Irradiation Growth of Zr-2.5 wt% Nb, ibid.

V. Fidleris, The Irradiation Creep and Growth Phenomenon, Fundamental Mechanisms of Radiation-Inducted Creep and Growth, Proceedings of an International Conference, June 1987, Journal of Nuclear Materials Vol 159.

Details on Damage and Deformation Mechanisms are Presented in Papers in the Proceeding of the Following Conferences:

Radiation Damage in Metals, Cincinnati, 1975, ASM.

Fundamental Mechanisms of Radiation-Induced Creep and Growth, Chalk River, May 1979, Journal of Nuclear Materials, Volume 90, 1980.

Fundamental Mechanisms of Radiation - Induced Creep and Growth, Hecla Island, June 1987, Journal of Nuclear Materials, Volume 159.

Measurements of Irradiation - Enhanced Creep in Nuclear Materials, Petten, The Netherlands, May, 1976, Journal of Nuclear Materials, Volume 65.

8.0 PRESSURE TUBE FRACTURE

B. Cox, Current Views of the Mechanisms of Cracking of Zr-2.5 wt% Nb Pressure Tubes, CRNL 1474, March 1976.

Pickering GS Unit 2 Failure of Pressure Tube G-16, Status Report 84-1, January 6, 1984, AECL-CO, Information Exchange System Technical Newsletter.

C.E. Ells, Hydride Precipitates in Zirconium Alloys (A Review), AECL-2720, Journal of Nuclear Materials, Vol 28, 1968.

C.E. Coleman and J.F.R. Ambler, Reviews on Coatings and Corrosion, Vol. III, Freund, Israel, 1979.

D.O. Northwood and V. Kosasih, Int. Metals Review, 28, 1983.

R.L. Eadie and R.R. Smith, Canadian Metall. Quarterly, Vol 27, No. 3, 1988.

R. Dutton, K. Nuttall, M.P. Puls and L.A. Simpson, Metallurgical Transactions 8A, 1977.

L.A. Simpson and M.P. Puls, Metallurgical Transactions A, Vol 10 A, 1979.

M.P. Puls, Acta Metallurgica, 29, 1981.

M.P. Puls, Acta Metallurgica, 31, 1984.

C.E. Coleman, B.A. Cheadle, J.F.R. Ambler, P.C. Lichtenberger, and R.L. Eadie, Canadian Metallurgical Quarterly, 24, 1985.

B.A. Cheadle, C.E. Coleman and J.F.R. Ambler, Proceedings of the International Conference on Zirconium in the Nuclear Industry, ASTM STP 939, 1987.

M. Leger, Hydride Blister Growth in Zr-2.5 wt% Nb Pressure Tube Material, CNS, Proceedings of the 12th Simulation Symposium on Reactor Dynamics and Plant Control, April 1986.

9.0 CORROSION AND HYDROGEN INGRESS

P.C. Lichtenberger, Hydrogen Ingress Mechanisms in Zr-2.5 wt% Nb Pressure Tubes - An Overview of some Recent Progress, Presented at the Annual CNA/CNS Conference, June 1988.

B. Cox, Mechanisms of Oxidation and Deuterium Pickup in Zirconium Alloys, CRNL 2950 OH D&D 85431, Fuel Channel Technology Seminar, February 1987.

B.D. Warr, A.H.C. Chan and S.R. Lukac, Modelling Deuterium Pickup In Operating Reactor Pressure Tubes, ibid.

V.F. Urbanic, Corrosion and Deuterium Uptake in Pressure Tubes, ibid.

10.0 ALLOY DEVELOPMENT

W. Chubb, Progress in the Development of Creep-Resistant Zirconium Alloys, Transactions of the ASM, Vol. 48, 1956.

C.D. Williams, C.E. Ells and P.R. Dixon, Development of High Strength Zirconium Alloys, Canadian Metallurgical Quarterly, Vol. 11, No. 2, 1972.

C.D. Williams, Development Potential of Zirconium Alloys for High - Temperature Applications, Reactor Technology, Vol. 13, No. 2, 1970.

N.R. McDonald, Prospects for High Strength Zirconium Alloys, The Journal of the Australian Institute of Metals, Vol. 16, No. 4, 1971.

B.A. Cheadle, A Comparison of Pressure Tube Materials for CANDU Reactors, CRNL 1720, 1978.

B.A. Cheadle, A Comparison of Cold-Worked Zr-2.5 wt% Nb and XL Alloy Pressure Tubes, CRNL 1674, 1977.

B.A. Cheadle, A Comparison of Cold-Worked Zr-2.5 wt% Nb and Heat Treated Zr-2.5 wt% Nb Pressure Tubes, CRNL 1624, 1977.

E.F. Ibrahim, E.G. Price and A.G. Wysiekierski, Canadian Metallurgical Quarterly, Vol 11, No. 1., 1972.

L.H. Keys, G. Johanson and A.S. Malin, The Physical Metallurgy of High Strength Zirconium Alloys, Journal of Nuclear Materials, 59, 1976.

E.M. Schulson and D.B. Graham, The Peritectoid of Ordered $Zr_3A\ell$, Acta Metallurgica, Vol. 24, 1976.

E.M. Schulson and M.J. Stewart, The Forming of $Zr_3A\ell$ Base Alloys, Metallurgical Transactions B, Vol 7B, 1976.

GENERAL REFERENCES

For all of the topics presented in this report relevant papers can be found in the Proceedings on the International Conferences on Zirconium in the Nuclear Industry as published in the following references:

ASTM STP 551, 1974
ASTM STP 633, 1977
ASTM STP 681, 1979
ASTM STP 754, 1982
ASTM STP 824, 1984
ASTM STP 939, 1987
ASTM STP 1023, 1989

Other relevant papers can be found in the Proceedings of the AECL and Ontario Hydro Fuel Channel Technology Seminars:

CRNL 2259, July 1981.
CRNL 2950, OH D&D Gen. 85431, February 1987.